‘Le charme discret’ of the von Willebrand factor - factor VIII complex

Małgorzata Przeradzka

‘Le charme discret’
of the von Willebrand factor - factor VIII complex

Małgorzata Przeradzka

Cover: Cartoon representation of the von Willebrand factor and factor VIII molecules. Design by Erwin Timmerman. With use of modeling software: https://ccsb.scripps.edu/

The research described in this thesis was performed at the department of Plasma Proteins, Sanquin Research, Amsterdam, The Netherlands

ISBN: 978-94-6361-442-9.
Lay out and printed by: Optima grafische communicatie, Rotterdam, The Netherlands.

Financial support for printing was kindly provided by Sanquin Research.

‘Le charme discret’

of the von Willebrand factor - factor VIII complex

De discrete charme van het von Willebrand factor-factor VIII complex
(met een samenvatting in het Nederlands)

Proefschrift

ter verkrijging van de graad van doctor aan de
Universiteit Utrecht
op gezag van de
rector magnificus, prof.dr. H.R.B.M. Kummeling,
ingevolge het besluit van het college voor promoties
in het openbaar te verdedigen op

maandag 26 oktober 2020 des middags te 12.45 uur

door

Małgorzata Aniela Przeradzka

geboren op 17 maart 1989
te Łódź, Polen

Promotoren: Prof. dr. A.B. Meijer
Prof. dr. K. Mertens

Copromotor: Dr. M. van den Biggelaar

Financial support by the Dutch Hear Fundation for the publication of this thesis is gratefully acknowledged

TABLE OF CONTENT

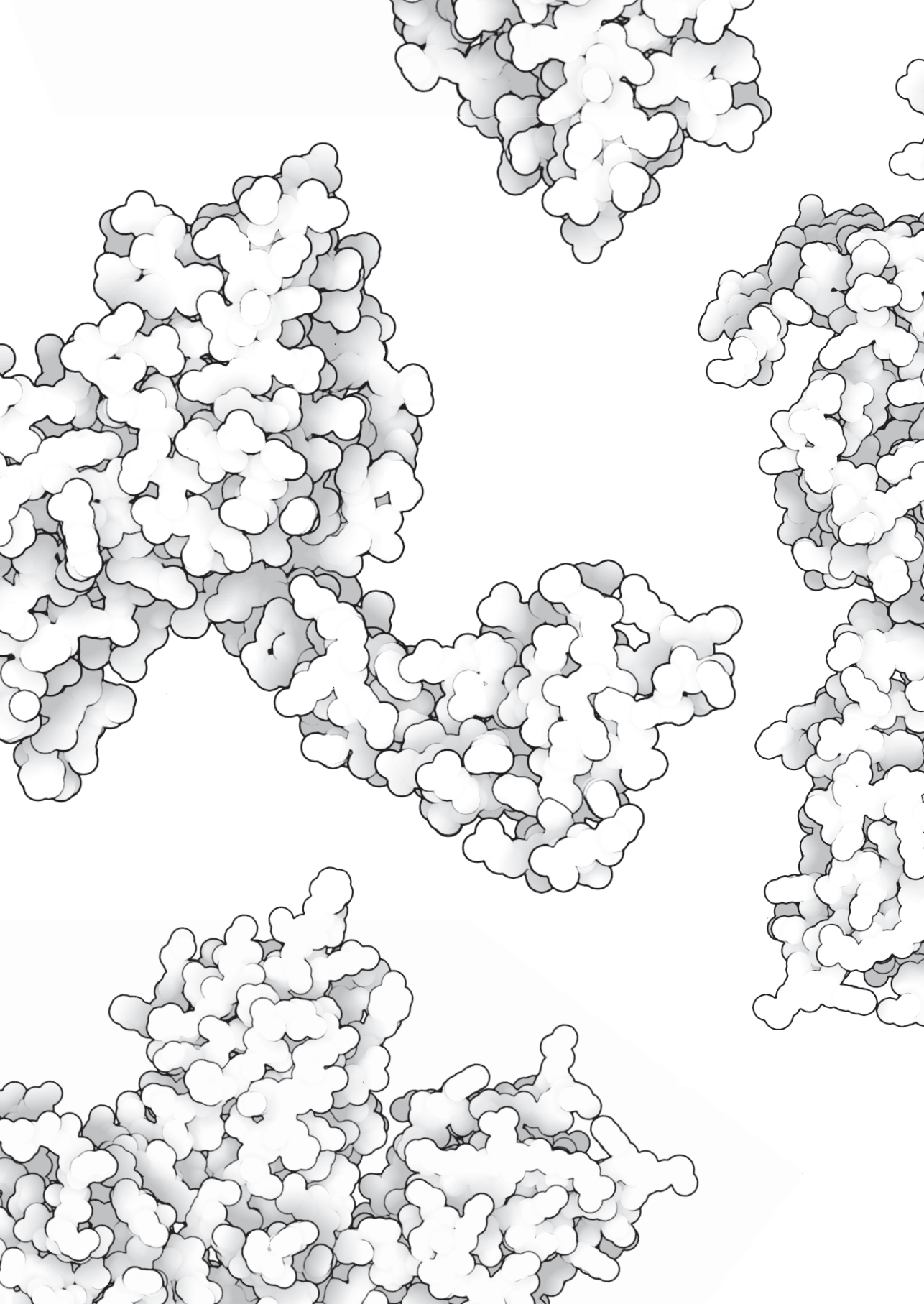

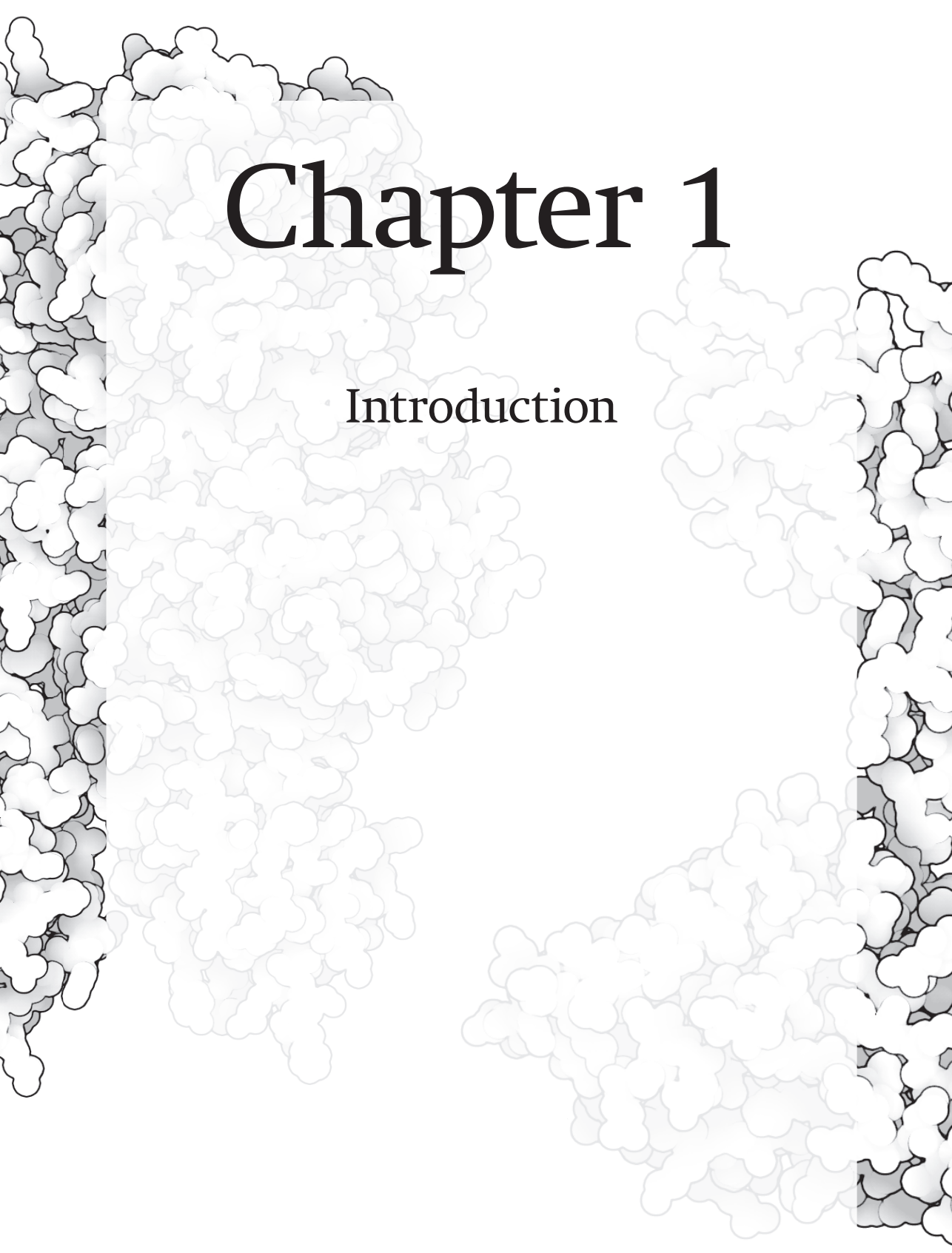

Chapter 1

Introduction

SCOPE OF THIS THESIS

Von Willebrand Factor (VWF) and Factor VIII (FVIII) are key players in the molecular mechanisms behind bleeding arrest at sites of vascular injury. Whereas VWF is indispensable for platelet plug formation, FVIII serves its role in the coagulation cascade as a cofactor for the serine protease Factor IX (FIX). VWF also acts as a carrier protein for FVIII and has a dual role in regulating the FVIII half-life *in vivo*. On the one hand, VWF mediates the catabolism of FVIII via poorly understood cellular mechanisms. On the other hand, VWF protects FVIII from fast clearance from the circulation. The high macromolecular complexity of the multimeric VWF has always been a major obstacle for resolving the mechanisms by which VWF interacts with its clearance receptors and FVIII. In chapter 2 and 3 of the present thesis, we employ domain-truncation variants of VWF to assess the role of the domains for the interaction with FVIII. Using hydrogen-deuterium exchange mass spectrometry (HDX-MS) followed by site-directed mutagenesis and protein-binding studies, detailed information is obtained about the identity of the amino acids that directly contribute to FVIII binding. The combined studies revealed the identity of the FVIII binding site in the N-terminal D' domain of VWF. These studies also provided an answer to the question why mutations in VWF that are associated with impaired VWF-FVIII complex formation have been identified outside the main FVIII binding region. The truncation variants of VWF were also employed in cell internalization experiments in chapter 4 to assess the role of the multiple putative receptors that may mediate the cellular uptake of VWF. This led to the identification of a shared mechanism by which the macrophage-scavenger receptor and low-density lipoprotein receptor-related protein mediate the uptake of VWF. In chapter 5, we addressed the binding site of VWF on FVIII using primary sequence and crystal structure analysis of FVIII. Site-directed mutagenesis of FVIII followed by binding studies and cofactor function studies were employed to identify FVIII residues that contribute to the interaction with VWF and/or activated FIX. In chapter 6, the findings and the future implications of this thesis are discussed. In the following paragraphs, the current understanding of the structure, role, interaction and clearance mechanism of VWF and FVIII is described in more detail.

THE ROLE OF VWF AND FVIII IN HAEMOSTASIS

The simultaneously acting processes involved in primary and secondary haemostasis effectively mediate bleeding arrest at vessel injury. Primary haemostasis regulates the initial formation of an instable platelet plug and secondary haemostasis results in the generation of insoluble fibrin. The interaction between platelets and fibrin leads to a stable platelet aggregate that effectively stops the bleeding at the site of injury[1]. VWF plays a central role in primary haemostasis. Upon vessel damage, collagens that are

normally underneath the endothelial cells of the vessel wall come into contact with VWF in plasma. The interaction between VWF and collagens induces the exposure of a binding site in VWF for the platelet receptor glycoprotein Ib. This mediates platelet adhesion followed by platelets activation at the site of injury. Further activation of the platelets eventually results in the formation of the instable platelet plug[2]. VWF is also stored in the secretory organelles, i.e. the Weibel-Palade bodies, of the endothelial cells and the alpha-granules of platelets. Activation of the platelets and endothelial cells triggers the release of VWF from these secretory organelles which also assist in the adhesion and activation of platelets at the site of damage[3].

Vessel damage results into the exposure to the blood of tissue factor which is expressed on the perivascular cells. This initiates the process of secondary haemostasis involving a cascade of activation reactions of serine proteases and their cofactors. It eventually leads to a boost in the generation of thrombin that converts fibrinogen into fibrin [4]. Coagulation FVIII plays a central role in the coagulation cascade. It serves its role as a cofactor for the serine protease FIX. The complex of activated FVIII (FVIIIa) and activated FIX (FIXa) on procoagulant phospholipid surfaces effectively converts Factor X (FX) into activated FX (FXa)[5]. In the complex with activated cofactor V and procoagulant phospholipids, FXa proteolytically cleaves prothrombin into thrombin.

Prior to activation, FVIII circulates in a tight complex with VWF in the circulation. In this complex, FVIII is protected from premature interaction with its ligands FIXa, FX and phospholipids. In addition, the *in vivo* half-life is increased from about 1 hour in absence of VWF to about 14 hours in presence of VWF[6]. Figure 1 shows a schematic overview of the haemostatic processes.

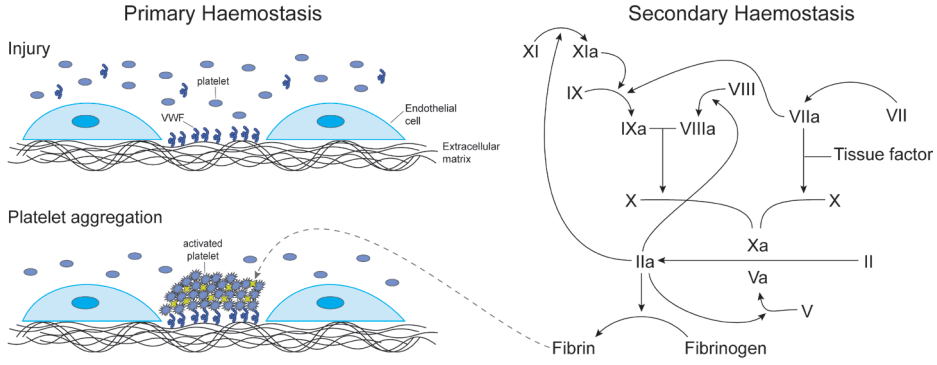

Figure 1. Schematic representation of haemostasis. Primary haemostasis and secondary haemostasis.

THE STRUCTURE AND FUNCTION OF VWF

VWF is synthesized by endothelial cells and megakaryocytes as a single chain protein comprising 2813 amino acids[7]. After synthesis, VWF is stored as a large multimeric protein in the Weibel-Palade bodies of the endothelial cells and the alpha-granules of the platelet precursor-cells, the megakaryocytes. VWF is also constitutively secreted by these endothelial cells and megakaryocytes[8]. Several protein domains have initially been identified in VWF, i.e. D1-D2-D'-D3-A1-A2-A3-D4-C1-C2-C3-C4-C5-C6-CK[9]. The D1-D2 domains form the pro-peptide and the fragment starting with D' represents the mature sequence of the protein. In 2012 the domain organisation has been refined by Zhou et al. For the D'-D3 domains, they suggested that it can be further subdivided into TIL'-E'-VWD3-C8_3-TIL3-E3 domains[10]. A full overview of the domains of VWF is shown in Figure 2.

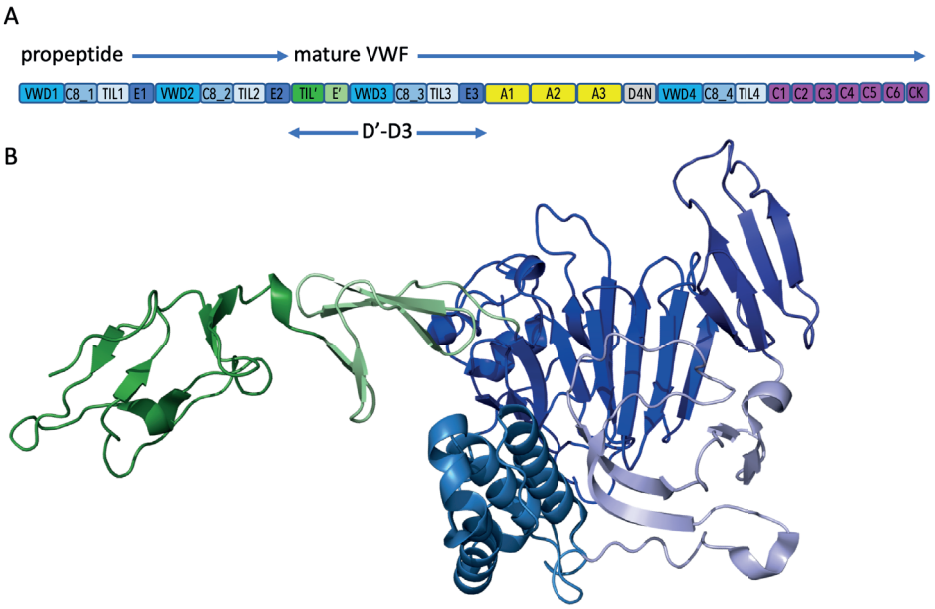

Figure 2. VWF structure and domain organisation. (A) Schematic representation of the domain organisation of VWF[10]. (B) Crystal structure of the TIL'-E'-VWD3-C8_3-TIL3-E3 fragment of VWF. The domains are coloured as indicated in panel A [PDB entry:6n29][14].

Multimerization of VWF starts in the endoplasmatic reticulum (ER) where the CK domains of two VWF monomers are tail-to-tail linked via disulphide bridges[11]. The dimers are transported to the trans-Golgi network where the D3 domains are head-to-head connected via disulphide bridges. This involves Cys1099 of the C8-3 domain and Cys1142 of the TIL3 domain[12]. Within the ER, it has been proposed that these cysteine residues are buried in the structure to protect VWF from premature dimerization

via the D3 domains. The acid environment within the Golgi is thought to induce a conformational change in D3, thereby exposing the cysteine residues to the protein surface to mediate dimerization of the D3 domains[12-14]. The VWF pro-peptide assists in this process and is removed from the mature VWF via furin-assisted proteolysis[15]. Under the acidic trans-Golgi conditions, the C domains dimerise in a non-covalent manner to further allow the tubular packing of the VWF multimers in the Weibel-Palade bodies[16].

The homologous VWF A domains are not unique to this protein. The VWF-type A domains have also been identified in short-chain collagens and cellular adhesion proteins[17]. The VWF A2 domain is known for its mechano-sensitivity as a consequence of lacking the particular disulphide bridge that is conserved in the other A domains[18]. This makes the A2 domain more susceptible to unfolding under shear flow conditions. The unfolded A2 domain exposes a cleavage site for the protease "a disintegrin-like and metalloprotease with thrombospondin type 1 repeat motifs 13" (ADAMTS13), which can cleave the VWF multimers into smaller fragments[19,20]. This serves as a feed-back mechanism to prevent uncontrolled platelet adhesion. Shear flow also exposes a binding-site for the platelet receptor glycoprotein Ib in the A1 domain of VWF[21]. This maybe be the consequence of a macromolecular rearrangement of the interactions between the A and D3 domains of VWF[22].

Interaction sites for other ligands have also been identified in VWF. The C4 domain comprises a binding site for the platelet integrin GPIIb-IIIa, and interactive regions for collagens have been found in the A1 and A3 domain[23-26]. The first 272 amino acid residues of the D'-D3 domains of VWF have been demonstrated to comprise the high affinity binding site for FVIII[27,28]. The amino acid residues of D'-D3 that directly contribute to FVIII binding are, however, still unknown.

THE STRUCTURE AND FUNCTION OF FVIII

FVIII is synthesised as a polypeptide chain of 2351 amino acids. The domain structure is organised as follows: A1-a1-A2-a2-B-a3-A3-C1-C2 (Figure 3). The A domains are homologous to the A domains of ceruloplasmin and the C domains to the discoidin-like domains of discoidin. The a1, a2 and a3 are short spacer regions that are rich in acidic amino acids and comprise sulphated tyrosine residues. The B domain of FVIII shares no sequence homology with any other known protein domain[29]. Mediated by limited proteolysis of the B domain, FVIII is cleaved into a heterogenous heavy chain (domains: A1-a1-A2-a2-B) that is non-covalently linked to a light chain (domains: a3-A3-C1-C2)[5].

To perform its role as co-factor in the coagulation cascade, FVIII requires activation by thrombin, which proteolytically cleaves at arginine residues that flank the acidic regions. Upon activation, the heavy chain is cleaved at position Arg372 at the

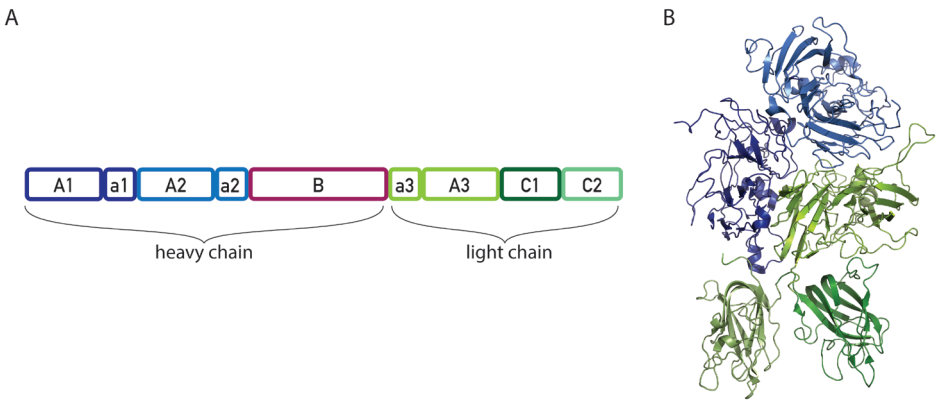

Figure 3. FVIII structure and domain organisation. (A) Domain organisation of FVIII. a1, a2 and a3 represent short spacer regions rich in acidic amino acid residues and sulphated tyrosine residues (B) Crystal structure of FVIII [PDB entry: 3cdz] [30]. The domains are coloured as indicated in panel A.

C-terminal side of the acidic a1 region and at position Arg740 at the C-terminal side of the acidic a2 region. One additional cleavage at the C-terminal side of the acid a3 region (Arg1689) is required to fully activate FVIII[31,32]. As a consequence of activation, B domain and acidic a3 region are released from FVIII and the A1 and A2 domain are bisected[31]. It has also been shown that FXa can proteolytically activate FVIII. Whether or not this is of physiological relevance is unclear[33,34]. Upon activation, FVIII dissociates from its carrier protein VWF leading to exposure of interactive sites on FVIII for its ligands. To date, several ligand interaction sites have been identified in FVIII. An overview of the proposed sites is given below.

Interaction of FVIII with von Willebrand factor

Multiple amino acid regions in the FVIII light chain have been implicated to contribute to VWF binding[35,36]. A recently published model based on an electron microscopy study of FVIII in interaction with D'-D3 shows that VWF may bind the C1 domain[37,38]. Previous reports demonstrated that the acidic a3 region is essential for FVIII-VWF complex formation as well[39]. An HDX-MS study by Chiu et al. showed, however, multiple sites of structural perturbation spread throughout the FVIII light chain upon FVIII binding to the D'-D3 fragment of VWF. Multiple studies further suggest a role of the FVIII C2 domain for the interaction of FVIII with VWF. This is based on the observation that antibodies directed against the C2 domain affect FVIII-VWF complex formation. Several mutations have also been identified in the C2 domain that reduce the affinity for VWF[40-43]. In spite of the putative role of the C2 domain in VWF binding, a FVIII variant in which the C2 domain was replaced with that of FV showed near normal

VWF binding[44]. The above-mentioned studies show that the molecular mechanism by which VWF binds FVIII is not fully understood.

Interaction of FVIII with FIX

In 1994, the group of Mertens et al proposed that the light chain mediates high affinity binding to FIXa[45]. It has been demonstrated that FVIII region 1811-1818 contributes to the interaction with FIXa[46,47]. Fay et al. has suggested that the A2 domain acts as a modulator of FIXa activity via an FXa interactive region that is located at position 558-565[43,48]. A FIXa binding site has also been identified in C2 region 2228-2240[49]. The C1 residues Q2042/Y2043 and R2090/Q2091 were all implied to take part in interaction with FIX[50]. Intriguingly, a FVIII/FV-C1 chimera and not a FVIII/FV-C2 chimera displayed markedly reduced cofactor activity[44]. These results show that the C2 domain may not comprise FIXa interactive regions after all. Taken together, resolving the full identity of the FIXa interactive regions on FVIII remains a topic for investigation.

Interaction of FVIII with phospholipids

The C domains of FVIII are required for effective binding of FVIII to phospholipid membranes comprising phosphatidyl-serine (PS) in the outer leaflet. Each of the C domains comprise 4 flexible β-hairpin loops, so called “spikes”, that mediate phospholipid binding[50]. Based on cryo-EM studies of FVIII bound to a phospholipid membrane, it was initially thought that only the C2 domain of FVIII mediates phospholipid binding. In the proposed model, the C1 domain was placed on top on the C2 domain at an angle of approximately 90 degrees[51]. The crystal structures of FVIII, however, show the C1 domain in a parallel position next to the C2 domain placing the spikes of the C1 and C2 domain next to each other[30,52]. This orientation implied that both C domains may contribute to the interaction with the phospholipid membrane[30,52]. The role of the C1 domain was confirmed by the study of Wakabayashi et al and showed that a FVIII variant lacking the C2 domain still displays phospholipid-dependent cofactor function[53].

THE CLEARANCE MECHANISMS OF VWF

VWF circulates in the blood stream in a tight non-covalent complex with FVIII. In absence of VWF, the low-density lipoprotein receptor 1 (LRP1) has been implicated as an endocytic receptor for FVIII[54]. Molecular mechanisms that mediate cellular uptake of VWF have been demonstrated to contribute to the clearance of FVIII in presence of VWF. *In vivo* studies have shown that the macrophages of the liver and spleen are actively involved in VWF uptake[55]. This finding is compatible with the observation that chemical inactivation of macrophages leads to increased levels of circulating VWF[56].

Macrophages derived from the THP-1 cell line have been shown to internalise VWF in a shear-independent manner. Monocyte-derived macrophages, however, only internalize VWF under conditions of shear stress[57]. The *in vivo* role of shear stress remains therefore unclear[58]. Another topic that remains to be resolved involves the numerous receptors that have been suggested to act as a clearance receptor for VWF on the macrophages. These include LRP-1, macrophage scavenger receptor-1 (MSR-1, SR-AI or CD204), scavenger-receptor macrophage galactose-type lectin (MGL), Siglec-5 and the Asialoglycoprotein receptor (ASGPR)[59]. The relative contribution of these receptor to the catabolism of VWF is a topic for further investigation.

BLEEDING DISORDERS ASSOCIATED WITH FUNCTIONAL ABSENCE OF FVIII OR VWF

The critical importance of FVIII and VWF for proper haemostasis is demonstrated by the observation that their functional absence is associated with the bleeding disorders haemophilia A and Von Willebrand Factor Disease (VWD), respectively. These disorders are among the most commonly inherited disorders[60]. Two distinct types of Haemophilia have been distinguished i.e. haemophilia A involving a qualitative or quantitative deficiency of FVIII, and haemophilia B that is associated with defects in FIX expression or function. Both haemophilia A and B are X-linked recessive disorders affecting 1 in 5000 males and 1 in 35 000 males, respectively[61,62]. Disease causing genetic variations in FVIII can lead to defects in FVIII binding to phospholipids, FIXa and/or VWF[48,63]. Some of the variations cause the formation of a premature stop codon leading to the expression of a truncated FVIII variant or a complete absence of the protein[64]. One treatment strategy for haemophilia A patients involves intravenous injections with concentrates of purified plasma-derived or recombinant FVIII[65]. As the half-life of FVIII is approximately 14 hours, patients have to infuse themselves up to 3 times a week with FVIII to reduce the risk for uncontrolled bleedings[66].

The clinical manifestations of disease-causing genetic variants of VWF are more complex. Consequently, multiple types of VWD are distinguished. VWD Type I is the most prevalent and is defined as "including partial quantitative deficiency of VWF"[67]. VWD Type C1 is the result of accelerated clearance of VWF from the circulation. An example of the latter disorder is referred to VWD Vicenza, and involves a single substitution of the Arginine residue at position 1205 for a Histidine residue in the D3 domain[68]. Complete deficiency of VWF in plasma is classified as VWD Type 3 and VWD Type 2 is characterised by missense mutations leading to qualitative defects. Table 1 shows an overview of the VWD types and subtypes thereof.

VWD Type 2 Normandy (2N) is special due to its association with an hemophilia-like phenotype caused by a particularly low plasma level of FVIII. The associated variants

Table 1 The VWD types and subtypes

Defect	Type	Description	Multimers
Quantitative	1	Partial quantitative deficiency of VWF	normal pattern
	3	Virtually complete deficiency in VWF	normal pattern
Qualitative	2A	Decreased VWF-dependent platelet adhesion associated with the absence of high-molecular weight VWF multimers	loss of high-molecular weight VWF multimers
	2B	Increased affinity for platelet glycoprotein Ib	loss of high-molecular weight VWF multimers
	2M	Decreased VWF-dependent platelet adhesion unrelated to the absence of high-molecular weight VWF multimers	normal pattern
	2N	Markedly decreased binding affinity for Factor VIII	normal pattern (with exceptions)

of VWF exhibit a reduced affinity for FVIII[69]. Amino acid substitutions are identified in the first 461 amino acids of mature VWF[67]. Although this is compatible with the observation that the FVIII binding region is at the N-terminus of VWF, it has remained unclear why these variants are scattered over this broad range of amino acids residues

MACROMOLECULAR MASS SPECTROMETRY AS A TOOL TO STUDY PROTEIN INTERACTIONS

Protein labeling approaches combined with mass spectrometry have been employed to identify protein interaction sites or conformational changes. Several methods rely on chemically modifying lysine residues in bound and unbound proteins using biotin or tandem mass tags (TMT)[70,71]. Lysine residues at the protein interface are expected to be more protected from chemical modification in the protein complex compared to the isolated proteins. Mass spectrometry analysis is a particularly powerful approach to identify the modified lysine residue based on their distinct difference in mass.

TMTs greatly facilitate quantifying the difference in chemical modification. In this approach, the protein complexes are modified with e.g. TMT-127 and the unbound proteins with TMT-126. The TMT-126 and TMT-127 labeled protein are then mixed and proteolyzed by trypsin and/or chymotrypsin followed by identification by mass spectrometry analysis. Both TMT-127 and TMT-126 have an identical mass but a different isotope distribution. Fragmentation of TMT modified peptides releases a unique reporter group from the TMT which allows for relative quantification in the mixed sample[70]. A disadvantage of this approach is that only information is obtained about lysine residues. In addition, modified lysine residues may affect the stability of the protein complex or the protein itself.

HDX-MS represents another powerful approach to study not only protein-protein interactions but also conformational changes within a protein. HDX-MS takes maximum

advantage of the mechanism that hydrogen of, amongst others, the protein backbone are exchanged with deuterium atoms when a protein is transferred from H_2O to D_2O[72]. The increase in mass in an amino acid region, caused by introduction of deuterium, can be accurately measured by MS analysis. The rate of exchange depends on solvent accessibility of the protein backbone and of the local conformation of the protein. Sites where proteins interact may also exhibit a reduced HDX[73]. HDX-MS has previously been successfully employed to identify the FVIII binding region of an antibody that markedly affects PS binding and endocytosis of FVIII[74]. This technology may also be particularly suitable to identify binding regions for FIXa, phospholipids and VWF in FVIII.

QUESTIONS ADDRESSED IN THIS THESIS

The VWF-FVIII complex is critical for proper functioning of the mechanisms behind bleedings arrest at sites of vessel injury. Whereas the individual constituents of the complex play a distinct role in haemostasis, the catabolic processes of FVIII and VWF partly share the same mechanisms. In the present thesis, we aim to gain insight into the interaction between VWF and FVIII as well as cellular uptake mechanism of VWF. In **chapter 2**, we set out to identify the residues of VWF that contribute to FVIII binding. To this end, HDX-MS studies of the FVIII-D'-D3 complex were combined with site-directed mutagenesis studies, and protein binding studies. The addressed questions include: Which residues of VWF are involved in the direct interaction with FVIII? What is the contribution of charged residues to FVIII-VWF complex formation?

In **chapter 3**, we study why VWF type 2N variants have been identified outside the main FVIII binding site in the D' domain of VWF. We have constructed and purified a set of C-terminal subdomain truncation variants of the D'-D3 fragment. Their affinity to FVIII was evaluated using surface plasmon resonance analysis and a competitive binding assay. Chemical footprinting was employed to assess the structural integrity of the D'-D3 truncations variants. We addressed questions like: Is there a role for the D3 domain in binding to FVIII? What is the impact on the FVIII binding affinity upon subsequent deletion of the subdomains in the D'-D3 fragment of VWF? Which subdomain is most critical for the interaction with FVIII? What is the structural impact on the D'-D3 fragment upon subdomain deletions?

To study the mechanism of VWF clearance, we have employed cell surface proteomics and cellular uptake studies in **chapter 4**. We have covered questions as: Which putative VWF receptors on macrophages mediate the uptake of VWF? How do these receptors contribute to the uptake of VWF?

Chapter 5 addresses the complementary binding site of VWF in FVIII. Previously, we have found that replacing the C1 domain of FVIII with that of the homologous

protein FV impairs VWF binding. Questions addressed are: Which residues in the C1 domain are unique to FVIII compared to the FV C1 domain? Do these residues contribute to VWF binding and/or to the cofactor function of FVIII? Finally, in **chapter 6,** the collective findings of this study are discussed.

REFERENCES

1 Davie, E. W., Fujikawa, K. and Kisiel, W. (1991) The coagulation cascade: initiation, maintenance, and regulation. *Biochemistry* **30**, 10363-10370.

2 Peyvandi, F., Garagiola, I. and Baronciani, L. (2011) Role of von Willebrand factor in the haemostasis. *Blood Transfus.* **9**, 3-8.

3 Wagner, D. D. (1993) The Weibel-Palade body: The storage granule for von Willebrand factor and P-selectin. *Thromb. Haemost.* **70**, 105-110.

4 Gale, A. (2011) Current understanding of hemostasis. *Toxicol Pathol.* **39**, 273-280.

5 Fay, P. J. (2006) Factor VIII Structure and Function. *Int. J. Hematol.* **83**, 103-108.

6 Pipe, S. W., Montgomery, R. R., Pratt, K. P., Lenting, P. J. and Lillicrap, D. (2016) Life in the shadow of a dominant partner: the FVIII-VWF association and its clinical implications for hemophilia A. *Blood* **128**, 2007-2016.

7 Wagner, D. D. (1990) Cell Biology of von Willebrand factor. *Annu. Rev. Cell Biol.* **6**, 217-246.

8 Sadler, J. E. (2009) von Willebrand factor assembly and secretion. *J. Thromb. Haemost.* **7**, 24-27.

9 Springer, T. A. (2011) Biology and physics of von Willebrand factor concatamers. *J. Thromb. Haemost.* **9 Suppl 1**, 130-43.

10 Zhou, Y. F., Eng, E. T., Zhu, J., Lu, C., Walz, T. and Springer, T. A. (2012) Sequence and structure relationships within von Willebrand factor. *Blood* **120**, 449-458.

11 Katsumi, A., Tuley, E. A., Bodo, I. and Sadler, J. E. (2000) Localization of disulfide bonds in the cystine knot domain of human von Willebrand factor. *J. Biol. Chem.* **275**, 25585-25594.

12 Purvis, A. R., Gross, J., Dang, L. T., Huang, R.-H., Kapadia, M., Townsend, R. R. and Sadler, J. E. (2007) Two Cys residues essential for von Willebrand factor multimer assembly in the Golgi. *Proc. Natl. Acad. Sci. U. S. A.* **104**, 15647-15652.

13 Zhou, Y. F. and Springer, T. A. (2014) Highly reinforced structure of a C-terminal dimerization domain in von Willebrand factor. *Blood* **123**, 1785-1793.

14 Dong, X., Leksa, N. C., Chhabra, E. S., Arndt, J. W., Lu, Q., Knockenhauer, K. E., Peters, R. T. and Springer, T. A. (2019) The von Willebrand factor D'D3 assembly and structural principles for factor VIII binding and concatemer biogenesis. *Blood* **133**, 1523-1533.

15 van de Ven, W. J. M., Voorberg, J., Fontijn, R., Pannekoek, H., van den Ouweland, A. M. W., van Duijnhoven, H. L. P., Roebroek, A. J. M. and Siezen, R. J. (1990) Furin is a subtilisin-like proprotein processing enzyme in higher eukaryotes. *Mol. Biol. Rep.* **14**, 265-275.

16 Huang, R.-H., Wang, Y., Roth, R., Yu, X., Purvis, A. R., Heuser, J. E., Egelman, E. H. and Sadler, J. E. (2008) Assembly of Weibel-Palade body-like tubules from N-terminal domains of von Willebrand factor. *Proc. Natl. Acad. Sci. U. S. A.* **105**, 482-487.

17 Colombatti, A., Bonaldo, P. and Doliana, R. (1993) Type A Modules: Interacting Domains Found in Several Non-Fibrillar Collagens and in Other Extracellular Matrix Proteins. *Matrix* **13**, 297-306.

18 Lynch, C. J. and Lane, D. A. (2016) N-linked glycan stabilization of the VWF A2 domain. *Blood* **127**, 1711-1718.

19 Tsai, H. M. (1996) Physiologic cleavage of von Willebrand factor by a plasma protease is dependent on its conformation and requires calcium ion. *Blood* **87**, 4235-44.

20 Furlan, M., Robles, R. and Lämmle, B. (1996) Partial purification and characterization of a protease from human plasma cleaving von Willebrand factor to fragments produced by in vivo proteolysis. *Blood* **87**, 4223-34.

21 Cruz, M. A., Handin, R. I. and Wise, R. J. (1993) The interaction of the von Willebrand factor-A1 domain with platelet glycoprotein Ib/IX: The role of glycosylation and disulfide bonding in a monomeric recombinant A1 domain protein. *J. Biol. Chem.* **268**, 21238-21245.
22 Ulrichts, H., Lenting, P. J., Pareyn, I., Vandeputte, N. and Vanhoorelbeke, K. (2006) Shielding of the A1 Domain by the D'-D3 Domains of von Willebrand Factor Modulates Its Interaction with Platelet Glycoprotein Ib-IX-V. *J. Biol. Chem.* **281**, 4699-4707.
23 Roth, G. J., Titani, K., Hoyer, L. W. and Hickey, M. J. (1986) Localization of binding sites within human von Willebrand factor for monomeric type III collagen. *Biochemistry* **25**, 8357-8361.
24 Kalafatis, M., Takahashi, Y., Girma, J. P. and Meyer, D. (1987) Localization of a collagen-interactive domain of human von Willebrand factor between amino acid residues Gly 911 and Glu 1,365. *Blood* **70**, 1577-83.
25 Ju, L., Chen, Y., Zhou, F., Lu, H., Cruz, M. A., Zhu, C. and Centre, P. (2016) Von Willebrand factor-A1 domain binds platelet glycoprotein Ibα in multiple states with distinctive force-dependent dissociation kinetics. *Thromb. Res.* **136**, 606-612.
26 Christophe, O., Obert, B., Meyer, D. and Girma, J. P. (1991) The binding domain of von Willebrand factor to sulfatides is distinct from those interacting with glycoprotein Ib, heparin, and collagen and resides between amino acid residues Leu 512 and Lys 673. *Blood* **78**, 2310-2317.
27 Foster, P. A., Fulcher, C. A., Marti, T., Titani, K. and Zimmerman, T. S. (1987) A major factor VIII binding domain resides within the amino-terminal 272 amino acid residues of von Willebrand factor. *J. Biol. Chem.* **262**, 8443-8446.
28 Shiltagh, N., Kirkpatrick, J., Cabrita, L. D., Mckinnon, T. a J., Thalassinos, K., Tuddenham, E. G. D., Hansen, D. F., Tuddenham, Edward GD, Hansen, D. F., Tuddenham, E. G. D., et al. (2014) Solution structure of the major factor VIII binding region on von Willebrand factor. *Blood* **123**, 4143-4152.
29 Pipe, S. W. (2009) Functional roles of the factor VIII B domain. *Haemophilia* **15**, 1187-1196.
30 Ngo, J. C. K., Huang, M., Roth, D. A., Furie, B. C. and Furie, B. (2008) Crystal Structure of Human Factor VIII: Implications for the Formation of the Factor IXa-Factor VIIIa Complex. *Structure* **16**, 597-606.
31 Fay, P. J. (2004) Activation of factor VIII and mechanisms of cofactor action. *Blood Rev.* **18**, 1-15.
32 Camire, R. M. and Bos, M. H. A. (2009) The molecular basis of factor V and VIII procofactor activation. *J. Thromb. Haemost.* **7**, 1951-1961.
33 Donath, M., Lenting, P. J., van Mourik, J. A. and Mertens, K. (1995) The Role of Cleavage of the Light Chain at Positions Arg1689 or Arg1721 in Subunit Interaction and Activation of Human Blood Coagulation Factor VIII. *J. Biol. Chem.* **270**, 3648-3655.
34 Plantier, J. L., Rolli, V., Ducasse, C., Dargaud, Y., Enjolras, N., Boukerche, H. and Négrier, C. (2010) Activated factor X cleaves factor VIII at arginine 562, limiting its cofactor efficiency. *J. Thromb. Haemost.* **8**, 286-93.
35 Lollar, P., Hill-Eubanks, D. C. and Parker, C. G. (1988) Association of the factor VIII light chain with von Willebrand factor. *J. Biol. Chem.* **263**, 10451-5.
36 Saenko, E. L. and Scandella, D. (1997) The Acidic Region of the Factor VIII Light Chain and the C2 Domain Together Form the High Affinity Binding Site for von Willebrand Factor. *J. Biol. Chem.* **272**, 18007-14.

37 Chiu, P.-L., Bou-Assaf, G. M., Chhabra, E. S., Chambers, M. G., Peters, R. T., Kulman, J. D. and Walz, T. (2015) Mapping the interaction between factor VIII and von Willebrand factor by electron microscopy and mass spectrometry. *Blood* **126**, 935-8.

38 Yee, A., Oleskie, A. N., Dosey, A. M., Kretz, C. a., Gildersleeve, R. D., Dutta, S., Su, M., Ginsburg, D. and Skiniotis, G. (2015) Visualization of an N-terminal fragment of von Willebrand factor in complex with factor VIII. *Blood* **126**, 939-943.

39 Leyte, A., van Schijndel, H. B., Niehrs, C., Huttner, W. B., Verbeet, M. P., Mertens, K. and van Mourik, J. A. (1991) Sulfation of Tyr 1680 of human blood coagulation factor VIII is essential for the interaction of factor VIII with von Willebrand factor. *J. Biol. Chem.* **266**, 740-746.

40 Gilbert, G. E., Kaufman, R. J., Arena, A. A., Miao, H. and Pipe, S. W. (2002) Four hydrophobic amino acids of the factor VIII C2 domain are constituents of both the membrane-binding and von Willebrand factor-binding motifs. *J. Biol. Chem.* **277**, 6374-6381.

41 Saenko, E. L., Shimag, M., Rajalakshmis, K. J. and Scandella, D. (1994) A Role for the C2 Domain of Factor VIII in Binding to von Willebrand Factor. *J. Biol. Chem.* **269**, 11601-11605.

42 Saenko, E. L. and Scandella, D. (1995) A mechanism for inhibition of factor VIII binding to phospholipid by von Willebrand factor. *J. Biol. Chem.* **270**, 13826-13833.

43 Fay, P. J., Beattie, T., Huggins, C. F. and Regan, L. M. (1994) Factor VIIIa A2 subunit residues 558-565 represent a factor IXa interactive site. *J. Biol. Chem.* **269**, 20522-20527.

44 Ebberink, E. H. T. M., Bouwens, E. A. M., Bloem, E., Boon-Spijker, M., van den Biggelaar, M., Voorberg, J., Meijer, A. B. and Mertens, K. (2017) Factor VIII/V C-domain swaps reveal discrete C-domain roles in factor VIII function and intracellular trafficking. *Haematologica* **102**, 686-694.

45 Lenting, P. J., Donath, M.-J., Mourik, J. A. Van and Mertens, K. (1994) Identification of a binding site for blood coagulation factor IXa on the light chain of human factor VIII. *J. Biol. Chem.* **269**, 7150-7155.

46 Lenting, P. J., van de Loo, J. W., Donath, M. J., van Mourik, J. A. and Mertens, K. (1996) The sequence Glu1811-Lys1818 of human blood coagulation factor VIII comprises a binding site for activated factor IX. *J. Biol. Chem.* **271**, 1935-1940.

47 Bloem, E., Meems, H., van den Biggelaar, M., Mertens, K. and Meijer, A. B. (2013) A3 domain region 1803-1818 contributes to the stability of activated factor VIII and includes a binding site for activated factor IX. *J. Biol. Chem.* **288**, 26105-26111.

48 Vincent Jenkins, P., Freas, J., Schmidt, K. M., Zhou, Q. and Fay, P. J. (2002) Mutations associated with hemophilia A in the 558-565 loop of the factor VIIIa A2 subunit alter the catalytic activity of the factor Xase complex. *Blood* **100**, 501-508.

49 Soeda, T., Nogami, K., Nishiya, K., Takeyama, M., Ogiwara, K., Sakata, Y., Yoshioka, A. and Shima, M. (2009) The Factor VIIIa C2 domain (residues 2228-2240) interacts with the factor IXa Gla domain in the factor Xase complex. *J. Biol. Chem.* **284**, 3379-3388.

50 Lü, J., Pipe, S. W., Miao, H., Jacquemin, M. and Gilbert, G. E. (2011) A membrane-interactive surface on the factor VIII C1 domain cooperates with the C2 domain for cofactor function. *Blood* **117**, 3181-3189.

51 Stoilova-McPhie, S., Villoutreix, B. O., Mertens, K., Kemball-Cook, G. and Holzenburg, A. (2002) 3-Dimensional structure of membrane-bound coagulation factor VIII: Modeling of the factor VIII heterodimer within a 3-dimensional density map derived by electron crystallography. *Blood* **99**, 1215-1223.

52 Shen, B. W., Spiegel, P. C., Chang, C., Huh, J., Lee, J., Kim, J., Kim, Y. and Stoddard, B. L. (2008) The tertiary structure and domain organization of coagulation factor VIII. *Blood* **111**, 1240-1247.

53 Gilbert, G. E. and Arena, A. A. (1996) Activation of the factor VIIIa-factor IXa enzyme complex of blood coagulation by membranes containing phosphatidyl-L-serine. *J. Biol. Chem.* **271**, 11120-11125.

54 Lenting, P. J., Neels, J. G., van den Berg, B. M., Clijsters, P. P., Meijerman, D. W., Pannekoek, H., van Mourik, J. A., Mertens, K. and van Zonneveld, A. J. (1999) The light chain of factor VIII comprises a binding site for low density lipoprotein receptor-related protein. *J. Biol. Chem.* **274**, 23734-23739.

55 Schooten, C. J. Van, Shahbazi, S., Groot, E., Oortwijn, B. D., Berg, H. M. Van Den, Denis, V. and Lenting, P. J. (2008) Macrophages contribute to the cellular uptake of von Willebrand factor and factor VIII in vivo. *Blood* **112**, 1704-1712.

56 Lenting, P. J., Westein, E., Terraube, V., Ribba, A.-S., Huizinga, E. G., Meyer, D., de Groot, P. G. and Denis, C. V. (2004) An Experimental Model to Study the *in Vivo* Survival of von Willebrand Factor. *J. Biol. Chem.* **279**, 12102-12109.

57 Castro-Núñez, L., Dienava-Verdoold, I., Herczenik, E., Mertens, K. and Meijer, A. B. (2012) Shear stress is required for the endocytic uptake of the factor VIII-von Willebrand factor complex by macrophages. *J. Thromb. Haemost.* **10**, 1929-37.

58 Wohner, N., Muczynski, V., Mohamadi, A., Legendre, P., Proulle, V., Aymé, G., Christophe, O. D., Lenting, P. J., Denis, C. V. and Casari, C. (2018) Macrophage scavenger receptor sr-ai contributes to the clearance of von willebrand factor. *Haematologica* **103**, 728-737.

59 O'Sullivan, J. M., Ward, S., Lavin, M. and O'Donnell, J. S. (2018) von Willebrand factor clearance - biological mechanisms and clinical significance. *Br. J. Haematol.* **183**, 185-195.

60 McDonald, V. and Austin, S. K. (2013) Inherited bleeding disorders. *Med. Elsevire* **41**, 231-233.

61 Bhatnagar, N. and Hall, G. W. (2017) Major bleeding disorders: diagnosis, classification, management and recent developments in haemophilia. *Arch. Dis. Child.* **103**, 509-513.

62 Castaman, G. and Matino, D. (2019) Hemophilia A and B: molecular and clinical similarities and differences. *Haematologica* **104**, 1702-1709.

63 Kemball-Cook, G., Tuddenham, E. G. and Wacey, A. I. (1998) The factor VIII Structure and Mutation Resource Site: HAMSTeRS version 4. *Nucleic Acids Res.* **26**, 216-9.

64 Zimmermann, M. A., Oldenburg, J., Müller, C. R. and Rost, S. (2014) Expression studies of mutant factor VIII alleles with premature termination codons with regard to inhibitor formation. *Haemophilia* **20**, 215-221.

65 Kevane, B. and O'Connell, N. (2018) The current and future role of plasma-derived clotting factor concentrate in the treatment of haemophilia A. *Transfus. Apher. Sci.*, *Elsevier* 0-1.

66 Powell, J. S., Josephson, N. C., Quon, D., Ragni, M. V., Cheng, G., Li, E., Jiang, H., Li, L., Dumont, J. A., Goyal, J., et al. (2012) Safety and prolonged activity of recombinant factor VIII Fc fusion protein in hemophilia A patients. *Blood* **119**, 3031-3037.

67 Sadler, J. E., Mannucci, P. M., Mazurier, C., Meyer, D., Nichols, W. L., Nishino, M., Peake, I. R., Rodeghiero, F., Schneppenheim, R., Ruggeri, Z. M., et al. (2006) Update on the pathophysiology and classification of von Willebrand disease: a report of the Subcommittee on von Willebrand Factor. *J. Thromb. Haemost.* **4**, 2103-2114.

68 Casonato, A., Pontara, E., Sartorello, F., Cattini, M. G., Gallinaro, L., Bertomoro, A., Rosato, A., Padrini, R. and Pagnan, A. (2006) Identifying type Vicenza von Willebrand disease. *J. Lab. Clin. Med.* **147**, 96-102.

69 Schneppenheim, R., Lenk, H., Obser, T., Oldenburg, J., Oyen, F., Schneppenheim, S., Schwaab, R., Will, K. and Budde, U. (2004) Recombinant expression of mutations causing von Willebrand disease type Normandy: Characterization of a combined defect of factor VIII binding and multimerization. *Thromb. Haemost.* **92**, 36-41.

70 Thompson, A., Schäfer, J., Kuhn, K., Kienle, S., Schwarz, J., Schmidt, G., Neumann, T. and Hamon, C. (2003) Tandem mass tags: A novel quantification strategy for comparative analysis of complex protein mixtures by MS/MS. *Anal. Chem.* **75**, 1895-1904.

71 Mendoza, V. L. and Vachet, R. W. (2009) Probing Protein Structure by Amino Acid-Specific Covalent Labeling and Mass Spectrometry. *Mass Spectrom. Rev* **28**, 785-815.

72 Marcsisin, S. R. and Engen, J. R. (2010) Hydrogen exchange mass spectrometry: what is it and what can it tell us? *Anal Bioanal Chem* **397**, 967-972.

73 Morgan, C. R. and Engen, J. R. (2009) Investigating solution-phase protein structure and dynamics by hydrogen exchange mass spectrometry. *Curr. Protoc. protein Sci.* **Chapter 17**, Unit 17.6.1-17.

74 van den Biggelaar, M., Madsen, J. J., Faber, J. H., Zuurveld, M. G., van der Zwaan, C., Olsen, O. H., Stennicke, H. R., Mertens, K. and Meijer, A. B. (2015) Factor VIII interacts with the endocytic receptor low-density lipoprotein receptor-related protein 1 via an extended surface comprising “hot-spot” lysine residues. *J. Biol. Chem.* **290**, 16463-16476.

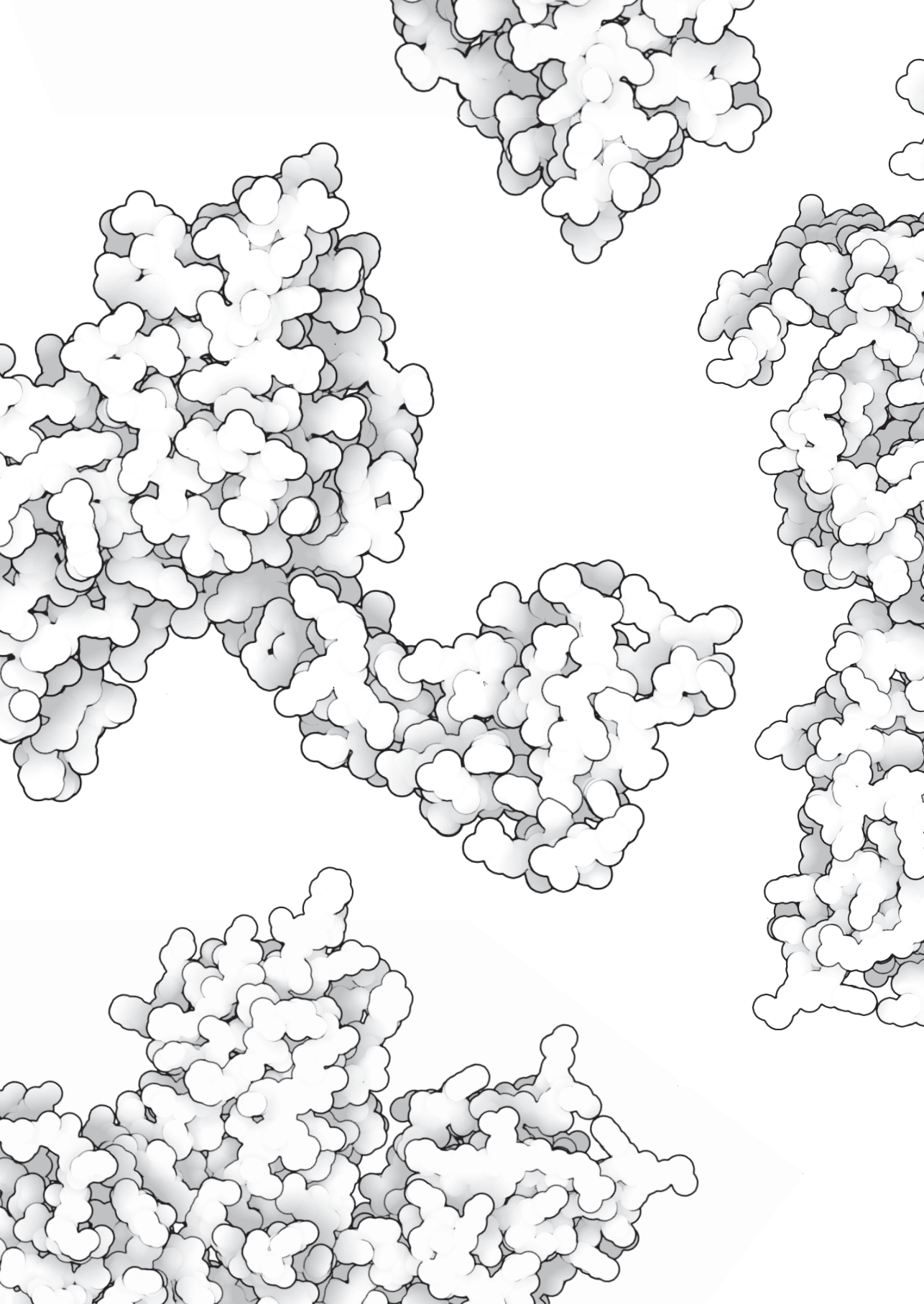

Chapter 2

D' domain region Arg782-Cys799 of Von Willebrand Factor contributes to Factor VIII binding

Małgorzata A. Przeradzka [1], Josse van Galen [1], Eduard H.T.M. Ebberink [1], Arie J. Hoogendijk [1], Carmen van der Zwaan [1], Koen Mertens [1], Maartje van den Biggelaar [1, 2] and Alexander B. Meijer [1,2]

Haematologica. 2020;105(6):1695-1703

[1]Molecular and Cellular Hemostasis, Sanquin Research, 1066 CX Amsterdam, The Netherlands,

[2]Department of Biomolecular Mass Spectrometry and Proteomics, Utrecht Institute for Pharmaceutical Sciences, Utrecht University, Utrecht, The Netherlands

ABSTRACT

In the complex with von Willebrand factor (VWF) factor VIII (FVIII) is protected from rapid clearance from circulation. Although it has been established that the FVIII binding site resides in the N-terminal D'-D3 domains of VWF, detailed information about the amino acid regions that contribute to FVIII binding is still lacking. In the present study, hydrogen-deuterium exchange mass spectrometry was employed to gain insight into the FVIII binding region on VWF. To this end, time-dependent deuterium incorporation was assessed in D'-D3 and the FVIII-D'-D3 complex. Data showed reduced deuterium incorporation in the D' region Arg782-Cys799 in the FVIII-D'-D3 complex compared to D'-D3. This implies that this region interacts with FVIII. Site-directed mutagenesis of the six charged amino acids in Arg782-Cys799 into alanine residues followed by surface plasmon resonance analysis and solid phase binding studies revealed that replacement of Asp796 affected FVIII binding. A marked decrease in FVIII binding was observed for the D'-D3 Glu787Ala variant. The same was observed for D'-D3 variants in which Asp796 and Glu787 were replaced by Asn796 and Gln787. Site-directed mutagenesis of Leu786, which together with Glu787 and Cys789 forms a short helical region in the crystal structure of D'-D3, also had a marked impact on FVIII binding. The combined results show that the amino acid region Arg782-Cys799 is part of a FVIII binding surface. Our study provides new insight into FVIII-VWF complex formation and defects therein that may be associated with bleeding caused by markedly reduced levels of FVIII.

INTRODUCTION

The multimeric glycoprotein von Willebrand factor (VWF) acts as a carrier protein for coagulation factor VIII (FVIII) in the circulation. [1] In the complex with VWF, FVIII is protected from rapid clearance from plasma. [2,3] Multiple amino acid substitutions have been identified in VWF that impair FVIII-VWF complex formation. The associated reduced plasma levels of FVIII can result in the bleeding disorder referred to as von Willebrand disease type 2 Normandy (VWD type 2N). [4] Most of the aberrant mutations in VWF involve substitutions of amino acid residues that have been proposed to affect the structural integrity of VWF. [5,6] These substitutions provide therefore only limited information about the identity of the FVIII binding site on VWF.

Distinct protein domains can be identified in the primary amino acid sequence of VWF. These domains are arranged in the order: D'-D3-A1-A2-A3-D4-B-C1-C2-C2-CK. [7] Zhou *et al.* have refined the domain organization within VWF. For D'-D3, they proposed that these domains can be further divided into TIL'-E'-VWD3-C8_3-TIL3-E3 subdomains. [8] In plasma, VWF circulates as an ensemble of multimeric proteins of varying size. In these multimers, the VWF monomers are head-to-head and tail-to-tail connected *via* disulphide bridges between two D3 domains and two CK domains. [9] FVIII also comprises multiple domains that together constitute a light chain of the domains A3-C1-C2 and a heavy chain comprising the domains A1-A2-B. [10] Because of limited proteolysis of the B domain, FVIII is heterogeneous in size with molecular weights ranging from 160 kDa to 330 kDa. [11,12]

For effective binding to FVIII, VWF requires the presence of a short acidic amino acid region at the start of the FVIII A3 domain. This region, which includes sulphated tyrosine residues, is referred to as the a3 region. [13,14] Next to this VWF binding region, hydrogen-deuterium exchange mass spectrometry (HDX-MS) and previous site-directed mutagenesis studies have identified binding sites for VWF in the C1 and C2 domain of FVIII as well. [15-19] During activation of FVIII, the a3 region is removed from FVIII leading to the dissociation of the FVIII-VWF complex. Additional cleavages by thrombin generates activated FVIII that can perform its role in the coagulation cascade as a cofactor for activated factor IX ultimately leading to fibrin formation. [20]

It has previously been established that the N-terminal D'-D3 domains of VWF comprise the binding site for FVIII. In 1987, limited proteolysis studies of VWF revealed that a VWF fragment comprising the residues 764-1036 harbors the interaction site for FVIII. [21] Based on cryoelectron microscopy (cryo-EM) structures of FVIII in complex with D'-D3, it has later been shown that the main interactive region for FVIII resides in the D' domain. [19] Recently, we have found that the presence of the VWD3 subdomain of the D3 domain is required to optimally support the interaction between D' and FVIII. [22] Using a primary amine-directed chemical foot printing approach combined with mass spectrometry analysis, we have further demonstrated that Lys773 contrib-

utes to FVIII binding. [23] In the present study, we have employed HDX-MS combined with site-directed mutagenesis and protein binding studies to further explore the FVIII binding regions on VWF. The combined results show that the D' domain region Arg782-Cys799 is part of the FVIII binding interface.

METHODS

Materials

Tris-HCl was from Invitrogen (Breda, the Netherlands), NaCl was obtained from Fagron (Rotterdam, the Netherlands) and HEPES was from Serva (Heidelberg, Germany), FreeStyle 293 expression medium was obtained from Gibco (Thermo Fisher Scientific). Tween 20 and D_2O was from Sigma-Aldrich (St Louis, MO, USA). Human serum albumin (HSA) was obatined from the Division of Products at Sanquin (Amsterdam, the Netherlands). All other chemicals were from Merck (Darmstadt, Germany), unless indicated otherwise.

Proteins

Antibody CLB-EL14 (EL14), CLB-Rag20, CLB-CAg12 (CAg12) and HPC4 have been described before. [22,24,25] D'-D3 fragment, FVIII lacking the B domain residues 746-1639 (referred to as FVIII throughout this paper) and VWF were obtained essentially as described before. [26-28] Purified proteins were dialyzed against a buffer with 50 mM HEPES (pH 7.4), 150 mM NaCl, 10 mM $CaCl_2$, 50% (v/v) glycerol and stored at −20°C. Site-directed mutagenesis of the D'-D3 fragment was employed using Quik Change (Agilent Technologies) according to the manufacturer's instructions.

HDX-MS

D'-D3 was pre-incubated in presence or absence of FVIII in 1:1 molar ratio for 5 min at 4°C. Samples were subsequently diluted ten times in deuterated binding buffer (98% D_2O) or standard binding buffer and incubated for 10 sec, 100 sec or 1,000 sec at 24°C. A detailed description is available in the *Online Supplementary Materials and Methods*.

Solid-phase competition assays

Recombinant VWF (1 mg/mL) was immobilized overnight at 4°C in a buffer containing 50mM $NaHCO_3$ pH 9.8 in a 96-wells microtiter plate (Nunc Maxisorp). Increasing concentrations (0.3-900 nM) of D'-D3 and variants with single mutations were pre-incubated with 0.3 nM FVIII in a buffer containing 50 mM Tris, 150 mM NaCl, 2% human serum albumin, 0.1% Tween 20, pH 7.4 for 30 min at 37°C. These mixtures were transferred to the VWF coated plate and incubated for 2 hours at 37°C. Then,

the plate was washed three times with 50 mM Tris (pH 7.4), 150 mM NaCl, 5mM $CaCl_2$, 0.1% Tween 20 after which FVIII bound to VWF was detected with an HRP-labeled monoclonal antibody (CAg12).[26]

Surface plasmon resonance analysis

Surface plasmon resonance (SPR) analysis was carried out using a Biacore T-200 biosensor system (GE Healthcare) as previously described.[22] A monoclonal antibody to FVIII (EL14) was coupled to a CM5 sensor chip (GE Healthcare) to 5,000 response units (RU) density using the amino coupling activation method according to manufacturer's suggestions (GE Healthcare). Subsequently, 3,000 RU of FVIII were immobilized to the chip *via* EL14 antibody. Next, increasing concentrations of D'-D3 fragments were passed over the chip at a flow rate of 30 mL/min in a buffer containing 20 mM HEPES (pH 7.4), 150 mM NaCl, 5 mM $CaCl_2$ and 0.05% Tween 20 at 25°C. An empty channel was utilized to correct for non-specific binding to the dextran matrix.

RESULTS

HDX-MS on the isolated D'-D3 fragment of VWF

To facilitate identification of the FVIII binding residues within the D' domain (TIL'-E' subdomains), we made use of the D'-D3 monomer in which the cysteine residues involved in dimerization of the D3 domains (VWD3-C8_3-TIL3-E3 subdomains) were replaced by serine residues.[29] The D'-D3 fragment was transferred from H_2O to D_2O-containing buffer to assess time-dependent deuterium incorporation into the protein backbone. 178 peptides were identified covering 92% of the D'-D3 sequence (Figure 1A and *Online Supplementary Table S1*). For each peptide, we plotted the percentage of deuterium incorporation of the identified peptides at three different time points (Figure 1B). The overall result showed that almost all peptides from the N-terminal TIL' subdomain of D'-D3 exhibit limited to no change in deuterium incorporation at these time points. Only the peptide that includes the N-terminus of the TIL' subdomain showed increased deuterium incorporation. Apart from several peptides in the C8_3 subdomain of the D3 domain, most of the peptides in the other subdomains showed incorporation of deuterium in time. Peptides with the most marked change in deuterium incorporation correspond to unstructured regions in the recently published crystal structure of D'-D3.[30] This finding confirms that amino acid backbone hydrogens in unstructured regions exhibit an enhanced rate of hydrogen-deuterium exchange compared to structured regions. It further implies that these regions are unstructured in solution as can be predicted by the crystal structure.

Figure 1. HDX-MS analysis of the D'-D3 fragment. D'-D3 was incubated for 10s, 100s and 1000s in a deuterium buffer consisting of 20 mM HEPES (pH 7.4), 150 mM NaCl and 5 mM $CaCl_2$. D'-D3 was processed for HDX-MS analysis as described in methods. Panel A shows the identified peptides as blue lines underneath the primary sequence of D'-D3. Panel B shows the percentage of deuterium incorporation for the individual identified peptides for the different incubation times with deuterium buffer. The sequence of the peptide's numbers, shown on the x-axis, is displayed in Supplemental Table SI.

D' region Arg782-Cys799 shows reduced deuterium incorporation in the presence of FVIII. HDX-MS was employed on the FVIII-D'-D3 complex

The complex was transferred to D_2O-containing buffer and the incorporation of deuterium was assessed at three different time points. The obtained results were compared to the time-dependent deuterium incorporation in D'-D3 in the absence of FVIII. Most peptides originating from the FVIII-D'-D3 complex did not show a change in deuterium uptake compared to isolated D'-D3 (Figure 2 and *Online Supplementary Figure S1*). Several overlapping peptides in the TIL' subdomain of D', however, did show a reduced deuterium incorporation in the complex. The peptide region that is shared by the overlapping peptides includes the amino acids Arg782-Cys799 (Figure 2B-C). The HDX-MS results suggest that the local hydrogen bonding network is altered in this VWF region upon FVIII binding implying that this region contributes to FVIII binding.

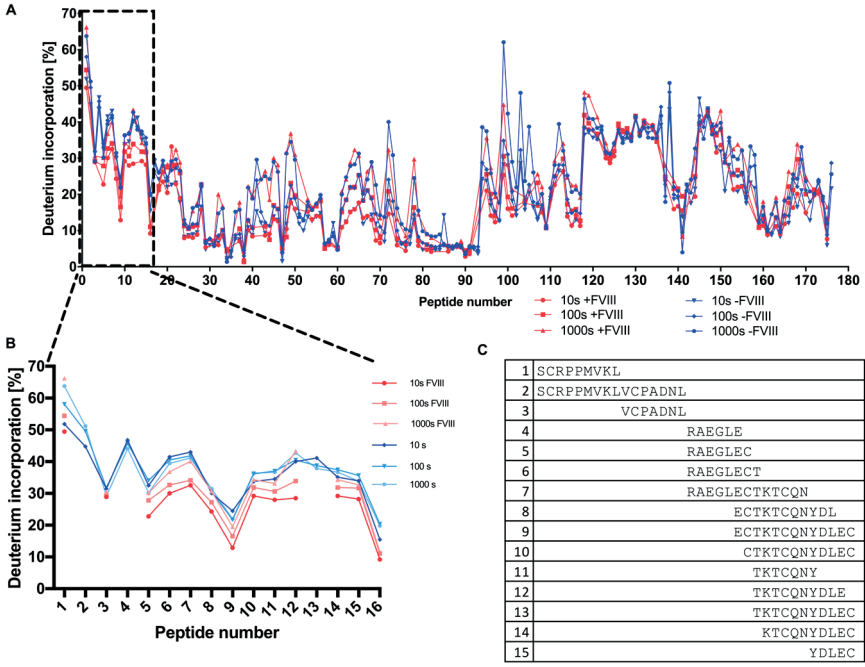

1	SCRPPMVKL	766-774
2	SCRPPMVKLVCPADNL	766-781
3	VCPADNL	775-781
4	RAEGLE	782-787
5	RAEGLEC	782-788
6	RAEGLECT	782-799
7	RAEGLECTKTCQN	782-794
8	ECTKTCQNYDL	787-797
9	ECTKTCQNYDLEC	787-799
10	CTKTCQNYDLEC	788-799
11	TKTCQNY	789-795
12	TKTCQNYDLE	789-798
13	TKTCQNYDLEC	789-799
14	KTCQNYDLEC	790-799
15	YDLEC	795-799

Figure 2. HDX-MS analysis of the D'-D3 - FVIII complex. The D'-D3 was incubated for 10s, 100s and 1000s in a deuterium buffer consisting of 20 mM HEPES (pH 7.4), 150 mM NaCl and 5 mM $CaCl_2$ in presence and absence of FVIII. The proteins were processed for HDX-MS analysis as described in methods. Panel A shows the percentage of deuterium incorporation of the identified peptides of D'-D3 at the indicated incubation times in deuterium buffer in presence and absence of FVIII. The sequence of the peptide numbers, shown on the x-axis, is displayed in Supplemental Table SI. Panel B shows the percentage of time-dependent deuterium incorporation for the 15 identified peptides that cover part of the TIL' subdomain of D'. The sequence of the peptide numbers, shown on the x-axis, in displayed in panel C.

SPR analysis reveals that charged residues in D' region Arg782-Cys799 contribute to FVIII binding

Site-directed mutagenesis of the D'-D3 fragment was employed to verify the contribution of the region Arg782-Cys799 to FVIII binding. As electrostatic interactions have been proposed to mediate FVIII-VWF complex assembly, [31,32] the charged amino acids in this region were replaced by alanine residues resulting in six new D'-D3 variants *i.e.* Arg782Ala, Glu784Ala, Glu787Ala, Lys790Ala, Asp796Ala and Glu798Ala. SPR analysis was performed to assess their FVIII binding efficiency. To this end, increasing concentrations of the D'-D3 variants were passed over FVIII that was immobilized *via* antibody EL14 to the surface of a CM5 sensor chip (Figure 3A-G). The Arg782Ala, Glu784Ala and Glu798Ala variants revealed association and dissociation binding responses that closely resembled those of the wild-type (WT) D'-D3. The Lys790Ala and Aps796Ala variants showed decreased binding responses compared to WT D'-D3. Almost no binding was observed for the Glu787Ala variant. The association and dissociation responses revealed complex binding kinetics comprising at least two components. To estimate the binding affinities, we plotted the maximum binding response as a function of the D'-D3 variant concentration (Figure 3H). The concentration at which the half-maximum binding response is reached, represents an estimation of the average binding affinities (K_D) of the involved components. Compared to the K_D obtained for the WT D'-D3 (~50 nM), results showed a more than four-fold increase in K_D for D'-D3 Asp796Ala (~190 nM) and a five-fold increase for D'-D3 Lys790Ala (~240 nM). These findings together show that charged amino acid residues in the region Arg782-Cys799 contribute to FVIII binding. A glutamic acid at position 787 appears most critical for effective interaction between FVIII and D'-D3.

A solid phase competition assay reveals that charged residues contribute to FVIII binding. The efficiency by which the D'-D3 variants were able to compete with VWF for FVIII binding was assessed using a competitive binding assay as also employed in previous studies. [22,23] FVIII was incubated with immobilized VWF in the presence of increasing concentrations of the D'-D3 variants. Residual FVIII binding to immobilized VWF was assessed using an antibody against FVIII that does not interfere with the complex formation between FVIII and VWF (Figure 4). Results showed that about 50 nM of WT D'-D3 was required to reduce FVIII binding to immobilized VWF by 50%. For the Arg782Ala, Glu784Ala, and Glu798Ala variants of D'-D3 about 100 nM was required to reach the same effect. A markedly reduced competition efficiency was observed for the Asp796Ala variant as more than 800 nM was required to reduce the binding to 50%. Almost no competition was observed for D'-D3 Glu787Ala. The data further reveal a biphasic competition curve for the Lys790Ala variant. This implies that D'-D3 Lys790Ala may exist in two conformations that differentially interfere with complex formation between FVIII and VWF. We therefore cannot make any reliable

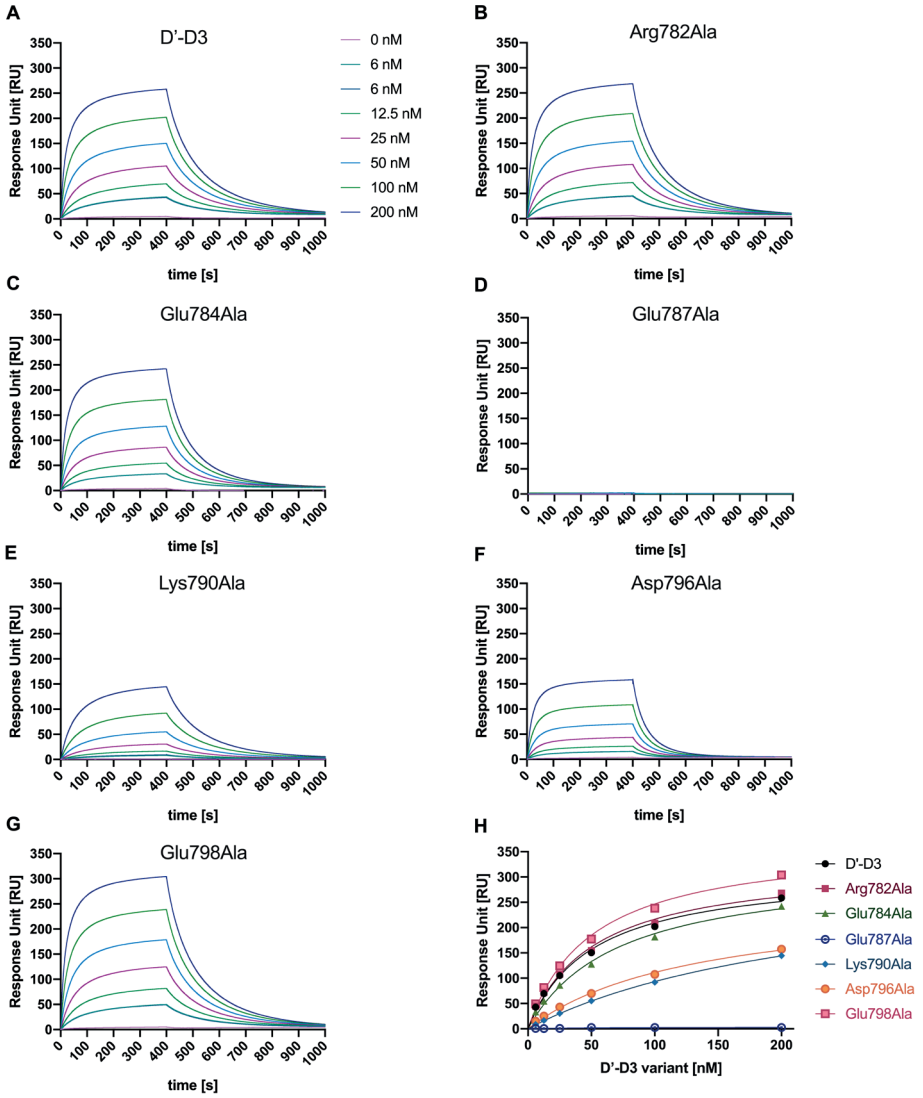

Figure 3. SPR analysis of D'-D3 variants in interaction with FVIII. (panel A-G) Multiple concentrations (0-200 nM) of the indicated D'-D3 variants were passed over FVIII that was immobilized via antibody EL14 to the surface of a CM5 sensor chip. The binding response is represented in Response Units and was assessed in 20 mM HEPES (pH 7.4), 150 mM NaCl, 5 mM $CaCl_2$, 0.05% (v/v) Tween 20 at a flow rate of 30 µl/min at 25°C. Panel H show the maximum binding response in Response Units of the D'-D3 variants at a function of the employed concentration.

conclusions about the putative role of Lys790 for FVIII binding. Based on the results, we also constructed two new D'-D3 variants *i.e.* Glu787Gln and Asp796Asn and assessed their FVIII binding efficiency using SPR analysis. Results showed that changing the charged amino acids with their neutral counterpart also affected FVIII binding (*Online*

Supplementary Figure S2). Changing Glu787 for a Gln in full-length VWF also revealed a major impact on FVIII using a solid phase binding assay (*Online Supplementary Figure S3*). The data together confirm the observation that amino acid residues in the region Arg782-Cys799 are involved in FVIII binding. In particular, the glutamic acid residue at position 787 seems critical for the interaction between FVIII and D'-D3.

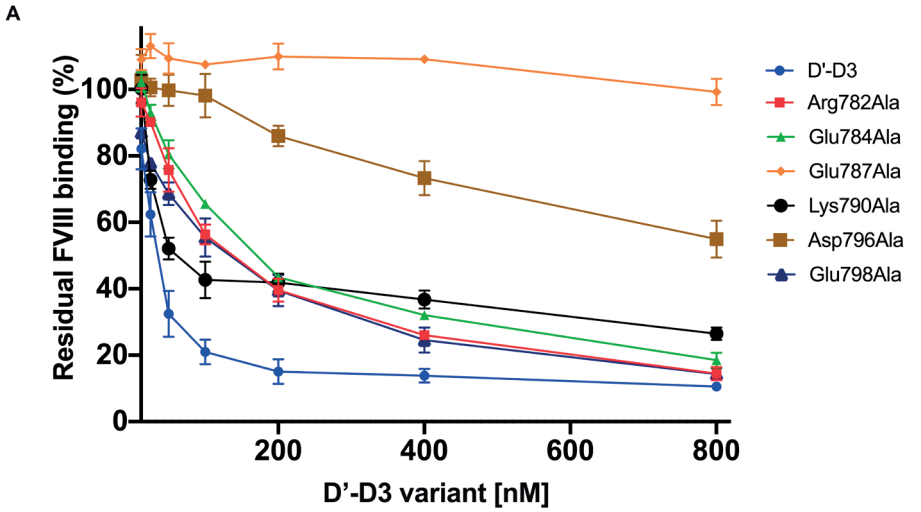

Figure 4. D'-D3 variants in competition with immobilized VWF for binding FVIII. FVIII was incubated with increasing concentrations of the indicated D'-D3 variants in a buffer comprising 50 mM Tris (pH 7.4), 150 mM NaCl, 5mM $CaCl_2$, 2% human serum albumin and 0.1% Tween 20 at 37 °C. The protein mixtures were next incubated with immobilized VWF in the same buffer. Residual FVIII binding to immobilized VWF was assessed employing HRP-conjugated CAg12 antibody as described in methods. Data represents mean ± SD of three independent experiments.

A leucine at position 786 is important for effective interaction with FVIII

Analysis of the crystal structure of D'-D3 shows that Glu787 is part of a short helical region that also includes Leu786 and Cys788 (Figure 5A).[30] We speculate Leu786 and Cys788 are critical to maintain the structural integrity of this helix, and therefore the spatial position of Glu787 in D'-D3. We therefore decided to destabilize this helical structure by replacing Leu786 for an alanine residue and study the effect thereof on FVIII binding. SPR analysis showed a markedly reduced FVIII binding response of the Leu786Ala variant with an estimated K_D of ~500 nM (Figure 5C). The competitive binding assay revealed that about 400 nM of the variant was required to reduce FVIII binding to VWF by 50% (Figure 5B). These findings together demonstrate an impaired FVIII binding efficiency of D'-D3 Leu786Ala. We propose therefore that the stability of the helical region may indeed be of importance for FVIII binding.

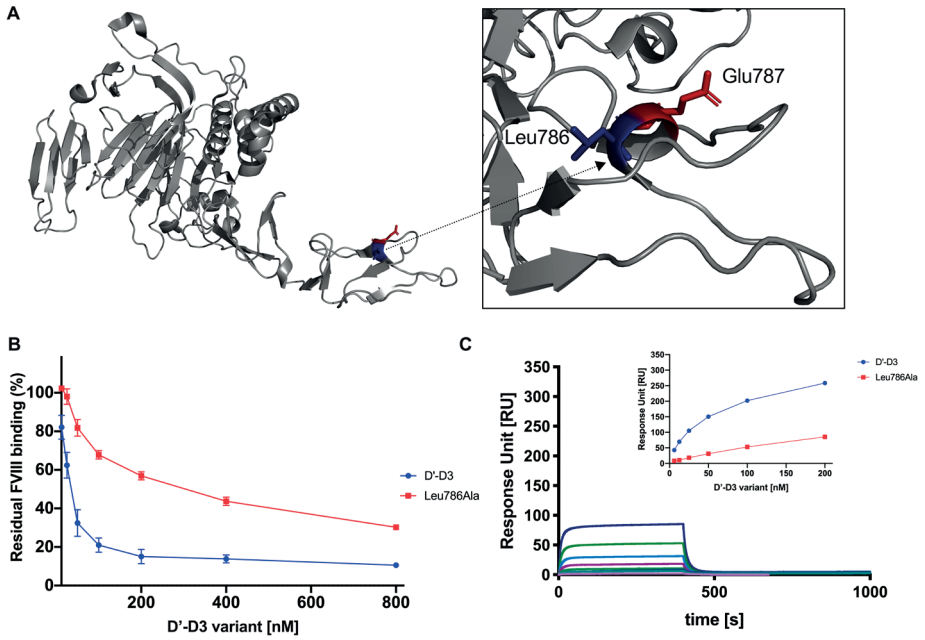

Figure 5. The FVIII binding efficiency of D'-D3 Leu786Ala. (Panel A) Part of the crystal structure of D'-D3 (PDB entry: 6n29) [30] with a zoom-in of the helical region comprising the residues 786-Leu-Glu-Cys-789 (Panel B) Multiple concentrations of D'-D3 Leu786Ala were passed over FVIII that was immobilized via antibody EL14 to the surface of a CM5 sensor chip. The binding response is indicated as Response Units and was assessed in 20 mM HEPES (pH 7.4), 150 mM NaCl, 5 mM $CaCl_2$, 0.05% (v/v) Tween 20 at a flow rate of 30 µl/min at 25ºC. (Panel C) FVIII was pre-incubated with increasing concentrations of D'-D3 and D'-D3 Leu786Ala in a buffer comprising 50 mM Tris (pH 7.4), 150 mM NaCl, 5mM $CaCl_2$, 2% human serum albumin and 0.1% Tween 20 at 37 ˚C. The protein mixtures were next incubated with immobilized VWF in the same buffer. Residual FVIII binding to immobilized VWF was assessed employing HRP-conjugated CAg12 antibody as described in methods. Data represents mean ± SD of three independent experiments.

DISCUSSION

The particularly high complexity of the molecular architecture of VWF has always posed a major challenge for the identification of the FVIII interactive regions within VWF. We therefore decided to utilize a short fragment of VWF that includes the FVIII binding site, *i.e.* D'-D3. [2] Previously, we have employed a primary amine-directed chemical foot printing approach on the FVIII-VWF complex and established that Lys773 contributes to FVIII binding. [23] This approach provided only information about the putative role of the side-chains of lysine amino acid residues for FVIII-VWF complex formation. HDX-MS as utilized in this study has the potential to provide information about the putative role of all amino acids in D'-D3. [33]

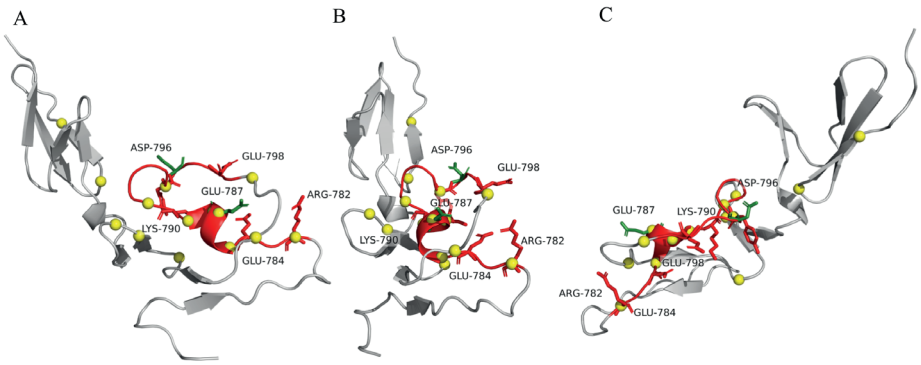

Figure 6. Amino acid region Arg782-Cys799 and sites involved in VWF type 2N indicated in the crystal structure of TIL' subdomain. Shown is the TIL' subdomain of the crystal structure of D'-D3 (PDB entry: 6n29) in a ribbon representation. Panel A, B and C present the same structure from different angels. Region Arg782-Cys799 is displayed in red. The yellow spheres indicated residues that have been mutated in VWD type 2N. [37]

With HDX-MS, the replacement of amide hydrogen atoms of the protein backbone by deuterium atoms can be assessed upon the transfer of a protein complex from H_2O to D_2O. Sites where proteins interact can show a reduced time-dependent deuterium incorporation usually because of local changes in the hydrogen bonding network of the protein backbone. This methodology has proven to be particularly powerful in the identification of protein interaction sites. [34] Applying HDX-MS on the FVIII-D'-D3 complex showed reduced deuterium incorporation in amino acid region Arg782-Cys799 in the presence of FVIII (Figure 2). This result strongly suggest that it is involved in the interaction with FVIII. This region is also particularly rich in amino acid residues that are mutated in VWD type 2N (Figure 6). This corroborates the functional importance of this region.

The role of Arg782-Cys799 for FVIII binding was further confirmed by replacing the charged amino acid residues by alanine residues. Especially replacement of Glu787 proved detrimental for the interaction between D'-D3 and FVIII (Figures 3-4). A major impact on FVIII binding was also observed for the Glu787Gln variant of D'-D3 and full-length VWF (*Online Supplementary Figure S2-3*). Patients with VWF type 2N have further been identified with a Glu787Lys variant of VWF. [35] These observations together demonstrate the importance of a glutamic acid at position 787. We cannot exclude that Glu787 may be critical for maintaining the local conformation of the D' domain. The crystal structure, however, reveals that Glu787 is exposed to the solvent and is not part of the internal protein core (Figure 5A). [30] We may therefore have identified one of the critical amino acids that directly interacts with FVIII rather than being important for stabilizing the local conformation. Th replacement of Leu786 by an alanine, most

likely, alters the conformation of the short helical region 786-Leu-Glu-Cys-789 thereby repositioning Glu787 (Figure 5A). This can explain, in our view, the altered FVIII binding efficiency of the Leu786Ala variant (Figure 5B-C). HDX-MS did not reveal reduced deuterium incorporation in peptides that include Lys773. This residue is part of a beta-sheet in which the amino backbone hydrogens tightly interact. Apparently, this secondary structure element does not change its conformation upon FVIII binding, which is required to detect altered deuterium incorporation.

Based on cryo-EM studies, Yee *et al*. proposed a model for the FVIII-D'-D3 complex. In this model the D' domain is in contact with the FVIII C1 domain. [18] The contribution of the C1 domain to VWF binding has also been demonstrated with HDX -MS studies on FVIII in the presence and of the D'-D3. [19] Because of the relatively low resolution of the structure, it was not possible to predict the orientation of the D' domain on FVIII. Results of this study now provide evidence that the region comprising Arg782-Lys790 may be oriented towards the C1 domain of FVIII. This sequence is part of a flat surface on the TIL' subdomain that may optimally interact with the C1 domain (*Online Supplementary Figure S4*).

How the sulphated acid a3 region at the start of the FVIII A3 domain interacts with D'-D3 remains, however, unclear from both the cryo-EM study and this study. Removal of this region upon activation of FVIII is the trigger for FVIII-VWF complex dissociation. [12] It has further been shown that replacement of the sulphated tyrosine residue 1680 with a phenylalanine leads to a VWF binding defect. [14] Recently, a well-designed nuclear magnetic resonance study was employed to assess the putative complex formation between the isolated a3 region and the isolated D' domain. Main changes in chemical shift were identified outside the region that was identified in our study, *i.e*. residues Val772, Asn819, Cys821 and Val 822, suggesting that the a3 region may interact with these residues. The isolated a3 binds the D' domain with a markedly reduced affinity compared to intact FVIII. [36] We have also found that the VWD3 subdomain of the D3 domain is required to support D' binding to FVIII as well. [22] These notions show that the mechanism by which FVIII and VWF interact and the role of the a3 region therein remains a topic for further investigation.

FUNDING

This study has been funded by Product and Process Development, Sanquin, the Netherlands (PPOP-13-002) and by the Landsteiner foundation of blood research (LSBR 1882).

REFERENCES

1. Brinkhous KM, Sanderg H, Garris JB, et al. Purified human factor VIII procoagulant protein : Comparative hemostatic response after infusions into hemophilic and von Willebrand disease dogs. Proc. Natl. Acad. Sci. U. S. A. 1985;82(24):8752-8756.
2. Yee A, Gildersleeve RD, Gu S, et al. A von Willebrand factor fragment containing the D'-D3 domains is sufficient to stabilize coagulation factor VIII in mice. Blood. 2014;124(3):445-452.
3. Pipe SW, Montgomery RR, Pratt KP, Lenting PJ, Lillicrap D. Life in the shadow of a dominant partner: the FVIII-VWF association and its clinical implications for hemophilia A. Blood. 2016;128(16):2007-2016.
4. Mazurier C, Goudemand J, Hilbert L, et al. Type 2N von Willebrand disease: clinical manifestations, pathophysiology, laboratory diagnosis and molecular biology. Best Pract. Res. Clin. Haematol. 2001;14(2):337-47.
5. Jorieux S, Fressinaud E, Goudemand J, et al. Conformational changes in the D' domain of von Willebrand factor induced by CYS 25 and CYS 95 mutations lead to factor VIII binding defect and multimeric impairment. Blood. 2000;95(10):3139-45.
6. Jorieux S, Gaucher C, Goudemand J, Mazurier C. A Novel Mutation in the D3 Domain of von Willebrand Factor Markedly Decreases Its Ability to Bind Factor VIII and Affects Its Multimerization. Blood. 1998;92:4663-4670.
7. Springer TA. Biology and physics of von Willebrand factor concatamers. J. Thromb. Haemost. 2011;9 Suppl 1(1):130-43.
8. Zhou YF, Eng ET, Zhu J, et al. Sequence and structure relationships within von Willebrand factor. Blood. 2012;120(2):449-458.
9. Marti T, Rösselet SJ, Titani K, Walsh KA. Identification of disulfide-bridged substructures within human von Willebrand factor. Biochemistry. 1987;26(25):8099-109.
10. Fay P. Factor VIII Structure and Function. Int. J. Hematol. 2006;83(2):103-108.
11. Stoilova-McPhie S, Villoutreix BO, Mertens K, Kemball-Cook G, Holzenburg A. 3-Dimensional structure of membrane-bound coagulation factor VIII: Modeling of the factor VIII heterodimer within a 3-dimensional density map derived by electron crystallography. Blood. 2002;99(4):1215-1223.
12. Lenting PJ, van Mourik JA, Mertens K. The life cycle of coagulation factor VIII in view of its structure and function. Blood. 1997;92(11):3983-3996.
13. Saenko EL, Scandella D. The acidic region of the factor VIII light chain and the C2 domain together form the high affinity binding site for von willebrand factor. J. Biol. Chem. 1997;272(29):18007-14.
14. Leyte A, van Schijndel HB, Niehrs C, et al. Sulfation of Tyr 1680 of human blood coagulation factor VIII is essential for the interaction of factor Viii with von Willebrand factor. J. Biol. Chem. 1991;266(2):740-746.
15. Hamer R, Koedam J, Besser-visser N, et al. Factor VIII binds to von Willebrand factor via its 80,000 light chain. Eur. J. Biochem. 1987;166(1):37-43.
16. Leyte A, Verbeet MP, Brodniewicz-Proba T, Van Mourik JA, Mertens K. The interaction between human blood-coagulation factor VIII and von Willebrand factor. Characterization of a high-affinity binding site on factor VIII. Biochem. J. 1989;257(3):679-83.
17. Lollar P, Hill-Eubanks DC, Parker CG. Association of the factor VIII light chain with von Willebrand factor. J. Biol. Chem. 1988;263(21):10451-5.

18. Yee A, Oleskie AN, Dosey AM, et al. Visualization of an N-terminal fragment of von Willebrand factor in complex with factor VIII. Blood. 2015;126(8):939-943.
19. Chiu P-L, Bou-Assaf GM, Chhabra ES, et al. Mapping the interaction between factor VIII and von Willebrand factor by electron microscopy and mass spectrometry. Blood. 2015;126(8):935-8.
20. Fay PJ. Activation of factor VIII and mechanisms of cofactor action. Blood Rev. 2004;18(1):1-15.
21. Foster PA, Fulcher CA, Marti T, Titani K, Zimmerman TS. A major factor VIII binding domain resides within the amino-terminal 272 amino acid residues of von Willebrand factor. J. Biol. Chem. 1987;262(18):8443-8446.
22. Przeradzka MA, Meems H, van der Zwaan C, et al. The D' domain of von Willebrand factor requires the presence of the D3 domain for optimal factor VIII binding. Biochem. J. 2018;475(17):2819-2830.
23. Castro-Núñez L, Bloem E, Boon-Spijker MG, et al. Distinct roles of Ser-764 and Lys-773 at the N terminus of von Willebrand factor in complex assembly with coagulation factor VIII. J. Biol. Chem. 2013;288(1):393-400.
24. van den Biggelaar M, Meijer AB, Voorberg J, Mertens K. Intracellular cotrafficking of factor VIII and von Willebrand factor type 2N variants to storage organelles. Blood. 2009;113(13):3102-3109.
25. Stel, H. V., Sakariassen, K. S. Scholte, B.J., Veerman, E. C. I., van der Kwast, Th. H., De Groot, Ph. G. SJJ and VMJA. Characterization of 25 Monoclonal Antibodies to FVIII-von Willebrand Factor: Relatioship Between Ristocetin-Induced Platelet Aggregation and Platelet Adherence to Subendothelium. Blood. 1984;63(6):1408-1415.
26. Meems H, Van Den Biggelaar M, Rondaij M, et al. C1 domain residues Lys 2092 and Phe 2093 are of major importance for the endocytic uptake of coagulation factor VIII. Int. J. Biochem. Cell Biol. 2011;43(8):1114-1121.
27. Bloem E, Meems H, van den Biggelaar M, et al. Mass spectrometry-assisted study reveals that lysine residues 1967 and 1968 have opposite contribution to stability of activated factor VIII. J. Biol. Chem. 2012;287(8):5775-5783.
28. van den Biggelaar M, Bouwens EAM, Voorberg J, Mertens K. Storage of factor VIII variants with impaired von Willebrand factor binding in Weibel-Palade bodies in endothelial cells. PLoS One. 2011;6(8):e24163.
29. Purvis AR, Gross J, Dang LT, et al. Two Cys residues essential for von Willebrand factor multimer assembly in the Golgi. Proc. Natl. Acad. Sci. U. S. A. 2007;104(40):15647-15652.
30. Dong X, Leksa NC, Chhabra ES, et al. The von Willebrand factor D'D3 assembly and structural principles for factor VIII binding and concatemer biogenesis. Blood. 2019;133(14):1523-1533.
31. Dimitrov JD, Christophe OD, Kang J, et al. Thermodynamic analysis of the interaction of factor VIII with von Willebrand factor. Biochemistry. 2012;51(20):4108-4116.
32. Owen WG, Wagner RH. Antihemophilic factor: separation of an active fragment following dissociation by salts or detergents. Thromb. Diath. Haemorrh. 1972;27(3):502-515.
33. Marcsisin SR, Engen JR. Hydrogen exchange mass spectrometry: what is it and what can it tell us? Anal Bioanal Chem. 2010;397(3):967-972.
34. Morgan CR, Engen JR. Investigating solution-phase protein structure and dynamics by hydrogen exchange mass spectrometry. Curr. Protoc. protein Sci. 2009;Chapter 17(17):Unit 17.6.1-17.

35. Schneppenheim R, Budde U, Drewke E, et al. Results of a screening for von Willebrand disease type 2N in patients with suspected haemophilia A or von Willebrand disease type 1. Thromb. Haemost. 1996;76(4):598-602.
36. Dagil L, Troelsen KS, Bolt G, et al. Interaction Between the a3 Region of Factor VIII and the TIL'E' Domains of the von Willebrand Factor. Biophys. J. 2019;3:1-11.
37. de Jong A, Eikenboom J. Von Willebrand disease mutation spectrum and associated mutation mechanisms. Thromb. Res. 2017;159(July):65-75.

SUPPLEMENTARY SECTION

Methods:

Hydrogen- Deuterium Exchange Mass Spectrometry

4.5 µM D'-D3 was pre-incubated in presence or absence of FVIII in 1:1 molar ratio for 5 min at 4˚C in binding buffer (20 mM HEPES, 150 mM NaCl and 10 mM $CaCl_2$). Samples were subsequently placed in a LEAP PAL pipetting robot (LEAP Technologies, Morrisville, NC, USA). Samples were diluted 10 times in deuterated binding buffer (98% D_2O) (Sigma-Aldrich, St Louis, USA) or standard binding buffer and incubated for 10 sec, 100 sec or 1000 sec at 24 ˚C. Deuterium exchange was quenched by mixing the sample 1:1 with quenching solution (1 g TCEP dissolved in 2 ml 2M Urea, 1M NaOH) for 5 min at 4 ˚C. The sample was digested by passing it over a Poroszyme Immobilized Pepsin Cartridge (Thermo Scientific) with an isocratic flow of 5% acetonitrile, 0.1% formic acid for 5 minutes at 4 ˚C. After collection on a trap (Acclaim Guard Column. 120, C18, 5 µm, 2.0x10 mm Thermofisher), the peptides were washed for 30 sec at 4 ˚C. Subsequently, peptides were eluted and passed over an analytic C18 column (Hypersil Gold C18, Thermo) using a gradient from 4-64% acetonitrile at 50 µl/min at 4 ˚C. Peptides were injected online into an LTQ Orbitrap-XL (Thermo Scientific) operating in positive mode. In order to identify peptides and their retention times, peptides were fragmented by collision induced dissociation. The resulting data was analysed using PEAKS software (PEAKS 7.0, Bioinformatics Solutions Inc.). Deuterium uptake of the samples was calculated using HDExaminer 2.2.0 (Sierra Analytics). Three independent experiments were performed to collect to the required data. In the figures, data are presented as percent of deuterium update calculated respectively to peptide size and maximal amount of deuterium incorporation. The results were visualised on a 3D model using PyMol (Schrödinger, Cambridge, MA, USA).

Immunosorbent assay

The anti-VWF monoclonal antibody CLB-RAg20 (2.5 µg/ml) was immobilized overnight at 4˚C in a buffer containing 50 mM $NaHCO_3$ pH 9.8 in a 96-wells microtiter plate (Nunc Maxisorp). The plate was washed 3 times with 50 mM Tris (pH 7.4), 150 mM NaCl, 5 mM $CaCl_2$, 0.1% Tween 20. Then VWF and VWF-Glu787Gln (0.25 nM) were added in a buffer containing 50 mM Tris pH 7.4, 150 mM NaCl, 5 mM $CaCl_2$, 1% bovine serum albumin, 0.1% Tween 20 to anti-VWF antibody coated plate and incubated for 2h at 37 ˚C. The unbound VWF was washed with 50 mM Tris (pH 7.4), 150 mM NaCl, 5 mM $CaCl_2$, 0.1% Tween 20. Next, increasing concentrations of FVIII (0,01875-1,2 nM) were added to the plate and incubated for 45 min at 37 ˚C. The bound FVIII was detected with an HRP-labelled monoclonal antibody (CAg 12) [1] after another 45 min of incubation 37 ˚C.

REFERENCES

1. Meems H, Van Den Biggelaar M, Rondaij M, et al. C1 domain residues Lys 2092 and Phe 2093 are of major importance for the endocytic uptake of coagulation factor VIII. *Int. J. Biochem. Cell Biol.* 2011;43(8):1114-1121.

Supplementary Figures and Table are available in the online version of the manuscript and upon request (http://www.haematologica.org/content/haematol/suppl/2020/06/01/haematol.2019.221994.DC1/2019.221994.PRZERADZKA_SUPPL.pdf)

Supplemental Table SI. Primary sequence and peptide numbers of the peptides identified using HDXMS.

SUPPLEMENTARY FIGURES

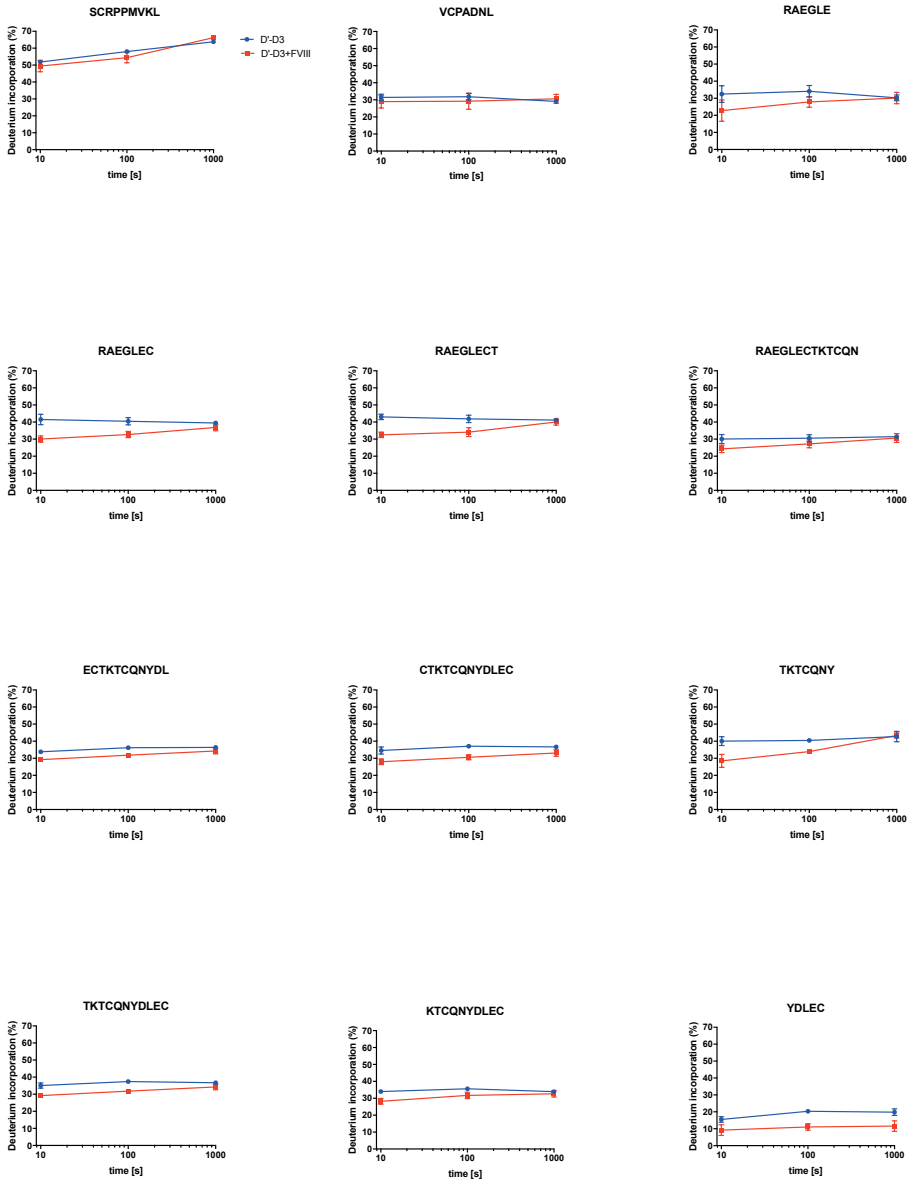

Supplemental Figure S1. HDX-MS analysis of D'-D3 in presence and absence of FVIII. (Other panels are available in the online version of the manuscript). D'-D3 was incubated for 10s, 100s and 1000s in a deuterium buffer consisting of 20 mM HEPES (pH 7.4), 150 mM NaCl and 5 mM $CaCl_2$ in presence or absence of FVIII. The proteins were processed for HDX-MS analysis as described in methods. Shown is the percentage of deuterium incorporation of the indicated peptides as a function of time. Data represents mean ± SD of three independent experiments.

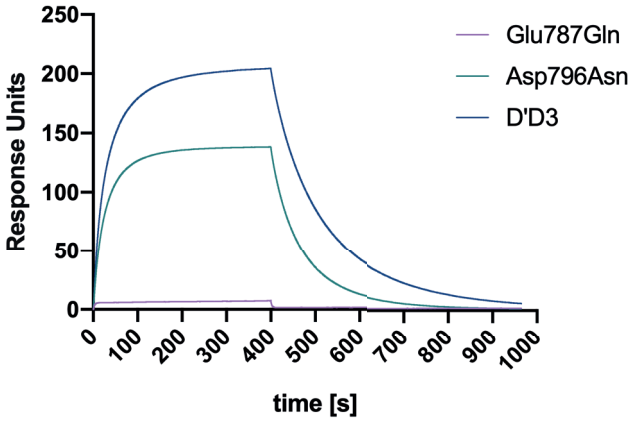

Supplemental Figure S2. SPR analysis of D'-D3 variants Glu787Gln and Asp796Asn in interaction with FVIII. 200 nM of the D'-D3 variants were passed over FVIII that was immobilized via antibody EL14 to the surface of a CM5 sensor chip as described in the methods section of the manuscript. The binding response is represented in Response Units and was assessed in 20 mM HEPES (pH 7.4), 150 mM NaCl, 5 mM $CaCl_2$, 0.05% (v/v) Tween 20 at a flow rate of 30 µl/min at 25°C.

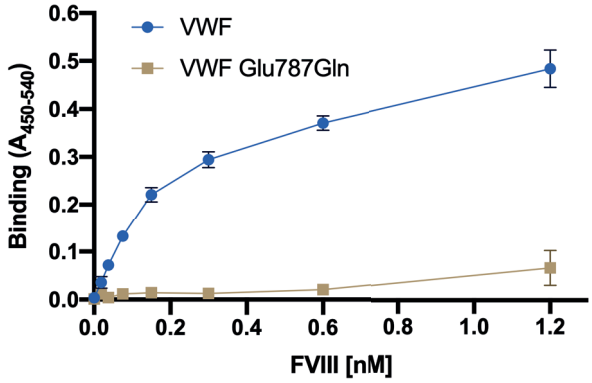

Supplemental Figure S3. Changing Glu787 for Gln in full length VWF affects FVIII binding Increasing concentrations of FVIII were added to WT-VWF or VWF Glu787Gln that was immobilized via antibody Rag-20 in a buffer comprising of 50 mM Tris pH 7.4, 150 mM NaCl, 5 mM $CaCl_2$, 1% bovine serum albumin, 0.1% Tween 20. FVIII binding to immobilized VWF was assessed employing HRP-conjugated CAg12. The binding curves were corrected for the binding response that was measured in the absence of VWF. Data represents mean ± SD of three independent experiments.

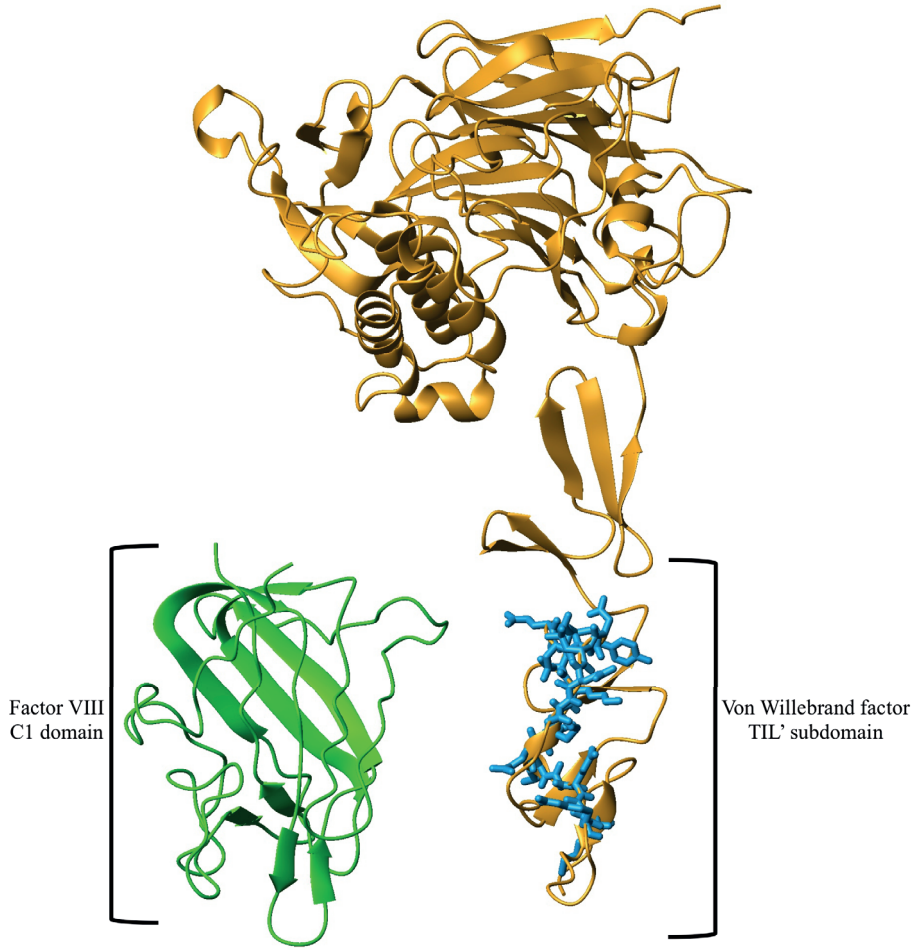

Supplemental Figure S4. Crystal structure of D'-D3 in a ribbon representative in yellow. Residues Arg782-Cys799 and Lys773 are shown in blue represented by sticks. The C1 domain of FVIII is shown in a ribbon presentation in green.

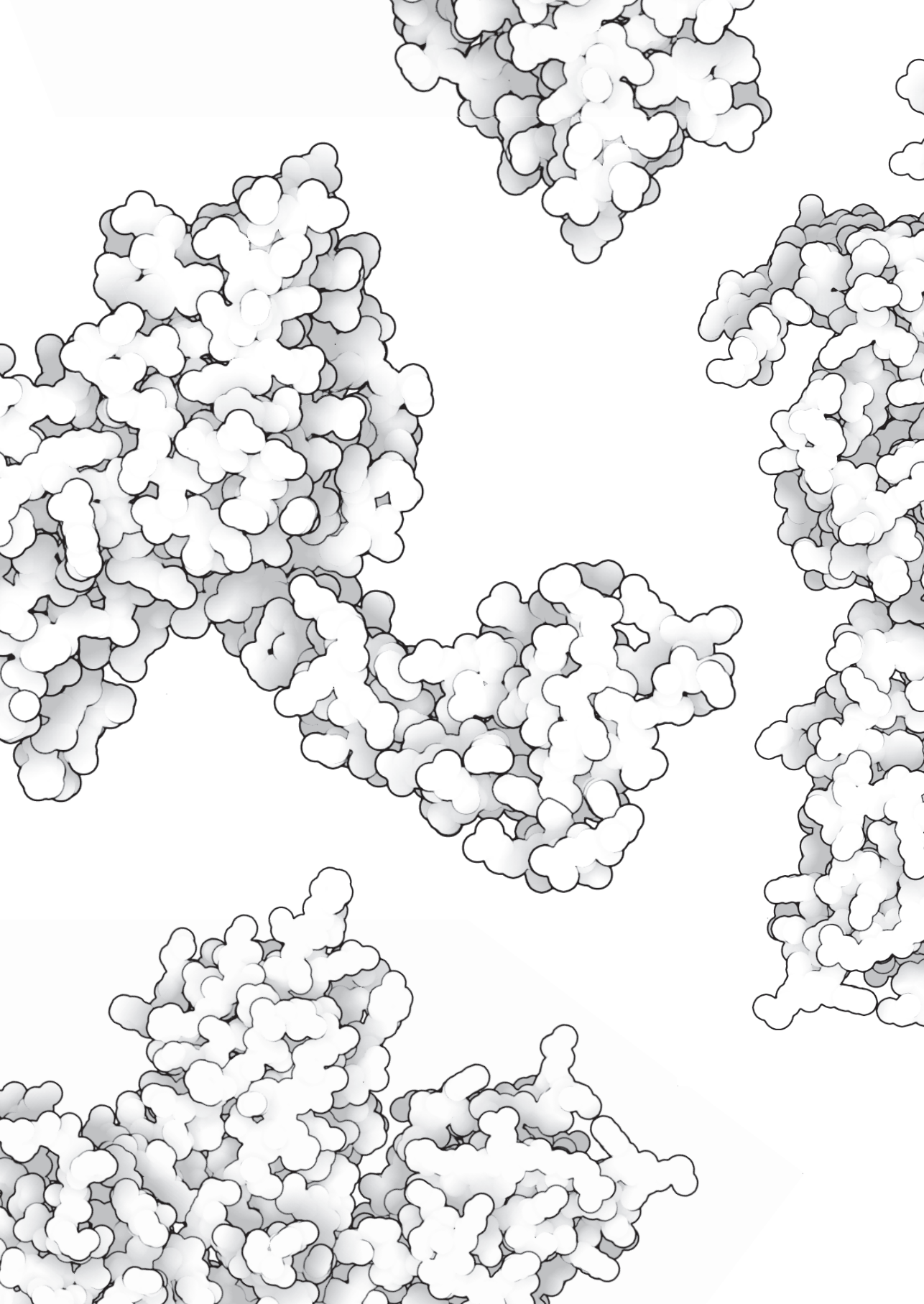

Chapter 3

The D' domain of von Willebrand factor requires the presence of the D3 domain for optimal factor VIII binding

Małgorzata A. Przeradzka [1], Henriet Meems [1], Carmen van der Zwaan [1], Eduard H.T.M. Ebberink [1], Maartje van den Biggelaar [1], Koen Mertens [1] and Alexander B. Meijer [1,2]

Biochem. J. 2018;475(17):2819-2830.

[1]Molecular and Cellular Hemostasis, Sanquin Research, 1066 CX Amsterdam, The Netherlands,

[2]Department of Biomolecular Mass Spectrometry and Proteomics, Utrecht Institute for Pharmaceutical Sciences, Utrecht University, Utrecht, The Netherlands

ABSTRACT

The D'-D3 fragment of von Willebrand factor (VWF) can be divided into TIL'-E'-VWD3-C8_3-TIL3-E3 subdomains of which TIL'-E'-VWD3 comprises the main factor VIII (FVIII)-binding region. Yet, von Willebrand disease (VWD) Type 2 Normandy (2N) mutations, associated with impaired FVIII interaction, have been identified in C8_3-TIL3-E3. We now assessed the role of the VWF (sub)domains for FVIII binding using isolated D', D3 and monomeric C-terminal subdomain truncation variants of D'-D3. Competitive binding assays and surface plasmon resonance analysis revealed that D' requires the presence of D3 for effective interaction with FVIII. The isolated D3 domain, however, did not show any FVIII binding. Results indicated that the E3 subdomain is dispensable for FVIII binding. Subsequent deletion of the other subdomains from D3 resulted in a progressive decrease in FVIII-binding affinity. Chemical footprinting mass spectrometry suggested increased conformational changes at the N-terminal side of D3 upon subsequent subdomain deletions at the C-terminal side of the D3. A D'-D3 variant with a VWD type 2N mutation in VWD3 (D879N) or C8_3 (C1060R) also revealed conformational changes in D3, which were proportional to a decrease in FVIII-binding affinity. A D'-D3 variant with a putative VWD type 2N mutation in the E3 subdomain (C1225G) showed, however, normal binding. This implies that the designation VWD type 2N is incorrect for this variant. Results together imply that a structurally intact D3 in D'-D3 is indispensable for effective interaction between D' and FVIII explaining why specific mutations in D3 can impair FVIII binding.

INTRODUCTION

Coagulation factor VIII (FVIII) circulates in plasma in complex with von Willebrand Factor (VWF). In this complex, FVIII is protected from rapid clearance from the circulation[1,2]. FVIII performs its role in secondary haemostasis as a cofactor for activated factor IX (FIXa) during the proteolytic conversion of factor X (FX) to activated FX[3]. VWF, on the other hand, is involved in primary haemostasis where it contributes to the initial platelet plug formation at sites of vessel injury[4]. The protective role of VWF for FVIII is demonstrated by the observation that impaired FVIII-VWF complex formation, caused by genetic variants of VWF, can lead to markedly reduced FVIII plasma levels. The associated bleeding disorder has been referred to as von Willebrand disease (VWD) type 2 Normandy (2N)[5]. The involved mutations are not confined to a specific site in VWF, but are distributed over an amino acid region spanning the first 486 amino acid residues of mature VWF[6]. This phenomenon has remained poorly understood.

FVIII circulates in plasma as a heavy chain (domains A1-*a1*-A2-*a2*-B) that is non-covalently linked to a light chain (domains *a3*-A3-C1-C2). *a1*, *a2* and *a3* are spacer regions rich in acidic amino acid residues[7]. VWF requires the acidic *a3* region and several sites in the C1 and C2 domain for high affinity binding to FVIII[7-9]. VWF itself is synthesized as a large multidomain glycoprotein of which the domain organization is represented as D1-D2-D'-D3-A1-A2-A3-D4-B-C1-C2-CK[10]. Guided by the location of disulfide bridges within VWF, limited proteolysis studies, and electron microscopy studies, Zhou et al. have refined the domain organization of VWF. The D'-D3 part of VWF has, for instance, been further dissected into TIL'-E'-VWD3-C8_3-TIL3-E3 subdomains [6]. After biosynthesis, VWF forms dimers in the endoplasmatic reticulum via disulfide bridge formation between two CK domains. These dimers are transported to the trans Golgi network where large VWF multimers can be formed through disulfide bridge formation between the D3 domains[11-13]. The VWF propeptide comprising the D1-D2 domains is critical for this process. After multimerization, the propeptide is removed from VWF mediated by furin cleavage leaving a mature VWF protein that starts with the D' domain[10].

Foster et al.[14] have suggested that the binding site of FVIII resides within the first 272 amino acids of D'-D3 covering the subdomains TIL'-E'-VWD3. In a more recent study addressing the NMR structure of the TIL'-E' (i.e. D') fragment, Shiltagh et al.[15] proposed that the major FVIII-binding site is localized within this structure. Electron microscopy studies also suggested that the interaction between FVIII and VWF primarily involves an interaction between D' and FVIII[16]. Using a chemical footprinting mass spectrometry approach, we have previously shown that amino acid residues at the start of the TIL' subdomain of mature VWF contribute to FVIII binding[17]. This agrees with the observation that the TIL' subdomain comprises the major binding site for FVIII. In spite of these observations, mutations in VWF in patients with VWD type

2N have been identified outside the TIL'-E' subdomains, i.e. in the subdomains of the D3 domain[18-23]. This shows that the function of these subdomains with respect to FVIII binding is unclear. Using surface plasmon resonance (SPR) analysis, competitive binding assays and chemical footprinting mass spectrometry on monomeric D'-D3 fragments and type 2N variants thereof, we now show that these subdomains contribute to the structural integrity of the D3 domain, which is indispensable for effective FVIII binding.

MATERIALS AND METHODS

Materials

HEPES was from Serva (Heidelberg, Germany), Tris was from Invitrogen (Breda, Netherlands) Tween 20 was from Sigma and NaCl was obtained from Fagron (Rotterdam, The Netherlands). Human serum albumin (HSA) was from the Division of Products at Sanquin (Amsterdam, The Netherlands). FreeStyle 293 expression medium was obtained from Gibco (Thermo Fisher Scientific). All other chemicals were from Merck (Darmstadt, Germany), unless indicated otherwise.

Proteins

Monoclonal antibody CLB-EL14 (EL14) has been described before[24]. CLB-Rag20 and CLB-CAg12 have been reported by Stel et al.[25]. HPC4 mouse hybridoma (HB9892) was obtained from ATCC and cultured in IMDM (Lonza) supplemented with 2% FCS (Bodinco). HPC4 antibody was purified with protein G sepharose (GE Heath Care) according to the manufacturer's procedures. The TIL'-E'-VWD3-C8_3-TIL3-E3 and TIL'-E' fragments and truncated variants thereof were designed in pcDNA3.1 (+) with two point mutations at position C1099S and C1142S to prevent dimerization of the fragments. A HPC4 tag was fused at the C-terminus for purification purpose. In addition, the sequence was codon-optimized for enhanced expression in human cells. Truncated variants of the D'-D3 fragment were constructed using Quick Change (Agilent Technologies) mutagenesis. The primers that were used in the present study are displayed in Table 1. Coding regions of all constructs were verified by sequence analysis. Sequence reactions were performed using BigDye Terminator Sequencing kit (Applied Biosystem, Foster City, CA, U.S.A.). Recombinant proteins were transiently expressed in a HEK 293 Freestyle cell line by means of polyethylenimine (PEI) (Polysciences) transfection as described in van den Biggelaar et al.[26]. Five days after transfection, proteins were purified from the medium by immunoaffinity chromatography using activated CNBr-Sepharose 4B coupled with anti-HPC4. The D'-D3 fragments were loaded on the anti-HPC4 column in 20 mM Tris-HCl (pH 7.4), 100 mM NaCl, 10 mM $CaCl_2$. After loading, the column

Table 1 Set of primers used in the study to obtain truncated fragments and single mutations in D'-D3.

construct		primer sequence
TIL'-E'-VWD3-C8_3-TIL3	sense	5'-CTGGGTCTCGTAACGGGGCTTCTAGTCCACCTGGGA-3'
	anti-sense	5'-GACCCAGAGGATTGCCCCGAAGATCAGGTGGACCCT-3'
TIL'-E'-VWD3-C8_3	sense	5'- AGGGTCCACCTGATCTTCGCACAGGGTGGCGGTTCT-3'
	anti-sense	5'- AGAACCGCCACCCTGTGCGAAGATCAGGTGGACCCT-3'
TIL'-E'-VWD3	sense	5'- AGGGTCCACCTGATCTTCCACCTTTCTGGTGTCGGC-3'
	anti-sense	5'- GCCGACACCAGAAAGGTGGAAGATCAGGTGGACCCT-3'
VWD3-C8_3-TIL3-E3	sense	5'-AACGGTCCCTGGGAAACACGGTGCACGAGGTGCTAG-3'
	anti-sense	5'-CTAGCACCTCGTGCACCGTGTTTCCCAGGGACCGTT-3'
D'-D3 D879N	sense	5'-GCCCACTACCTGACCTTCAACGGCCTGAAGTACCTGTTC-3'
	anti-sense	5'-GAACAGGTACTTCAGGCCGTTGAAGGTCAGGTAGTGGGC-3'
D'-D3 C1060R	sense	5'-ACAATGGTGGACAGCAGCCGCAGAATCCTGACCTCCGAT-3'
	anti-sense	5'-ATCGGAGGTCAGGATTCTGCGGCTGCTGTCCACCATTGT-3'
D'-D3 C1225G	sense	5'-CCCGAGCACTGCCAGATCGGTCACTGCGACGTCGTGAAC-3'
	anti-sense	5'-GTTCACGACGTCGCAGTGACCGATCTGGCAGTGCTCGGG-3'

was washed with 20 mM Tris-HCl (pH 7.4), 1 M NaCl, 10 mM $CaCl_2$. Next, proteins were eluted from the anti-HPC4 column with 20 mM Tris-HCl (pH 7.4), 100 mM NaCl, 5 mM EDTA. Subsequently, protein-containing fractions were dialyzed against 50 mM HEPES (pH 7.4), 150 mM NaCl, 10 mM $CaCl_2$, 50% (v/v) glycerol and stored at −20°C. Concentration of the D'-D3 fragments was assessed using Pierce BCA Protein Assay Kit using HSA as a standard according to the manufacturer's instructions (Thermo Fisher Scientific, Rockford, IL, U.S.A.). Recombinant VWF and FVIII lacking the B domain residues 746-1639 (referred to as FVIII throughout this paper) were expressed and purified as described previously[27,28]. FVIII antigen and activity levels were determined as described[27]. Protein deglycosylation of the fragments was performed using Rapid PNGase F according to the instructions of the manufacture (New England BioLabs, Ipswich, MA, U.S.A.).

Solid-phase competition assays

Recombinant VWF (1 µg/ml) was immobilized in the microtiter wells of a Nunc Maxisorp immunoplate by overnight incubation at 4°C in a buffer containing 50 mM $NaHCO_3$ pH 9.8. Next, FVIII was pre-incubated with increasing concentrations of VWF fragments for 30 min at 37°C in a buffer containing 50 mM Tris, 150 mM NaCl, 2% HSA, 0.1% Tween 20, pH 7.4. Subsequently, mixtures were added to the VWF containing wells and incubated for 2 h at 37°C. Plates were washed three times with 50 mM Tris (pH 7.4), 150 mM NaCl, 5 mM $CaCl_2$, 0.1% Tween 20 and residual FVIII binding to immobilized VWF was assessed using HRP-labelled CLB-CAg12 antibody as described [17].

Surface plasmon resonance analysis

SPR analysis was performed employing a Biacore T-200 biosensor system (GE Healthcare). For assessment of FVIII-VWF interaction, antibody CLB-EL14 was covalently coupled (5000 RU) to the dextran surface of an activated CM5 sensor chip via primary amino groups, using the amine-coupling method prescribed by the manufacturer (GE Healthcare). Subsequently, 3700 RU FVIII was loaded on the chip via CLB-EL14 and varying concentrations of the D'-D3 fragments were passed over immobilized FVIII at a flow rate of 30 µl/min in a buffer containing 20 mM HEPES (pH 7.4), 150 mM NaCl, 5 mM $CaCl_2$ and 0.05% Tween 20 at 25°C. The sensor chip was regenerated once after each experiment using the same buffer containing 1 M NaCl instead of 150 mM NaCl. A CLB-EL14-coated CM5 channel was used to correct for nonspecific binding.

Tandem mass tag modification

Tandem mass tag (TMT) (Thermo Fisher Scientific) modification of the lysine residues of the D'-D3 truncated fragments in comparison with D'-D3 was performed as follows. Each truncated variant or 2N variant was incubated with a 10 000-fold molar excess of TMT-126. The D'-D3 fragment was incubated with a 10 000-fold excess of TMT-127. After 5 min, the labelling reaction was quenched for 15 min by the addition of a 150-fold molar excess of hydroxylamine over the TMTs at 37°C. Next, protein mixtures were pooled at a 1:1 ratio and the cysteines were alkylated with 2-iodoacetamin as described [28]. The protein mixtures were proteolyzed overnight at 37°C with chymotrypsin using 0.05 µg chymotrypsin per µg protein (Thermo Fisher Scientific). Obtained peptides were concentrated and desalted using a C18 ZipTip (Millipore Corp.) according to the instructions of the manufacturer.

Mass spectrometry analysis

Peptides were separated by nanoscale C18 reverse-phase chromatography and sprayed into a LTQ Orbitrap XL mass spectrometer (Thermo Fisher Scientific) via a nano electrospray ion source (Nanospray Flex Ion Source, Thermo Scientific). Peptides were loaded on a 20 cm 75-360 µm inner-outer diameter fused silica emitter (New Objective) packed in-house with ReproSil-Pur C18-AQ, 1.9 µm resin (Dr Maisch GmbH). The column was installed on a Dionex Ultimate3000 RSLC nanoSystem (Thermo Scientific) using a MicroTee union formatted for 360 µm outer diameter columns (IDEX) and a liquid junction. The spray voltage was set to 2.15 kV. Buffer A was composed of 0.5% acetic acid and buffer B of 0.5% acetic acid, 80% acetonitrile. Peptides were loaded for 17 min at 300 nl/min at 5% buffer B, equilibrated for 5 min at 5% buffer B (17-22 min) and eluted by increasing buffer B from 5 to 15% (22-87 min) and 15-38% (87-147 min), followed by a 10 min wash to 90% and a 5 min regeneration to 5%. Collision-induced dissociation (CID) spectra and higher-energy CID (HCD) spectra were acquired as de-

scribed[28,29]. The five most intense precursor ions in the full scan (300-2000 *m/z*, 30 000 resolving power) were fragmented by CID with normalized collision energy of 35, and rapid scan mass spectrometry analysis in the ion trap. The same precursor ions were subjected to HCD fragmentation with a normalized collision energy of 60%. The identification of the peptides, together with determination of their TMT-127/TMT-126 ratio, was evaluated using Proteome Discover software 1.4. The SEQUEST search algorithm was used with a protein database 25.H sapiens.fasta. including the amino acid sequence of human VWF with the addition of the D'-D3 fragment with the mutations C1099S and C1142S. To select peptides for further analysis, the following criteria were used: (i) all lysine residues are modified by a TMT label (+225.1558 Da), (ii) all cysteine residues are alkylated, (iii) methionine residues may be oxidized and (iv) a maximum false discovery rate of 5% was accepted. The TMT ratio of the identified peptides was normalized to the average TMT ratio obtained within that experiment.

RESULTS

Effect of subdomain truncation of the D'-D3 domain on FVIII binding

To assess the role of the VWF (sub)domains for FVIII binding, a monomeric D'-D3 fragment, D' domain and D3 domain were constructed, expressed by HEK293 cells, and purified. In addition, C-terminal subdomain truncation variants of D'-D3 were obtained (Figure 1A). Monomeric fragments were obtained by substituting the cysteine residues at position 1099 and 1142 by serine residues[30]. Analysis of the protein variants by SDS-PAGE showed a double protein for the VWF fragments. This was particularly evident for isolated D3 domain (Figure 1B). After PGNase F treatment of D'-D3 and the D3 domain, only a single band was observed on the gel (Figure 1C). These observations imply that partial glycosylation of the fragments is the cause for the double protein band on SDS-PAGE. To assess the FVIII-binding efficiency of the VWF fragments, we performed a competitive binding assay in which we evaluated the binding of FVIII to immobilized VWF in the presence of increasing concentrations of the D'-D3 fragments (Figure 2). Residual FVIII binding to immobilized VWF was detected using CLB-CAg12, which itself does not interfere with FVIII-VWF complex formation[17]. The results demonstrated that D'-D3 competes with full-length VWF for binding to FVIII. No competition was observed for the isolated D3 domain. The isolated D' fragment reduced the binding of FVIII to immobilized VWF but only at higher concentrations. The competition assay further showed that removal of the C-terminal E3 subdomain from D'-D3 has only a limited effect on FVIII binding, if any at all. Subsequent removal of the TIL3 and C8_3 subdomains markedly impairs the ability of the fragments to bind FVIII. These results together indicate that the main

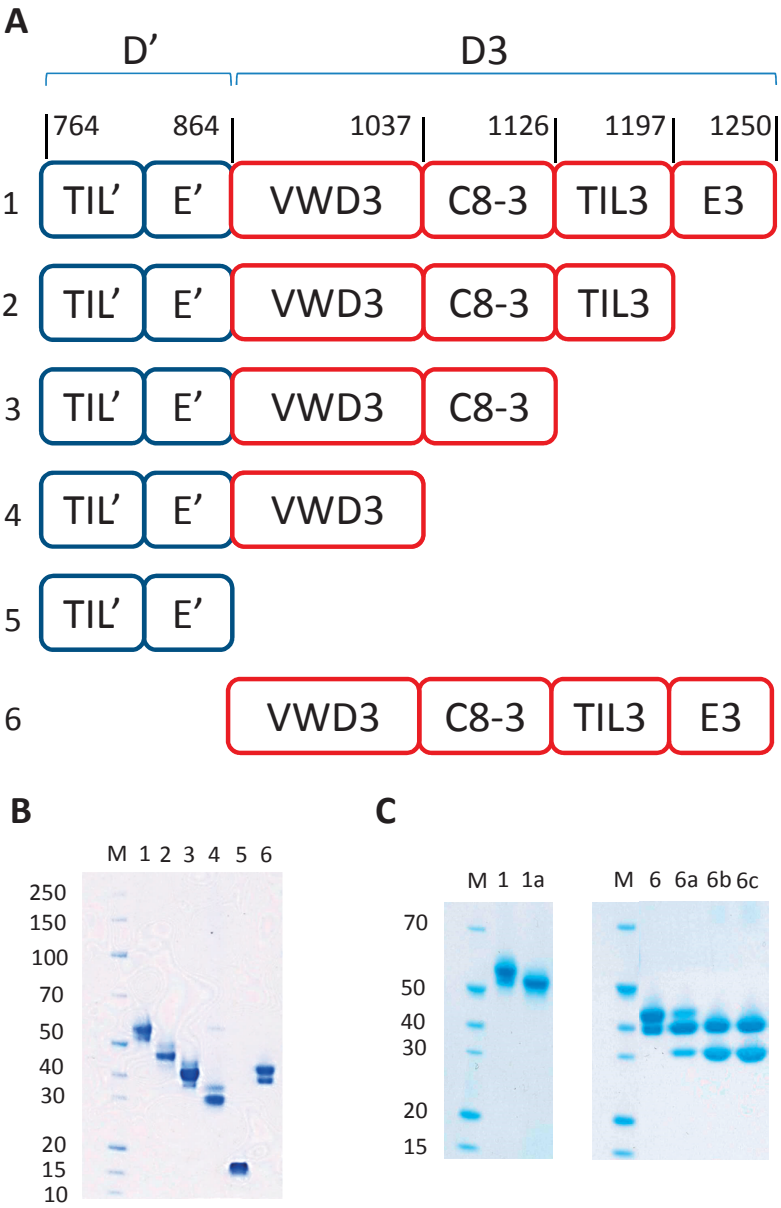

Figure 1. Construction and purification of VWF fragments. Panel A shows a schematic representation of the D'-D3 fragment variants of VWF that were employed in this study. Panel B and C show the purified fragments analyzed by SDS-PAGE. Proteins and marker were visualised using Coomassie Brilliant Blue staining. On the left side are indicated the molecular weights of the marker in kDa. Numbers at the bottom of the gel correspond with D'-D3 variants shown in panel A. Panel C shows analysis by SDS-PAGE of 2 µg D'-D3 that was treated with (1a) 0.5 µg or (1) without PNGase F and 2 µg D3 that was treated with increasing amounts of PNGase F (6) 0 µg, (6a) 0.5 µg, (6b) 1 µg or (6c) 2 µg PNGase F.

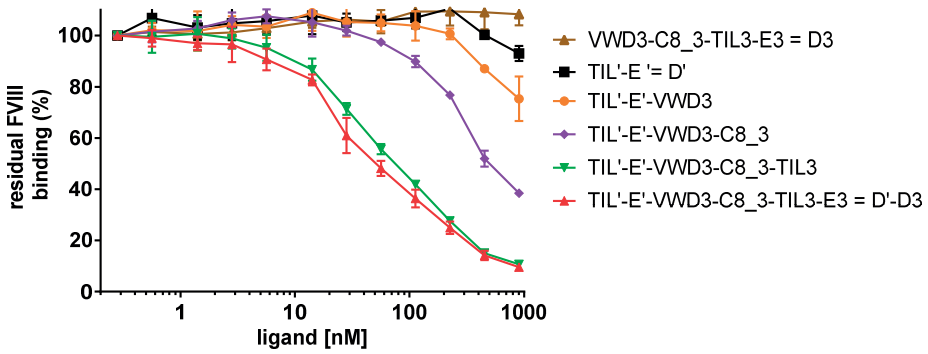

Figure 2. FVIII-VWF complex assembly in the presence of the D'-D3 fragments. FVIII (0.3 nM) was pre-incubated with increasing concentrations of VWF fragments ranging from 0.3 to 900 nM in a buffer containing 50 mM Tris (pH 7.4), 150 mM NaCl, 5 mM $CaCl_2$, 2% (v/v) human serum albumin and 0.1% Tween 20. Residual FVIII-VWF binding in the presence of D'-D3 fragments was determined with HRP-conjugated CLB-CAg12 antibody as described in Materials and Methods. Data represents mean ± SD of three independent experiments.

FVIII-binding region in the D' domain requires the presence of the VWD3-TIL3-C8_3 fragment for effective interaction with FVIII.

The VWF D3 subdomains contribute to FVIII binding

To gain additional insight into the binding efficacy of the truncated D'-D3 fragments to FVIII, we employed SPR analysis. To this end, FVIII was immobilized on a CM5 sensor chip via the C2 domain-directed antibody CLB-EL14, and increasing concentrations of the D'-D3 fragments were passed over immobilized FVIII (Figure 3). A dose-dependent increase in response units was observed employing increasing concentrations of D'-D3 and its variants. The data revealed effective FVIII binding of D'-D3 and D'-D3 lacking the E3 subdomain. However, markedly altered apparent association and dissociation curves were observed for fragments lacking TIL3-E3 and C8_3-TIL3-E3. To gain insight into the binding affinity, we estimated the K_D of the FVIII-VWF fragment complex by plotting the response at equilibrium as a function of the ligand concentration. Data showed a 4-fold increase in K_D for the TIL'-E'-VWD3-C8_3 variant compared with D'-D3 and 12-fold increase for the TIL'-E'-VWD3 fragment. The K_D of D'-D3 fragment that lacked the E3 subdomain was similar to that of D'-D3. These data show that the E3 subdomain is dispensable for effective FVIII binding. The N-terminal subdomains of D3 are, however, critical for the interaction with FVIII.

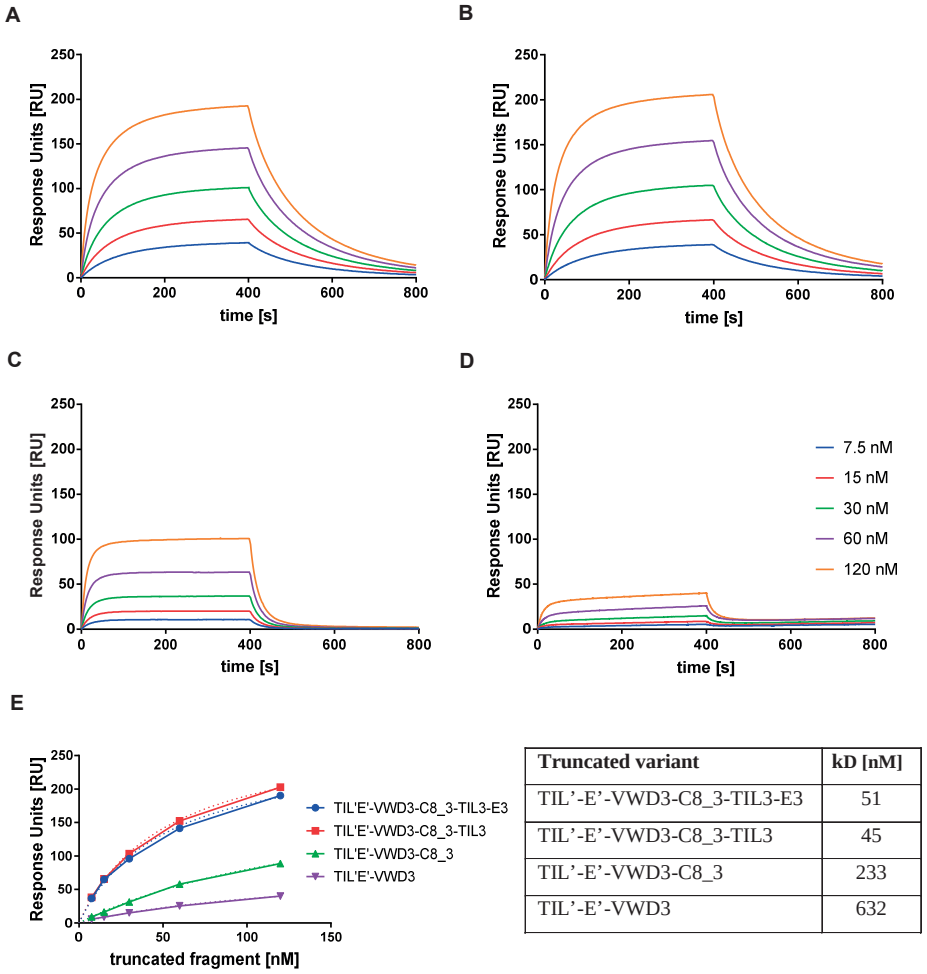

Truncated variant	kD [nM]
TIL'-E'-VWD3-C8_3-TIL3-E3	51
TIL'-E'-VWD3-C8_3-TIL3	45
TIL'-E'-VWD3-C8_3	233
TIL'-E'-VWD3	632

Figure 3. Binding of D'-D3 fragments to FVIII. Multiple concentrations (8-120 nM) of (panel A) D'-D3, (panel B) TIL'-E'-VWD3-C8_3-TIL3, (panel C) TIL'-E'-VWD3-C8_3, and (panel D) TIL'-E'-VWD3) were passed over FVIII that was immobilized via C2 domain-directed antibody EL14 on a CM5 sensor chip. Association and dissociation of the fragments was assessed in 20 mM HEPES (pH 7.4), 150 mM NaCl, 5 mM $CaCl_2$, 0.05% (v/v) Tween 20 at a flow rate of 30 µl/min at 25°C. The binding response is indicated as Response Units (RU) (panel E). The equilibrium dissociation constant (K_D) the complex between FVIII and the employed fragments was estimated by plotting the Response Unit at 120 s as a function of the fragment concentration. The fragment concentration at which half-maximum binding is reached reflects the estimated equilibrium dissociation constant (K_D).

Chemical footprinting reveals altered reactivity of lysine residues in the D3 domain upon C-terminal subdomain deletions from the D'-D3 fragment

Chemical footprinting mass spectrometry was employed to assess whether the C-terminal subdomain truncations may affect the reactivity of specific lysine residues for chemical modification in the D'-D3 fragment. To this end, lysine directed TMTs were utilized to chemically modify the lysine amino acid residues[31]. The truncation fragments were chemically modified with TMT-126 and the D'-D3 fragment with TMT-127. Removal of the E3 domain from D'-D3 resulted in an increase in TMT-126/TMT-127 ratio for lysine residues in the VWD3 domain and involved the lysine residues K1026/K10136, K985 and K882 (Figure 4). Upon deletion of the TIL3 and C8_3 subdomains, a further increase in TMT-126/TMT-127 ratio was observed for these lysine residues. These findings imply that subdomain deletion at the C-terminal side of the D3 domain affect amino acid regions in the N-terminal VWD3 subdomain of the D3 domain.

VWF type 2N variants differentially affect FVIII binding

The natural variants D'-D3 D879N (located in VWD3 subdomain), D'-D3 C1060R (C8_3 subdomain) and D'-D3 C1225G (E3 subdomain) have been suggested to impair FVIII-VWF complex formation[20]. We now evaluated FVIII binding of the D'-D3 variants comprising these VWD type 2N mutations using SPR analysis. FVIII was immobilized on a CM5 sensor chip via an anti-C2 domain antibody and the binding of the fragments was evaluated (Figure 5). Compared with D'-D3, results revealed a major decrease in FVIII-binding response for D'-D3 D879N and D'-D3 C1060R. Remarkably, the D'-D3 variant with the amino acid substitution in the E3 domain, i.e. C1225G, had only a limited decrease in binding response compared with D'-D3. Data show that the mutations in the VWD3 and C8-3 domains affect the interaction with FVIII.

Chemical footprinting reveals that VWF type 2N mutations affect the reactivity of lysine amino acid residues in the D3 domain

Chemical footprinting by TMT labels was employed to assess putative changes in lysine amino acid reactivity in the VWD type 2N variants of D'-D3. The VWF type 2N variants were labelled with TMT-126 and the D'-D3 fragment with TMT-127. Data showed an increase in TMT-126/TMT-127 ratio in a region comprising K1026/K1036 comparing the D'-D3 C1225G variant with D'-D3 (Figure 6). For the D'-D3 C1060R variant, multiple lysine residues were affected. Several lysine comprising regions showed a decreased reactivity toward the TMT labels and other regions displayed an increased reactivity. The D'-D3 D879N variant especially revealed a major change in the region comprising the lysine residues K1026 and K1036. No TMT-126/TMT-127 ratio could be obtained for K882 for the D'-D3 D879N variant. The TMT-labelled peptide comprising K882 also

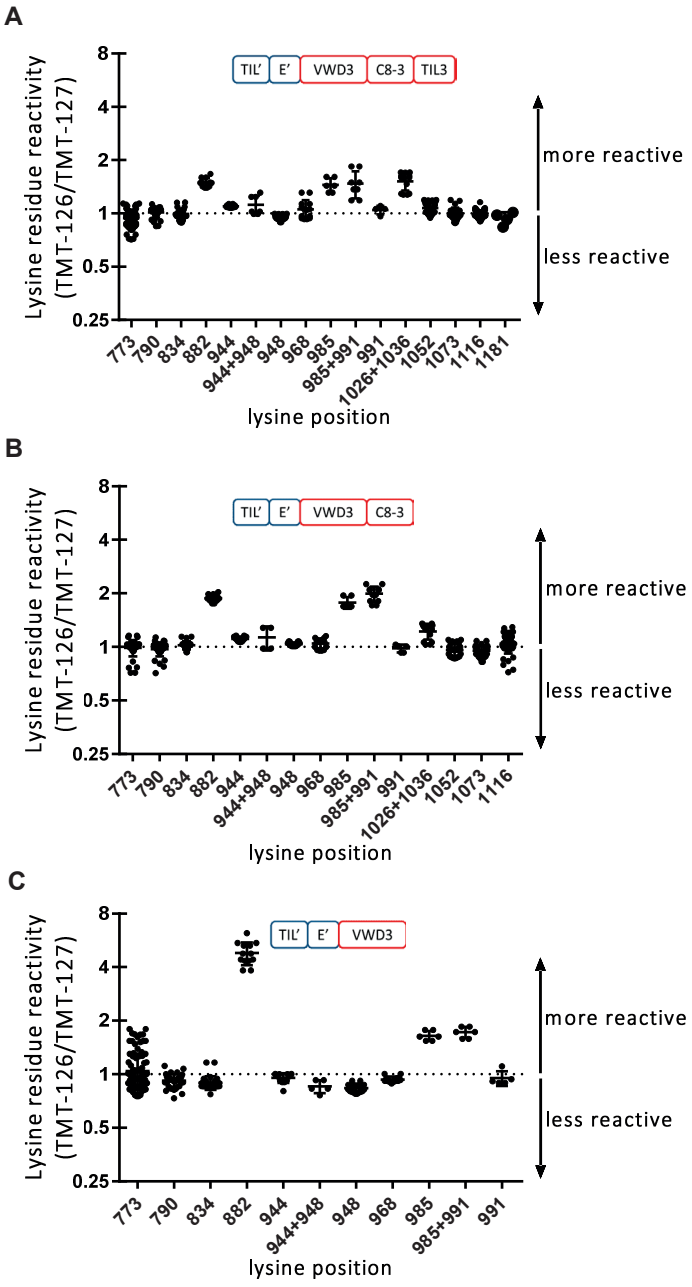

Figure 4. Chemical modification of D'-D3 fragments reveals conformational changes in D3. The truncated D'-D3 fragments (panel A) TIL'-E'-VWD3-C8_3-TIL3, (panel B) TIL'-E'-VWD3-C8_3 and (panel C) TIL'-E'-VWD3 were labelled with TMT-126 and the D'-D3 fragment with TMT-127. Proteins were mixed in a 1:1 molar ratio. The obtained average TMT-126/TMT-127 ratios of the lysine residues are shown on the x-axis and the position of the lysine residue on the y-axis. Data represents the average ± SD TMT-126/TMT-127 ratios of three independent experiments.

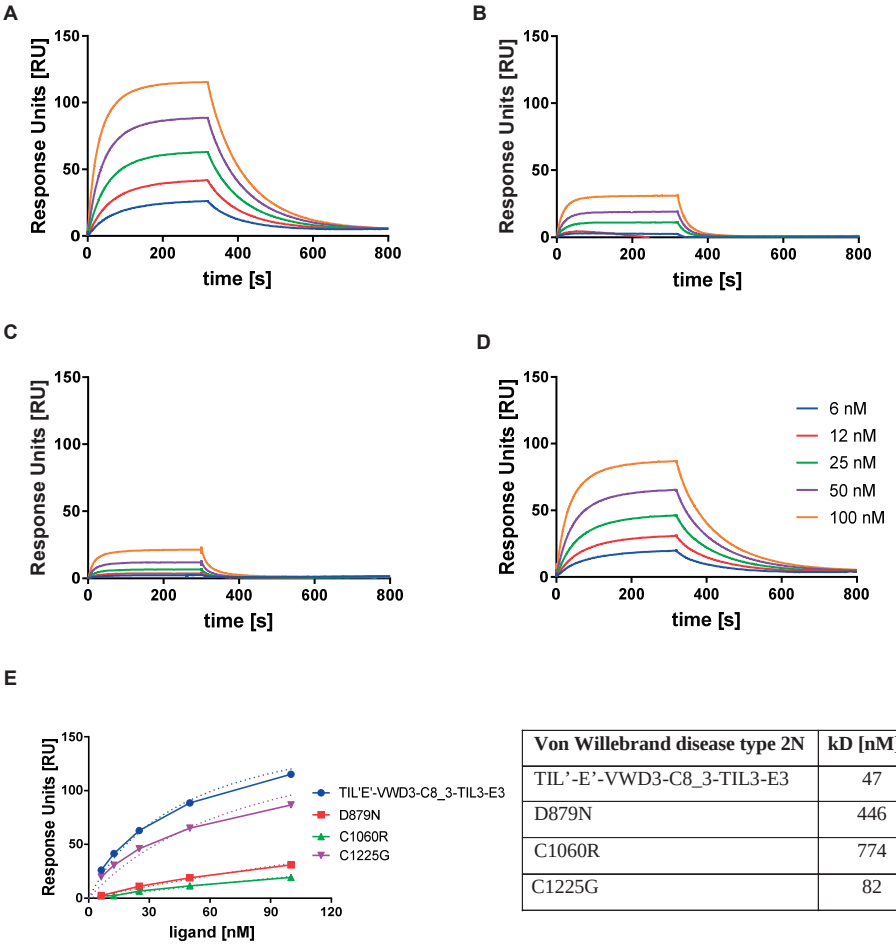

Von Willebrand disease type 2N	kD [nM]
TIL'-E'-VWD3-C8_3-TIL3-E3	47
D879N	446
C1060R	774
C1225G	82

Figure 5. Binding of D'-D3 and VWF type 2N variants to FVIII. Various concentrations (0-100 nM) of (panel A) D'-D3, (panel B) D'-D3 D879N, (panel C) D'-D3 C1060R or (panel D) D'-D3 C1225G were passed over FVIII that was immobilized via C2 domain-directed antibody CLB-EL14 on a CM5 sensor chip. The binding response is indicated as Response Units (RU) (panel E) and was assessed in 20 mM HEPES (pH 7.4), 150 mM NaCl, 5 mM $CaCl_2$, 0.05% (v/v) Tween 20 at a flow rate of 30 µl/min at 25°C. A CM5 channel coated with CLB-EL14 lacking FVIII was used to correct for background binding. Response unit as a function of ligand concertation for tested 2N variants in comparison to D'-D3.

includes the D879N substitution and has different physio-chemical properties from those of the reference TMT-labelled peptide of WT-D'-D3. In spite of this limitation, data together imply changes in the D3 domain for especially D'-D3 C1060R and D'-D3 D879N.

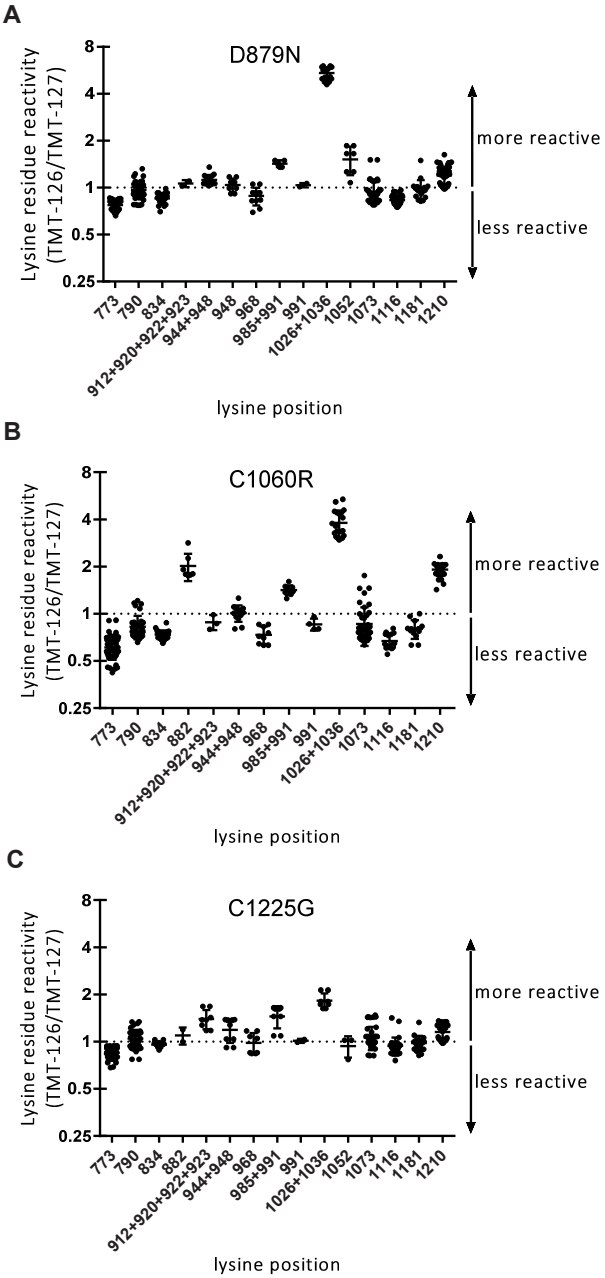

Figure 6. Chemical modification of VWF type 2N variants of the D'-D3 fragments reveals conformational changes in D3. (panel A) D'-D3 D879N, (panel B) D'-D3 C1060R and (panel C) D'-D3 C1225G were labelled with TMT-126 and the D'-D3 fragment with TMT-127. The obtained average TMT-126/TMT-127 ratios of the lysine residues are shown on the y-axis and the position of the lysine residue on the x-axis. Data represents the average ± SD TMT-126/TMT-127 ratios of three independent experiments.

DISCUSSION

Studies addressing VWF-FVIII complex formation have been hampered by the fact that VWF circulates in plasma as dimers up to ultra-large multimers[32]. The tertiary and quaternary structures of VWF are further altered by shear stress conditions or by immobilization on surfaces[33,34]. This has led to confusion about the number of FVIII molecules that can bind VWF as well as the actual binding affinity of FVIII for VWF[35-37]. Critical analysis of the VWF type 2N mutations also shows that several variants affect VWF multimerization and not merely the interaction with FVIII[18,21,38]. Assessing the role of individual VWF (sub)domain for FVIII binding has, therefore, remained a challenge. To overcome this issue, we now have studied the interaction between FVIII and monomeric truncation fragments of VWF as well as type 2N mutations thereof.

It has been shown that the N-terminal D' domain of VWF comprises the main binding region for FVIII[14,15,39]. Results of this study surprisingly showed that the isolated D' domain poorly binds FVIII and that the isolated D3 domain did not bind FVIII at all (Figure 2). Except for the fragment lacking the E3 subdomain, the subsequent deletion of the other C-terminal subdomains from D'-D3 resulted in a major decrease in FVIII binding. These observations imply that the D' domain requires the presence of the D3 domain until at least the TIL3 subdomain for high affinity interaction with FVIII. The VWD3 domains seem, however, indispensable for the interaction with FVIII (Figure 3). Our findings agree with earlier studies that show that fragments of VWF comprising the residues S764-R1035 bind with a reduced affinity to FVIII although the proposed main FVIII-binding site is in D' (residues S764-864)[15,40].

Chemical footprinting mass spectrometry of lysine residues in D'-D3 provides insight into the reactivity of lysine residues towards the TMT labels in the individual VWF fragments and type 2N variants thereof. Residues at the surface of a fragment are expected to be more reactive to the TMT label compared with residues in the protein core, or those that contribute to e.g. salt-bridge formation[28,41]. Comparing the reactivity of the same lysine residues between fragments provides therefore insight into a putative change in the local structure surrounding this residue. Results showed that deletion of subdomains from the C-terminal side of the D3 domain impacts the labelling efficiency of lysine residues at the N-terminal side of the D3 domain. This change is most notable for lysine residue 882 in the VWD3 subdomain. This implies that the local structure is increasingly altered upon subsequent deletions of the C-terminal subdomains from the D3 domain (Figure 4). This suggests that interdomain contacts between these subdomains contribute to the structural integrity of the entire D3 domain. To date, no three-dimensional structure is available of the D3 domain in VWF or homologous D3 domains in other proteins. Our results predict that the structure will reveal a tight interaction between the subdomains within the D3 domain.

Removal of the E3 subdomain from the D3 domain has the least impact on the reactivity of the lysine residues in the remaining fragment. The same was observed for the VWD type 2N variant in which the cysteine residue at position 1225 is substituted for an arginine residue in the E3 subdomain (Figure 6). Apparently, the E3 subdomain is of less importance for the stability of the D3 domain, and may be more loosely associated in the D3 domain structure. The D'-D3 C1060R variant, however, revealed a marked change in reactivity of almost all lysine residues at C- and N-terminal side of this mutation implying a major impact on the structural integrity of the D3 domain. It may be expected that substitution of the structurally conserved cysteine residue at position 1060 affects the structure of the C8_3 domain. Compatible with our suggestion that interdomain interactions contribute to the stability of the D3 domain, a distorted C8_3 domain may affect the structure of the other domains as well.

The extent of reactivity of the lysine residues towards the TMTs in the subdomain deletion variants is reciprocal to the decrease in binding efficiency between FVIII and the VWF subdomain truncation variants (Figures 3 and 4). The same is true for the VWD type 2N variants. Only a limited effect on FVIII-binding efficiency was observed for the C1225G variant of D'-D3 and the variant lacking the E3 domain (Figures 5D and 6C). These variants also showed the least change in reactivity of the lysine residues. The C1060R variant, on the other hand, revealed a major change in lysine reactivity and FVIII binding. The later observation is in agreement with the study of Hilbert et al., who showed a poor FVIII-binding efficiency of the C1060R variant as well[20]. These findings together imply that the extent of distortion of the D3 domain is proportional to the decrease in binding affinity for FVIII. The reason why the C1225G variant has been designated as a VWD type 2N variant is at present unclear. An earlier study did reveal, however, an altered multimerization pattern for this VWF variant[21]. This suggests that the C1225G mutation may lead to incorrect dimerization of the D3 domains. This may lead, in turn, to a distortion of the structure of the D3 domain thereby affecting complex formation between FVIII and VWF. If so, requires further investigation. Results from the present study show that the E3 domain has a limited contribution to FVIII interaction.

Based on electron microscopy studies and molecular modelling of the D'-D3 fragment in complex with FVIII, it has been suggested that complex formation is primarily established via the interaction between the FVIII C1 domain and the D' domain. A weaker interaction was proposed to mediate the interaction between the C domains and the D3 domain[16]. Results from our and other studies show that the presence of part of the D3 domain is indispensable for effective complex formation with FVIII [37]. Our results do not exclude that there may be a secondary FVIII-binding site in the VWD3 subdomain that assists in the interaction between the D' domain and FVIII as has been proposed by the EM and molecular modelling studies[16,42]. Distortion of the

VWD3 domain in the truncation variants or VWF type 2N variants of D'-D3 may alter this FVIII binding site, and therefore the avidity of the complex between FVIII and the D'-D3 variant. Alternatively, there may be an interaction between the D' domain and the D3 domain in the complex with FVIII. This interaction may be required to stabilize the D' domain in an optimal FVIII-binding conformation. Distortion of the D3 domain structure leading to a reduced interaction between the D' domain and the D3 domain would then also lead to an impaired complex formation with FVIII. Irrespective of the existing binding mode between FVIII and D'-D3, both require a structurally intact D3 domain for effective interaction.

Taken together, we propose that an intact D3 domain is critical for the interaction between FVIII and VWF. We propose that VWF variants that disturb the structural integrity of the D3 domain will affect the complex formation with FVIII. This provides an explanation why mutations outside the main binding region in the D' domain can lead to VWD type 2N.

ABBREVIATIONS

CID, collision-induced dissociation; FIX, factor IX; FVIII, factor VIII; HCD, high-energy collisional dissociation; HSA, human serum albumin; PEI, polyethylenimine; SPR, surface plasmon resonance; TMT, tandem mass tag; VWD, von Willebrand disease; VWF type 2N, von Willebrand disease Type 2 Normandy; VWF, von Willebrand factor.

AUTHOR CONTRIBUTION

M.A.P. and H.M. performed experiments; C.v.d.Z. provided technical assistance; M.A.P., M.v.d.B., K.M. and A.B.M. designed the research; E.H.T.M.E. assisted with MS experiments, M.A.P. and A.B.M. analysed results; M.A.P. made the figures, M.A.P., H.M. and A.B.M. wrote the paper.

FUNDING

The present study has been funded by Product and Process Development, Sanquin, The Netherlands (PPOP-13-002).

REFERENCES

1 Brinkhous, K. M., Sanderg, H., Garris, J. B., Mattsson, C., Palm, M., Griggs, T. and Read, M. S. (1985) Purified human factor VIII procoagulant protein : Comparative hemostatic response after infusions into hemophilic and von Willebrand disease dogs. *Proc. Natl. Acad. Sci. U. S. A.* **82**, 8752-8756.

2 Morfini, M., Mannucci, P. M., Tenconi, P. M., Longo, G., Mazzucconi, M. G., Rodeghiero, F., Ciavarella, N., De Rosa, V. and Arter, A. (1993) Pharmacokinetics of monoclonally-purified and recombinant factor VIII in patients with severe von Willebrand disease. *Thromb. Haemost.* **70**, 270-272.

3 Fay, P. J. (2006) Factor VIII structure and function. *Int. J. Hematol.* **70**, 63-67.

4 Bryckaert, M., Rosa, J.-P., Denis, C. V and Lenting, P. J. (2015) Of von Willebrand factor and platelets. *Cell. Mol. Life Sci.* **72**, 307-326.

5 Sadler, J. E., Mannucci, P. M., Mazurier, C., Meyer, D., Nichols, W. L., Nishino, M., Peake, I. R., Rodeghiero, F., Schneppenheim, R., Ruggeri, Z. M., et al. (2006) Update on the pathophysiology and classification of von Willebrand disease: a report of the Subcommittee on von Willebrand Factor. *J. Thromb. Haemost.* **4**, 2103-2114.

6 Zhou, Y. F., Eng, E. T., Zhu, J., Lu, C., Walz, T. and Springer, T. A. (2012) Sequence and structure relationships within von Willebrand factor. *Blood* **120**, 449-458.

7 Saenko, E. L. and Scandella, D. (1997) The acidic region of the factor VIII light chain and the C2 domain together form the high affinity binding site for von Willebrand factor. *J. Biol. Chem.* **272**, 18007-18014.

8 Leyte, A., Van Schijndel, H. B., Niehrs, C., Huttner, W. B., Verbeet, M. P., Mertens, K. and Van Mourik, J. A. (1991) Sulfation of Tyr1680 of human blood coagulation factor VIII is essential for the interaction of factor VIII with von Willebrand factor. *J. Biol. Chem.* **266**, 740-746.

9 Foster, P. A., Fulcher, C. A., Houghten, R. A. and Zimmerman, T. S. (1988) An immunogenic region within residues Val1670-Glu1684 of the factor VIII light chain induces antibodies which inhibit binding of factor VIII to von Willebrand factor. *J. Biol. Chem.* **263**, 5230-5234.

10 Sadler, J. E. (2009) von Willebrand factor assembly and secretion. *J. Thromb. Haemost.* **7**, 24-27.

11 Marti, T., Rosselet, S. J., Titani, K. and Walsh, K. A. (1987) Identification of disulfide-bridged substructures within human von Willebrand factor. *Biochemistry* **26**, 8099-8109.

12 Katsumi, A., Tuley, E. A., Bodo, I. and Sadler, J. E. (2000) Localization of disulfide bonds in the cystine knot domain of human von Willebrand factor. *J. Biol. Chem.* **275**, 25585-25594.

13 Lenting, P. J. and Christophe, O. D. (2015) von Willebrand factor biosynthesis, secretion, and clearance: connecting the far ends **125**, 2019-2028.

14 Foster, P. A., Fulcher, C. A., Marti, T., Titani, K. and Zimmerman, T. S. (1987) A major factor VIII binding domain resides within the amino-terminal 272 amino acid residues of von Willebrand factor. *J. Biol. Chem.* **262**, 8443-8446.

15 Shiltagh, N., Kirkpatrick, J., Cabrita, L. D., Mckinnon, T. A. J., Thalassinos, K., Tuddenham, E. G. D. and Hansen, D. F. (2014) Solution structure of the major factor VIII binding region on von Willebrand factor. *Blood* **123**, 4143-4152.

16 Yee, A., Oleskie, A. N., Dosey, A. M., Kretz, C. a., Gildersleeve, R. D., Dutta, S., Su, M., Ginsburg, D. and Skiniotis, G. (2015) Visualization of an N-terminal fragment of von Willebrand factor in complex with factor VIII. *Blood* **126**, 939-942.

17 Castro-Núñez, L., Bloem, E., Boon-Spijker, M. G., van der Zwaan, C., van den Biggelaar, M., Mertens, K. and Meijer, A. B. (2013) Distinct roles of Ser-764 and Lys-773 at the N terminus of von Willebrand factor in complex assembly with coagulation factor VIII. *J. Biol. Chem.* **288**, 393-400.

18 Jorieux, S., Gaucher, C., Goudemand, J. and Mazurier, C. (1998) A Novel Mutation in the D3 Domain of von Willebrand Factor Markedly Decreases Its Ability to Bind Factor VIII and Affects Its Multimerization. *Blood* **92**, 4663-4670.

19 Casais, P., Carballo, G. A., Woods, A. I., Kempfer, A. C., Farías, C. E., Grosso, S. H. and Lazzari, M. A. (2006) R924Q substitution encoded within exon 21 of the von Willebrand factor gene related to mild bleeding phenotype. *Thromb. Haemost.* **96**, 228-230.

20 Hilbert, L., Jorieux, S., Proulle, V., Favier, R., Goudemand, J., Parquet, A., Meyer, D., Fressinaud, E. and Mazurier, C. (2003) Two novel mutations, Q1053H and C1060R, located in the D3 domain of von Willebrand factor, are responsible for decreased FVIII-binding capacity. *Br. J. Haematol.* **120**, 627-632.

21 Allen, S., Abuzenadah, A. M., Blagg, J. L., Hinks, J., Nesbitt, I. M., Goodeve, A. C., Gursel, T., Ingerslev, J., Peake, I. R. and Daly, M. E. (2000) Two novel type 2N von Willebrand disease-causing mutations that result in defective factor VIII binding, multimerization, and secretion of von Willebrand factor. *Blood* **95**, 2000-2007.

22 Hilbert, L., D'Oiron, R., Fressinaud, E., Meyer, D. and Mazurier, C. (2004) First identification and expression of a type 2N von Willebrand disease mutation (E1078K) located in exon 25 of von Willebrand factor gene. *J. Thromb. Haemost.* **2**, 2271-2273.

23 Berber, E., James, P. D., Hough, C. and Lillicrap, D. (2009) An assessment of the pathogenic significance of the R924Q von Willebrand factor substitution. *J. Thromb. Haemost.* **7**, 1672-1679.

24 Van Biggelaar, M. Den, Meijer, A. B., Voorberg, J. and Mertens, K. (2009) Intracellular cotrafficking of factor VIII and von Willebrand factor type 2N variants to storage organelles. *Blood* **113**, 3102-3109.

25 Stel, H. V., Sakariassen, K. S. Scholte, B.J., Veerman, E. C. I., van der Kwast, Th. H., De Groot, Ph. G., S. J. J. and V. M. J. A. (1984) Characterization of 25 Monoclonal Antibodies to FVIII-von Willebrand Factor: Relatioship Between Ristocetin-Induced Platelet Aggregation and Platelet Adherence to Subendothelium. *Blood* **63**, 1408-1415.

26 van den Biggelaar, M., Madsen, J. J., Faber, J. H., Zuurveld, M. G., van der Zwaan, C., Olsen, O. H., Stennicke, H. R., Mertens, K. and Meijer, A. B. (2015) Factor VIII Interacts with the Endocytic Receptor Low-density Lipoprotein Receptor-related Protein 1 via an Extended Surface Comprising "Hot-Spot" Lysine Residues. *J. Biol. Chem.* **290**, 16463-76.BN

27 Meems, H., van den Biggelaar, M., Rondaij, M., van der Zwaan, C., Mertens, K. and Meijer, A. B. (2011) C1 domain residues Lys 2092 and Phe 2093 are of major importance for the endocytic uptake of coagulation factor VIII. *Int. J. Biochem. Cell Biol.* **43**, 1114-1121.

28 Bloem, E., Meems, H., van den Biggelaar, M., van der Zwaan, C., Mertens, K. and Meijer, A. B. (2012) Mass spectrometry-assisted study reveals that lysine residues 1967 and 1968 have opposite contribution to stability of activated factor VIII. *J. Biol. Chem.* **287**, 5775-5783.

29 Dayon, L., Pasquarello, C., Hoogland, C., Sanchez, J. C. and Scherl, A. (2010) Combining low- and high-energy tandem mass spectra for optimized peptide quantification with isobaric tags. *J. Proteomics* **73**, 769-777.

30 Purvis, A. R., Gross, J., Dang, L. T., Huang, R.-H., Kapadia, M., Townsend, R. R. and Sadler, J. E. (2007) Two Cys residues essential for von Willebrand factor multimer assembly in the Golgi. *Proc. Natl. Acad. Sci. U. S. A.* **104**, 15647-15652.

31 Bloem, E., Ebberink, E. H. T. M., van den Biggelaar, M., van der Zwaan, C., Mertens, K. and Meijer, A. B. (2015) A novel chemical footprinting approach identifies critical lysine residues involved in the binding of receptor-associated protein to cluster II of LDL receptor-related protein. *Biochem. J.* **468**, 65-72.

32 Furlan, M., Robles, R. and Lämmle, B. (1996) Partial purification and characterization of a protease from human plasma cleaving von Willebrand factor to fragments produced by in vivo proteolysis. *Blood* **87**, 4223-34.

33 Wu, T., Lin, J., Cruz, M. A., Dong, J. F. and Zhu, C. (2010) Force-induced cleavage of single VWF A1A2A3-tridomains by ADAMTS-13. *Blood* **115**, 370-378.

34 Zhang, Q., Zhou, Y.-F., Zhang, C.-Z., Zhang, X., Lu, C. and Springer, T. A. (2009) Structural specializations of A2, a force-sensing domain in the ultralarge vascular protein von Willebrand factor. *Proc. Natl. Acad. Sci. U. S. A.* **106**, 9226-9231.

35 Vlot, A. J., Koppelman, S. J., van den Berg, M. H., Bouma, B. N. and Sixma, J. J. (1995) The affinity and stoichiometry of binding of human factor VIII to von Willebrand factor. *Blood* **85**, 3150-3157.

36 Vlot, A. J., Koppelman, S. J., Meijers, J. C., Dama, C., van den Berg, H. M., Bouma, B. N., Sixma, J. J. and Willems, G. M. (1996) Kinetics of factor VIII-von Willebrand factor association. *Blood* **87**, 1809-1816.

37 Yee, A., Gildersleeve, R. D., Gu, S., Kretz, C. a., McGee, B. M., Carr, K. M., Pipe, S. W. and Ginsburg, D. (2014) A von Willebrand factor fragment containing the D'-D3 domains is sufficient to stabilize coagulation factor VIII in mice. *Blood* **124**, 445-452.

38 Schneppenheim, R., Lenk, H., Obser, T., Oldenburg, J., Oyen, F., Schneppenheim, S., Schwaab, R., Will, K. and Budde, U. (2004) Recombinant expression of mutations causing von Willebrand disease type Normandy: Characterization of a combined defect of factor VIII binding and multimerization. *Thromb. Haemost.* **92**, 36-41.

39 Jorieux, S., Gaucher, C., Piétu, G., Chérel, G., Meyer, D. and Mazurier, C. (1994) Fine epitope mapping of monoclonal antibodies to the NH\subscript{2}-terminal part of von Willebrand factor (vWF) by using recombinant and synthetic peptides: interest for the localization of the factor VIII binding domain. *Br. J. Haematol.* **87**, 113-118.

40 Takahashi, Y., Kalafatis, M., Girma, J. P., Sewerin, K., Andersson, L. O. and Meyer, D. (1987) Localization of a factor VIII binding domain on a 34 kilodalton fragment of the N-terminal portion of von Willebrand factor. *Blood* **70**, 1679-1682.

41 Ebberink, E. H. T. M., Bouwens, E. A. M., Bloem, E., Boon-spijker, M., van den Biggelaar, M., Voorberg, J., Meijer, A. B. and Mertens, K. (2017) Factor VIII / V C-domain swaps reveal discrete C-domain roles in factor VIII function and intracellular trafficking. *Haematologica* **102**, 686-694.

42 Chiu, P. L., Bou-Assaf, G. M., Chhabra, E. S., Chambers, M. G., Peters, R. T., Kulman, J. D. and Walz, T. (2015) Mapping the interaction between factor VIII and von Willebrand factor by electron microscopy and mass spectrometry. *Blood* **126**, 935-938.

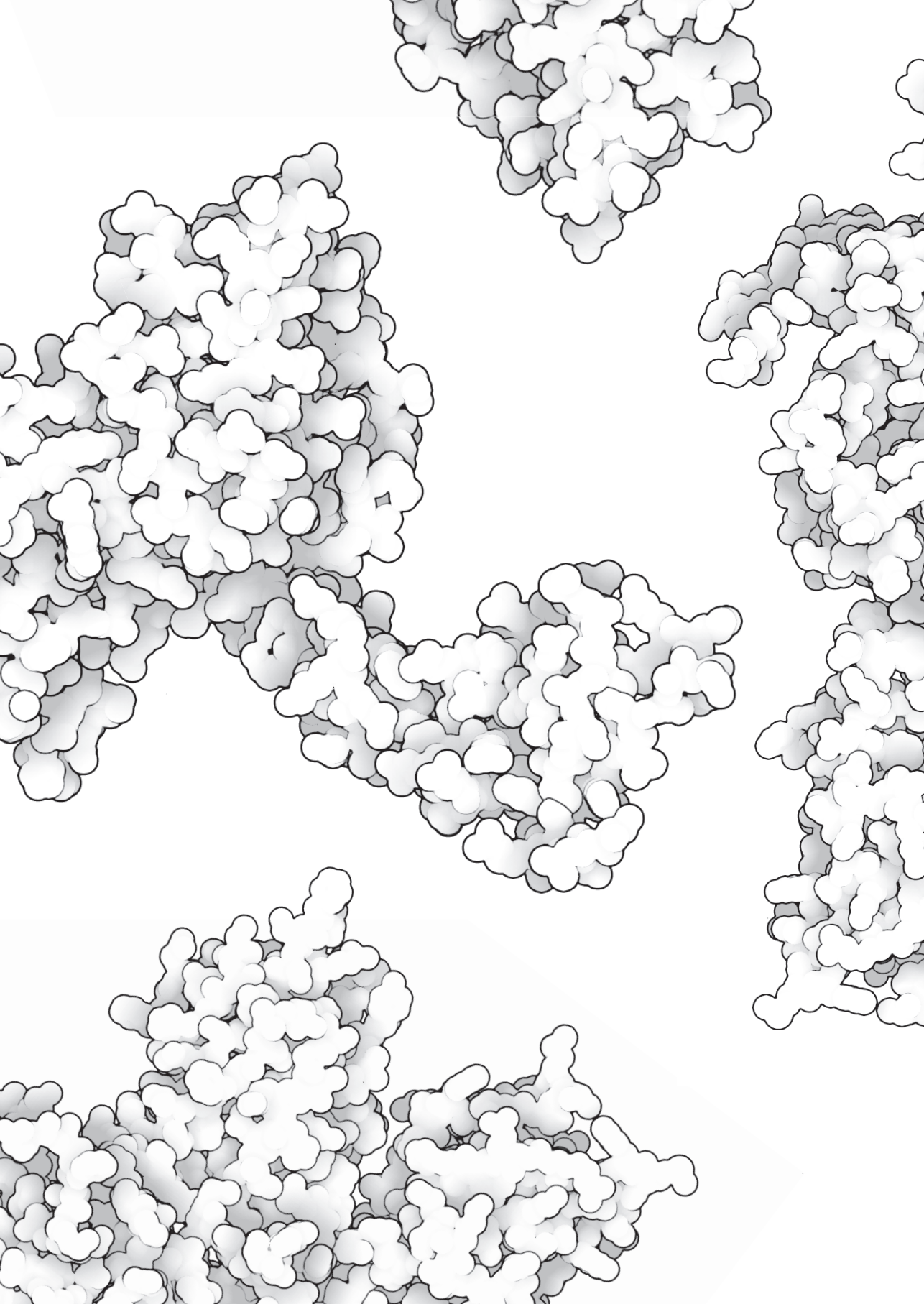

Chapter 4

Endocytosis by macrophages: Interplay of macrophage scavenger receptor-1 and LDL receptor-related protein-1

Eelke P. Béguin [1], Małgorzata A. Przeradzka [1], Esmée F.J. Janssen [1], Henriët Meems [1], Magdalena Sedek [1], Carmen van der Zwaan [1], Koen Mertens [1], Maartje van den Biggelaar [1,2], Alexander B. Meijer [1,2], Marjon J. Mourik [1]

Haematologica. 2020;105(3):E133-E137

[1]Molecular and Cellular Hemostasis, Sanquin Research, 1066 CX Amsterdam, The Netherlands,

[2]Department of Biomolecular Mass Spectrometry and Proteomics, Utrecht Institute for Pharmaceutical Sciences, Utrecht University, Utrecht, The Netherlands

Multiple receptors may mediate the cellular uptake of a single protein and thereby affect the plasma level of the involved protein. In case of Von Willebrand factor (VWF) these receptors include LDL receptor-related protein-1 (LRP-1), Macrophage scavenger receptor-1 (MSR-1, SR-AI or CD204), the Macrophage Galactose-type lectin (CLEC10A, MGL or CD301), Siglec-5 and the Asialoglycoprotein receptor (ASGPR).[1] In the present study, we aimed to gain insight into the interplay of multiple receptors to the cellular internalization of a single ligand like VWF.

The macrophages in the liver and spleen have been reported to contribute considerably to the cellular uptake of VWF.[2-4] Previously, we have shown that also human monocyte-derived macrophages (MDM) internalize VWF via a mechanism that depends on LRP-1.[5] We now analyzed the cell surface proteome of MDM using mass spectrometry analysis to identify putative other VWF clearance receptors on MDM. To this end, extracellular proteins were labelled with membrane impermeable sulfo-NHS-biotin after which samples were subjected to mass spectrometry processing and enrichment of biotin-labeled peptides using a biotin pull-down approach. Mass spectrometry analysis of the collected proteins resulted in the identification of more than a thousand potential cell surface proteins (*Online Supplementary Figure S1*). Several peptides of the VWF receptors LRP-1 and MSR-1 were identified as well as one peptide that is shared by Siglec-5 and Siglec-14. The estimated copy numbers of these receptors revealed a markedly higher expression of LRP-1 and MSR-1 compared to Siglec-5/14. We therefore focused our study on the possible dual mechanism by which LRP-1 and MSR-1 may cooperate in the cellular uptake of VWF by MDM.

Studying the uptake mechanism of VWF is hampered by the fact that flow-induced shear force is required to facilitate VWF internalization by MDM. For LRP-1, others have previously shown that full-length VWF only binds LRP-1 under shear stress conditions.[6] This observation is compatible with our previous finding the MDM internalize VWF via LRP-1 in a flow-dependent manner.[5] Shear force may induce a configurational change in VWF from a globular shape to an elongated shape, thereby exposing binding sites for clearance receptors like LRP-1 and possibly also MSR-1. In the present study, confocal microscopy and flow cytometry analysis showed that N-terminal VWF fragments, comprising the D'D3 and D'D3A1 domains, were effectively internalized by MDM in a shear-independent manner (Figure 1A-C). This observation may fit the model that the receptor binding sites of VWF are accessible for interaction with LRP-1 and/or MSR-1 within the D'D3A1 fragment.

To further dissect the role of LRP-1 in these observations, we utilized the U87MG cell line, which has been shown to express relatively high levels of LRP-1.[7] Our mass spectrometry approach confirmed the expression of LRP-1 in these cells and showed that MDM and U87MG cells contained similar levels of LRP-1 (*Online Supplementary Table S1*). Although we cannot fully exclude their presence using this approach, MSR-

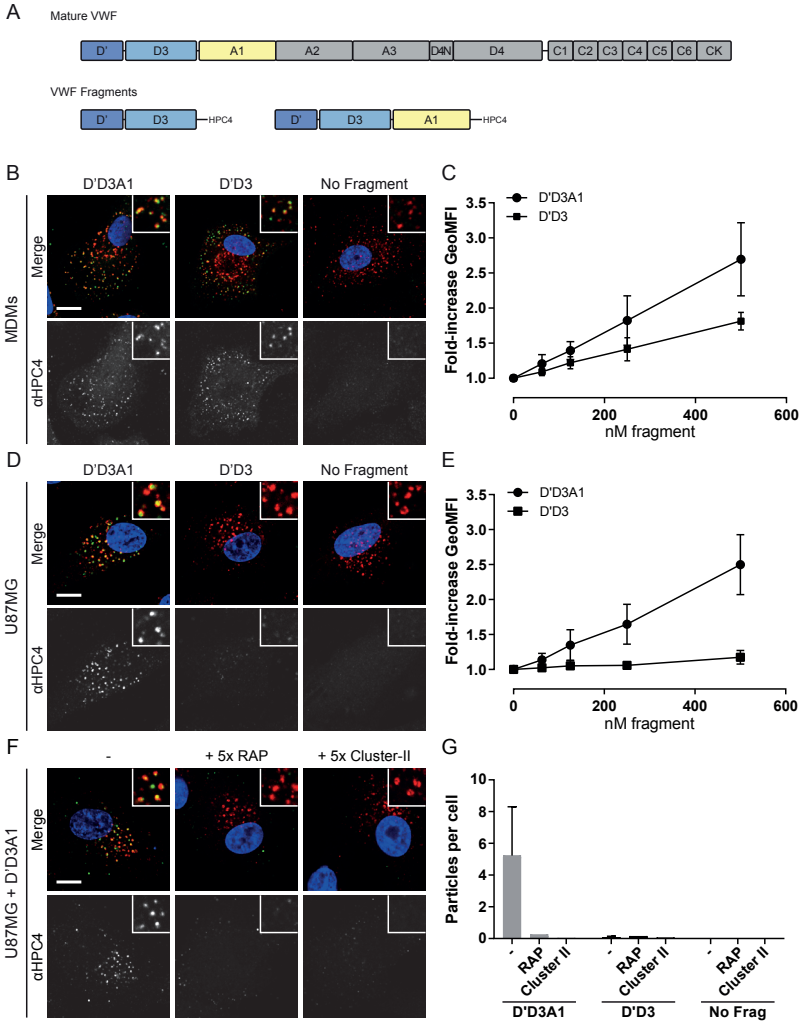

Figure 1, Uptake of VWF fragments D'D3A1 and D'D3 in MDMs and U87MG cells. (A) Schematic representation of the domains of VWF and the generated fragments. Both fragments were equipped with a C-terminal HPC4 tag for purification and detection purposes. (B,D) Uptake of 100 nM D'D3A1 or D'D3 in MDM and U87MG cells. Cells were stained with antibodies against HPC4 (green) and EEA1 (red), and Hoechst (blue). Scale bar represents 10 µm. Sites of co-localization result in a yellow staining. (C,E) Flow cytometry measurements of fragment uptake in MDM (C) and U87MG cells (E). Cells were incubated with concentrations of fragments of 0, 63, 125, 250 and 500 nM. Data show the fold-increase (mean ± standard deviation [SD]) of the geometric mean fluorescent intensity (GeoMFI) after correction for background staining in cells incubated with buffer only. Data were obtained from four independent experiments. (F) U87MG cells were incubated with 75 nM D'D3A1 or D'D3 with or without a five times molar excess of RAP or LRP-1 Cluster-II. Cells were stained with anti-HPC4 (green), anti-EEA1 (red) and Hoechst (blue). Scale bar represents 10 µm. Sites of co-localization result in a yellow staining (G) Quantification of confocal images. Number of particles per cell were counted in tile scans from four independent experiments. For each experiment 300-500 cells were analyzed. Data represent mean ± SD.

1 and other VWF clearance receptors were not identified on U87MG cells (*Online Supplementary Table S1*). Microscopy and flow cytometry studies revealed that U87MG cells effectively internalized D'D3A1, but not D'D3 (Figure 1D-E). The presence of LRP-antagonist Receptor Associated Protein (RAP) abrogated the internalization of D'D3A1 by these cells (Figure 1F-G). Likewise, the cellular uptake of D'D3A1 was blocked in the presence of an excess of purified LRP-1 domain Cluster II. These findings indicate that LRP-1 mediates the uptake of D'D3A1 by U87MG cells. These observations are in line with the finding that the A1 domain of VWF comprises a binding site for LRP-1.[8] Indeed, surface plasmon resonance (SPR) analysis showed that, in contrast to D'D3, D'D3A1 did bind to Cluster II, thereby confirming that the A1 domain of D'D3A1 is crucial for the interaction with LRP-1 (*Online Supplementary Table S2*).

In parallel, we investigated the role of MSR-1 in the internalization of VWF fragments D'D3 and D'D3A1. Binding studies showed a dose-dependent interaction of the extracellular domain of MSR-1 (sMSR-1) with both VWF fragments (*Online Supplementary Figure S3*). This observation is in agreement with the study by Wohner *et al*. that revealed binding sites for MSR-1 in the D'D3 and the A1 domain of VWF.[9] However, internalization experiments revealed that only the cellular uptake of D'D3 can be blocked by an antibody directed against MSR-1 (Figure 2). As the antibody inhibits both the binding of D'D3 and D'D3-A1 to the ligand binding domain of MSR-1 (*Online Supplementary Figure S4*), this indicates that the uptake of D'D3-A1 proceeds via an alternative mechanism, possibly via LRP-1. To address this issue, MDM were incubated with the fragments in the presence of the LRP antagonist RAP or an excess Cluster II. Competing with RAP or Cluster II minimized the uptake of the D'D3-A1 fragment in MDM (Figure 2B). Surprisingly, the uptake of D'D3 by MDM was similarly affected (Figure 2A). This suggests that internalization of both D'D3 and D'D3A1 is dependent on LRP-1 in spite of the notion that the LRP-1 binding site resides in the A1 domain of VWF.

To explain the remarkable dependence of D'D3 uptake by MDM on both LRP-1 and MSR-1, we hypothesized that MSR-1-induced D'D3 internalization may be mediated by LRP-1. We therefore assessed whether sMSR-1 can directly interact with LRP-1 using SPR analysis. To this end, sMSR-1 was passed over immobilized Cluster II on an SPR sensor chip. A dose dependent-binding response was observed that could be effectively blocked by prior incubation of sMSR-1 with Cluster II (Figure 3A). This finding implies that sMSR-1 may indeed interact with LRP-1. Subsequent confocal microscopy analysis showed that, upon incubation with U87MG cells, sMSR-1 was transported to the early endosomes via a process that was inhibited in presence of an excess of RAP or Cluster II (Figure 3B). These observations imply that sMSR-1 is endocytosed by U87MG cells via an LRP-1 dependent mechanism. In line with this hypothesis, we found that sMSR-1 could induce the internalization of D'D3 by U87MG cells (Figure 3C). Taken together,

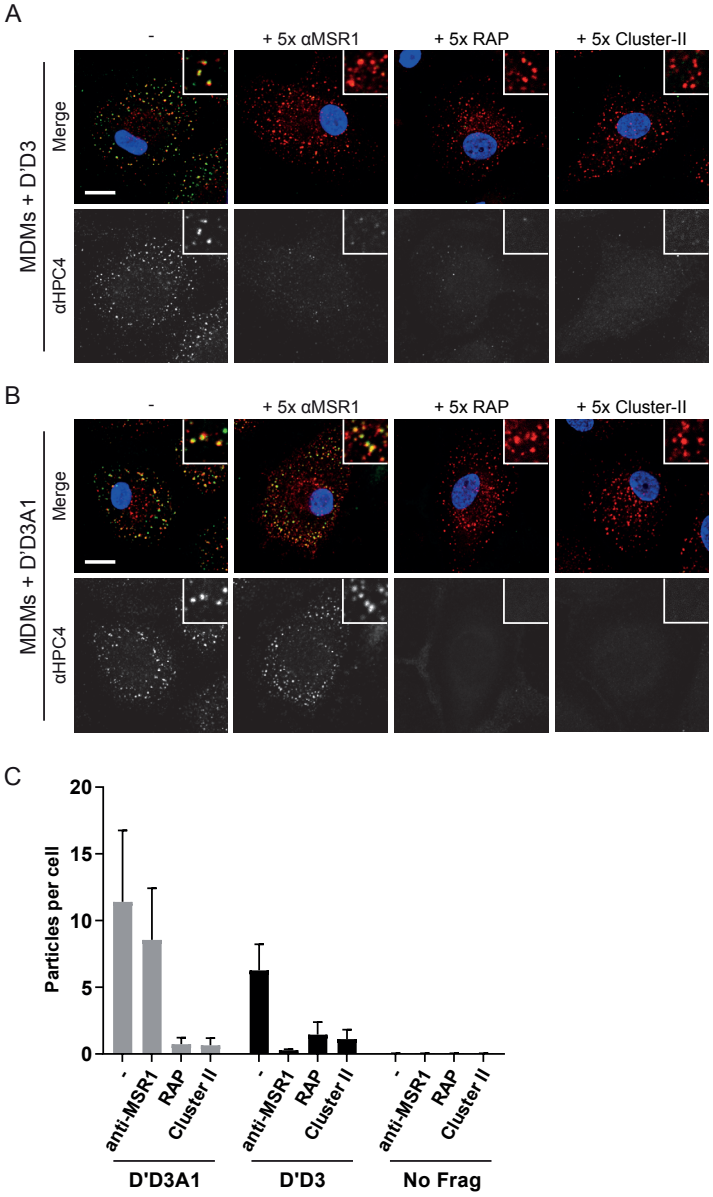

Figure 2. Uptake of D'D3 by MDM is mediated by MSR-1 and LRP-1. (A,B) Blocking MSR-1 only affects D'D3 interaction, whereas blocking LRP-1 affects both fragments. MDM were incubated with 75 nM D'D3A1 or D'D3 with or without a five times molar excess of anti-MSR1 blocking antibodies, RAP or LRP-1 Cluster-II. Cells were stained with anti-HPC4 (green), anti-EEA1 (red) and Hoechst (blue). Sites of co-localization result in yellow staining. In MSR-1 blocking conditions, red staining represents EEA-1 as well as MSR-1 as these antibodies were from the same species and isotype. Scale bar represents 10 µm. (C) Quantification of confocal images. Number of particles per cell were counted in tile scans from four independent experiments. For each experiment 300-500 cells were analyzed. Data in C represents mean ± SD.

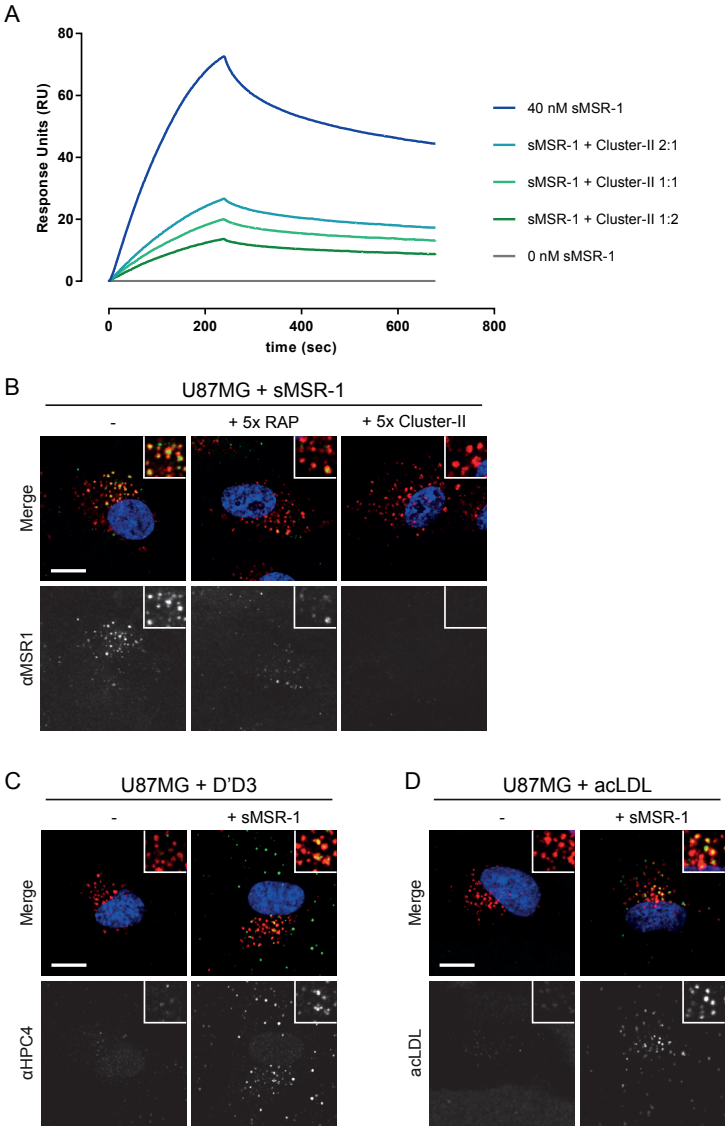

Figure 3. MSR-1 associates with LRP-1 to mediate D'D3 uptake. SPR and cell-based experiments to explore the interaction between MSR-1 and LRP-1. SPR and cell-based experiments to explore the interaction between MSR-1 and LRP-1. (A) Binding of soluble MSR-1 (sMSR-1) to 18 fmol/mm^2 immobilized LRP-1 Cluster-II in the absence and presence of increasing concentrations of soluble Cluster-II. The concentration of sMSR-1 was kept at 40 nM and the concentration of soluble Cluster-II was 20, 40 or 80 nM. (B) Uptake of 100 nM sMSR-1 by U87MG cells in the absence or presence of a five times molar excess of RAP or Cluster-II. Cells were stained with anti-MSR-1 (green), anti-EEA1 (red) and Hoechst (blue). Sites of co-localization result in yellow staining. (C) Uptake of 100 nM D'D3 in the absence and presence of 200 nM sMSR-1. Cells were stained for anti-HPC4 (green), anti-EEA1 (red) and Hoechst (blue). (D) Uptake of 2.5 µg/mL acLDL in the absence and presence of 200 nM sMSR-1. The scale bar represents 10 µm.

these data suggest that sMSR-1 may act as a bridging receptor between LRP-1 and D'D3, thereby mediating the uptake of this fragment via LRP-1. To assess whether this mechanism of endocytosis also holds true for another MSR-1 ligand, we incubated fluorescent acLDL with the U87MG cells in the presence and absence of sMSR-1. No uptake of acLDL was observed in the absence of sMSR-1, however, as for D'D3, the presence of sMSR-1 induced localization of acLDL to the early endosomes (Figure 3D).

These data provide evidence for a role for LRP-1 as a co-receptor for MSR-1 in the uptake of ligands by MDM. A similar mechanism has been proposed for the uptake of the uPA-PAI-1 complex via the urokinase plasminogen activator receptor (uPAR), although details are different. [10] The uPAR can bind urokinase plasminogen activator (uPA) with and without its inhibitor PAI-1. The uPAR-uPA complex is stable, whereas the uPAR-uPA-PAI-1 complex is internalized via LRP-1. [10] Also in this case, LRP-1 serves as a co-receptor which, in concert with a primary receptor (uPAR), mediates the internalization of a ligand (uPA-PAI-1). We and others have previously shown that the LRP-1 dependent uptake of Factor VIII (FVIII) also proceeds via a dual receptor mechanism. In addition to the interaction with LRP-1, FVIII requires prior binding to other structural elements on the cell surface to mediate the internalization by the cells. [11,12] These findings indicate that LRP-1 may serve as a co-receptor for multiple primary receptors, and multiple ligands.

Studies in mice have shown that LRP-1 and MSR-1 play a physiological role in VWF clearance as well. [6,9] However, many issues involving this mechanism remain to be resolved. For instance, others have shown that PMA-stimulated THP-1 cells can bind VWF and internalize it via a shear-independent mechanism. [9,13] In our hands, MDM only internalize VWF in a shear-dependent manner. Understanding the differences between these cellular systems remains a topic for further investigation. The same holds true for the expanding list of putative endocytic receptors for VWF. The relative importance of these receptors to mediate the uptake of VWF remains an open question.

Based on the data presented in this study, we propose the following model to explain the relationship between the two abundant VWF receptors on MDM. Both LRP-1 and MSR-1 associate with regions within D'D3A1, thereby initiating two endocytic pathways that are both regulated by LRP-1. The first pathway follows a direct association of the VWF A1 domain to LRP-1. In the second pathway, VWF interacts to MSR-1 via regions in the D'D3 assembly, which subsequently associates to LRP-1 for endocytosis.

REFERENCES

1. O'Sullivan JM, Ward S, Lavin M, O'Donnell JS. Von Willebrand factor clearance - biological mechanisms and clinical significance. Br J Haematol.2018;183(2):185-195.
2. Rawley O, O'Sullivan JM, Chion A, Keyes S, Lavin M, van Rooijen N, Brophy TM, Fallon P, Preston RJS, O'Donnell JS. Von Willebrand factor arginine 1205 substitution results in accelerated macrophage-dependent clearance in vivo. J Thromb Haemost.2015;13(5):821-826.
3. O'Sullivan JM, Aguila S, McRae E, Ward SE, Rawley O, Fallon PG, Brophy TM, Preston RJS, Brady L, Sheils O, Chion A, O'Donnell JS. N-linked glycan truncation causes enhanced clearance of plasma-derived von Willebrand factor. J Thromb Haemost.2016;14(12):2446-2457.
4. Van Schooten CJ, Shahbazi S, Groot E, et al. Macrophages contribute to the cellular uptake of Von Willebrand factor and factor VIII in vivo. Blood.2008;112(5):1704-1712.
5. Castro-Núñez L, Dienava-Verdoold I, Herczenik E, Mertens K, Meijer AB. Shear stress is required for the endocytic uptake of the factor VIII-von Willebrand factor complex by macrophages. J Thromb Haemost.2012;10(9):1929-1937.
6. Rastegarlari G, Pegon JN, Casari C, Soline Odouard, Ana-Maria Navarrete, Nathalie Saint-Lu, Bart J van Vlijmen, Paulette Legendre, Olivier D Christophe, Cécile V Denis, Peter J Lenting. Macrophage LRP1 contributes to the clearance of von Willebrand factor. Blood.2012;119(9):2126-2134.
7. Maletínská L, Blakely EA, Bjornstad KA, Deen DF, Knoff LJ, Forte TM. Human glioblastoma cell lines: levels of low-density lipoprotein receptor and low-density lipoprotein receptor-related protein. Cancer Res.2000;60(8):2300-2303.
8. Wohner N, Legendre P, Casari C, Christophe OD, Lenting PJ, Denis CV. Shear stress-independent binding of von Willebrand factor-type 2B mutants p.R1306Q & p.V1316M to LRP1 explains their increased clearance. J Thromb Haemost.2015;13(5):815-820.
9. Wohner N, Muczynski V, Mohamadi A, Paulette Legendre, Valérie Proulle, Gabriel Aymé, Olivier D. Christophe, Peter J. Lenting, Cécile V. Denis, Caterina Casari. Macrophage scavenger receptor SR-AI contributes to the clearance of von Willebrand factor. Haematologica.2018;103(4):728-737.
10. Conese M. alpha-2 Macroglobulin receptor/Ldl receptor-related protein (Lrp)- dependent internalization of the urokinase receptor. J Cell Biol.1995;131(6):1609-1622.
11. Sarafanov AG, Ananyeva NM, Shima M, Saenko EL. Cell Surface Heparan Sulfate Proteoglycans Participate in Factor VIII Catabolism Mediated by Low Density Lipoprotein Receptor-related Protein. J Biol Chem.2001;276(15):11970-11979.
12. Castro-Núñez L, Koornneef JM, Rondaij MG, Esther Bloem, Carmen van der Zwaan, Koen Mertens, Alexander B Meijer, Henriet Meems. Cellular uptake of coagulation factor VIII: Elusive role of the membrane-binding spikes in the C1 domain. Int J Biochem Cell Biol.2017;89:34-41.
13. Chion A, O'Sullivan JM, Drakeford C, Gudmundur Bergsson, Niall Dalton, Sonia Aguila, Soracha Ward, Padraic G Fallon, Teresa M Brophy, Roger J S Preston, Lauren Brady, Orla Sheils, Michael Laffan, Thomas A J McKinnon, James S O'Donnell. N-linked glycans within the A2 domain of von Willebrand factor modulate macrophage-mediated clearance. Blood.2016;128(15):1959-1968.

SUPPLEMENTARY SECTION:

Methods

Culture of MDMs and U87MG cells

Blood samples of healthy volunteers were used in accordance with Dutch regulations and after approval from the Sanquin Ethical Advisory Board in accordance with the Declaration of Helsinki. Written informed consent was given by all participants. Human monocytes were isolated from blood using MACS CD14-microbeads (Miltenyi Biotec) and were differentiated to macrophages using 50 ng/ml hrM-CSF (PeproTech) in RPMI-1640 (Lonza), supplemented with 10% FCS (Bodinco). [1] U87MG cells were obtained from ATCC (HTB-14) and cultured in phenol red-free DMEM-F12 with HEPES and L-glutamine (Thermo Fisher Scientific) supplemented with 10% FCS.

Expression and purification of recombinant proteins

HPC4 mouse hybridoma (HB9892) was obtained from ATCC and cultured in IMDM supplemented with 10% heat-inactivated fetal calf serum (FCS). HPC4 antibody was purified with protein G sepharose according to the manufacturer's protocol. The D'D3 and D'D3A1 fragments were designed in pcDNA3.1(+) and contained two point mutations at position C1099S and C1142S in order to prevent dimerization as described. [2] A HPC4 tag was fused to the C-terminus of both fragments which was used for purification and detection. Sequences were codon optimized to enhance expression in human cells. Coding regions of both constructs were verified by sequence analysis using the BigDye Terminator Sequencing kit (Applied Biosystem). Recombinant proteins were transiently expressed in HEK 293 Freestyle cells using Polyethylenimine (PEI) transfection. Cells were grown in Freestyle Expression medium (Thermo Fisher Scientific, Waltham, MA). Five days after transfection, proteins were purified from medium by immunoaffinity chromatography using CNBr-Sepharose 4B coupled with an anti-HPC4 antibody purified from mouse hybridoma HB9892. Fragments were loaded on the anti-HPC4 column in 20 mM Tris-HCl (pH 7.4), 100 mM NaCl, 10 mM $CaCl_2$. After loading, the column was washed with 20 mM Tris-HCl (pH 7.4), 1 M NaCl, 10 mM $CaCl_2$. Proteins were eluted with 20 mM Tris-HCl (pH 7.4), 100 mM NaCl, 5 mM EDTA. Subsequently, protein-containing fractions were dialyzed against 50 mM HEPES (pH 7.4), 150 mM NaCl, 10 mM $CaCl_2$, 50% (v/v) glycerol and stored at -20 °C. Concentration of the fragments was assessed using a Pierce BCA Protein Assay Kit (Thermo Fisher Scientific). Glutathione-S-transferase - Receptor Associated Protein (gst-RAP) and LRP1 Cluster-II expression and purification was performed as described. [3,4]

Uptake of VWF fragments

Cells were washed with HEPES buffer (10 mM HEPES (pH 7.4), 135 mM NaCl, 10 mM KCl, 5 mM $CaCl_2$ 2 mM MgSO4) and incubated with VWF fragments for 30 minutes at 37 °C in the absence or presence of a 5x molar excess of RAP, LRP-cluster II or mouse monoclonal anti-human SR-A1/MSR (clone #351620, R&D systems). After incubation, cells were washed and fixed in 4% paraformaldehyde (Electron microscopy sciences) in PBS for 15 minutes.

Immunofluorescence labeling and confocal imaging

After fixation, cells were washed with TBS followed by blocking and permeabilization with staining buffer (1% BSA, 0.1% saponin, 5 mM $CaCl_2$ in TBS). Cells were sequentially incubated with primary and secondary antibodies diluted in staining buffer and counter stained with Hoechst 33342 and HCS CellMask™ deep red (Thermo Fisher Scientific) for quantification purposes. Samples were imaged on a Leica SP8 confocal laser scanning microscope (Leica microsystems) equipped with a HC PL APO CS2 63x/1.40 oil immersion objective. Tile scans were collected for quantification and analyzed using ImageJ (version 1.52d, Wayne Rasband; National Institutes of Health) and Graphpad prism 7 (GraphPad Prism Software Inc.) software.

Antibodies for immunofluorescent labeling

Primary antibodies used for labeling were: mouse monoclonal EEA-1 IgG1(BD biosciences, San Jose, CA), mouse monoclonal anti-HPC4 IgG1 (see above, purified from mouse hybridoma HB9892), rabbit polyclonal HPC4 IgG (Cell Signaling technology, Beverly, MA) and mouse monoclonal IgG2b anti-MSR-1(Clone #351615, R&D Systems). Secondary antibodies were: goat anti-mouse Alexa Fluor 488, goat anti-mouse Alexa Fluor 568 and F (ab')2-Goat anti-Rabbit IgG Alexa Fluor 488 (all from Thermo Fisher Scientific).

Flow cytometry

Adherent cells were detached using a citric saline solution of 1% (w/v) KCl and 0.25% (w/v) Sodium citrate. After restoring the osmotic balance with the HEPES buffer described above, cells were placed in a V-bottom 96 wells plate using 2 x 10^5 cells per condition. Cells were incubated with VWF fragments for 30 minutes at 37 °C, washed and fixed similarly as described above. To stain for the VWF fragments directly, we conjugated anti-HPC4 antibodies to Pacific blue using a Pacific Blue™ protein labeling kit (Thermo Fisher Scientific). Since the binding of the HPC4 antibody is calcium sensitive we used the same staining protocol as described for immunofluorescence labeling. After incubating cells with antibodies, cells were washed twice with staining buffer and were then placed in TBS 2.5 mM $CaCl_2$ for analysis on a BD FACSCanto or

BD FACSCanto II (BD biosciences). Data was analyzed using FlowJo 10.4 (FlowJo, LLC, Ashland, OR) and Graphpad prism 7.

Cell surface labeling and mass spectrometry sample preparation

Cell surface proteins were labeled using a membrane-impermeable biotin label as described previously with minor modifications.[5] 10 cm Ø petri dishes of macrophages or U87MG cells were washed 3x with HEPES buffer and incubated for 30 min with 2 ml/dish 3 mM EZ-link Sulfo-NHS-LC-Biotin (Thermo Scientific) at 4 ºC. Excess label was quenched by washing 4x with ice-cold HEPES buffer with 100 mM glycine, and cells were lysed at RT with 100 µl 4% SDS, 100 mM Tris-HCl, 0.1 M DTT, 1x HALT protease inhibitor (Thermo Scientific). Lysates were processed using the FASP method.[6] 50 µg of the tryptic digests was subjected to strong-anion exchange using Empore Anion and Cation Exchange-SR Extraction disks (3M) as described[6], with elution buffer pHs of 11, 8, 6, 5, 4 and 3. The flow-through of fractions 8 and 11 were collected, acidified to pH <2.5 using trifluoroacetic acid and subjected to C18 desalting (named flow-through). Fractions were desalted using C18 StageTips.[7] The remainder of the tryptic digests was subjected to biotin pull-down by incubating peptides for 2 hours in 50 mM NH_4HCO_3, 150 mM NaCl pH 8.3 in 3 wells/sample of a SigmaScreen Streptavidin High Capacity Coated plates. Another round of pull-down was performed with the flow-through. Captured peptides were diluted using 70% acetonitrile, 5% formic acid. Samples were vacuum-dried to remove the acetonitrile and desalted in C18 StageTips.

Mass Spectrometry analysis and data processing

Peptides were separated on nanoscale C18 reverse chromatography coupled on line to an Orbitrap Fusion Tribrid mass spectrometer (Thermo Scientific) via a nanospray ion scource (Nanospray Flex Ion Scource, Thermo Scientific) as described previously previously.8 For the fractionated proteome the elution gradient was adjusted to 5-25% buffer B (pH 11), 5-30% buffer B (pH 5, 6, 8, flow-through) and 5-35% buffer B (pH 3, 4). For the biotin pull-down samples, the MS acquisition settings were adjusted to perform the MS2 analysis in the orbitrap analyzer, as has been described before for phosphopeptides.[8] All data were acquired with Xcalibur software. To identify proteins and peptides, raw files were analyzed with the MaxQuant (1.5.3.30) computational platform[9], using the Andromeda search engine by querying the human Uniprot database (release 3-2017, 70947 entries) using standard settings with the following adjustments. Protein quantification was based on unique peptides, the 'match between runs' option was enabled. In the cell surface samples, a variable modification comprising the biotin added mass (339.16166 Da), was added. Perseus 1.5.6.0 was used to estimate protein copy numbers with the proteomic ruler plugin.[10] These data, as well as the cell surface data, were loaded in Rstudio 1.1.383 (R version 3.4.2).[11] Reverse

values, potential contaminants and 'only identified by site' values were filtered out, as well as peptides without at least 2 valid values in 1 of the groups. Peptide numbers per protein were counted for the surface data, and these were coupled to the copy number estimates obtained from the proteome data. ComplexHeatmap 1.14.012 was used to generate heatmaps. The .raw MS files and search/identification files obtained with MaxQuant are available via ProteomeXchange [13] with identifier PXD011490.

Immunosorbent assay of VWF fragment binding to MSR-1

Microtiter plates were coated over night at 4 °C with human recombinant soluble MSR-1 (R&D Systems) or BSA using 50 µl/well of a 2.5 µg/ml solution. Wells were rinsed with wash buffer (50 mM Tris pH 7.4, 150 mM NaCl, 2 mM $CaCl_2$, 0.1% Tween 20) and blocked with working buffer (50 mM Tris pH 7.4, 150mM NaCl, 2 mM $CaCl_2$, 0.1% Tween 20, 0.1% PolyVinylPyrollidone) for 1 h at 37 °C to prevent non-specific binding. A concentration series of the VWF fragments diluted in working buffer were incubated for 2 h at 37 °C. On wells coated with BSA only the lowest and highest concentration of each fragment was examined. After incubation, unbound proteins were washed away and bound protein was detected by incubating sequentially with anti-HPC4 (10 µg/ml) and goat-anti-mouse HRP (1:5000, Southern biotech), both for 1 h. Peroxidase activity was detected using a tetramethylbenzidine substrate solution (TMB). Absorbance was measured at 450 nm.

Surface plasmon resonance analysis

SPR analysis was performed using a BIAcoreT200 biosensor system (Biacore AB, Uppsala, Sweden). For assessment of VWF fragment binding to LRP-1, LRP-1 purified from placenta (Biomac, Leipzig) was immobilized at ~2 fmol/mm^2 to a CM5-sensor chip via primary amino groups, using the amine-coupling kit as prescribed by the supplier. Varying concentrations of D'D3 and D'D3A1 ranging from 0 to 250 nM were passed over the immobilized LRP-1 for 240 s. For assessment of sMSR-1 (R&D systems) and Cluster-II binding to RAP, gst-RAP was coupled directly to a CM5 sensor chip at 8 fmol/mm^2. Concentrations ranging from 0 to 40 nM of Cluster-II and sMSR-1 were passed over immobilized gst-RAP for 240 s in SPR buffer. For assessment of sMSR-1 binding to LRP-1 Cluster-II, recombinant LRP-1 Cluster-II was directly coupled to a CM5 sensor chip at a density of ~18 fmol/mm^2. A concentration range of 0-80 nM sMSR-1 was passed over immobilized Cluster-II for 240 s. For the competition experiment we used 40 nM sMSR-1 and titrated in a concentration series of 0, 20, 40, and 80 nM Cluster-II. In all experiments, the proteins were diluted in SPR buffer containing 20 mM Hepes (pH 7.4), 150 mM NaCl, 5 mM $CaCl_2$ and 0.05% (v/v) Tween 20 and binding was measured at 25 °C at a flow rate of 30 µl/min. After each binding experiment the sensor chip was regenerated by washing repeatedly with 1M NaCl, 50 mM EDTA.

Binding curves were corrected for the binding response that was measured in the absence of an immobilized protein. Binding responses were plotted using Graphpad prism 7 software.

REFERENCES

1. Castro-Núñez L, Dienava-Verdoold I, Herczenik E, Mertens K, Meijer AB. Shear stress is required for the endocytic uptake of the factor VIII-von Willebrand factor complex by macrophages. J Thromb Haemost 2012;10(9):1929-1937.
2. Przeradzka MA, Meems H, van der Zwaan C, et al. The D' domain of von Willebrand factor requires the presence of the D3 domain for optimal factor VIII binding. Biochem J 2018;475(17):2819-2830.
3. Herz J, Goldstein JL, Strickland DK, Ho YK, Brown MS. 39-kDa protein modulates binding of ligands to low density lipoprotein receptor-related protein/a2-macroglobulin receptor. J Biol Chem 1991;266(31):21232-21238.
4. Bloem E, Ebberink EHTM, van den Biggelaar M, van der Zwaan C, Mertens K, Meijer AB. A novel chemical footprinting approach identifies critical lysine residues involved in the binding of receptor-associated protein to cluster II of LDL receptor-related protein. Biochem J 2015;468(1):65-72.
5. Béguin EP, van den Eshof BL, Hoogendijk AJ, et al. Integrated proteomic analysis of tumor necrosis factor α and interleukin 1β-induced endothelial inflammation. J Proteomics 2019;19289-101.
6. Wiśniewski JR, Zougman A, Nagaraj N, Mann M. Universal sample preparation method for proteome analysis. Nat Methods 2009;6(5):359-362.
7. Wisniewski JR, Zougman A, Mann M. Combination of FASP and StageTip-based fractionation allows in-depth analysis of the hippocampal membrane proteome. J Proteome Res 2009;8(12):5674-5678.
8. van den Eshof BL, Hoogendijk AJ, Simpson PJ, et al. Paradigm of Biased PAR1 (Protease-Activated Receptor-1) Activation and Inhibition in Endothelial Cells Dissected by Phosphoproteomics. Arterioscler Thromb Vasc Biol 2017;37(10):1891-1902.
9. Cox J, Mann M. MaxQuant enables high peptide identification rates, individualized p.p.b.-range mass accuracies and proteome-wide protein quantification. Nat Biotechnol 2008;26(12):1367-72.
10. Wiśniewski JR, Hein MY, Cox J, Mann M. A "Proteomic Ruler" for Protein Copy Number and Concentration Estimation without Spike-in Standards. Mol Cell Proteomics 2014;13(12):3497-3506.
11. Ritchie ME, Phipson B, Wu D, et al. limma powers differential expression analyses for RNA- sequencing and microarray studies. Nucleic Acids Res 2015;43(7):e47
12. Gu Z, Eils R, Schlesner M. Complex heatmaps reveal patterns and correlations in multidimensional genomic data. Bioinformatics 2016;32(18):2847-2849.
13. Vizcaíno JA, Deutsch EW, Wang R, et al. ProteomeXchange provides globally coordinated proteomics data submission and dissemination. Nat Biotechnol 2014;32(3):223-226.

Supplementary Table is available in the online version of the manuscript and upon request.

Supplemental Table S1. Protein copy number estimates and cell surface peptides of MDMs and U87MG cells. Cell surface peptides and estimated cell surface protein copy numbers per cell of MDMs (M1-3) and U87MG cells (U1-3). NA = not available.

SUPPLEMENTARY FIGURES:

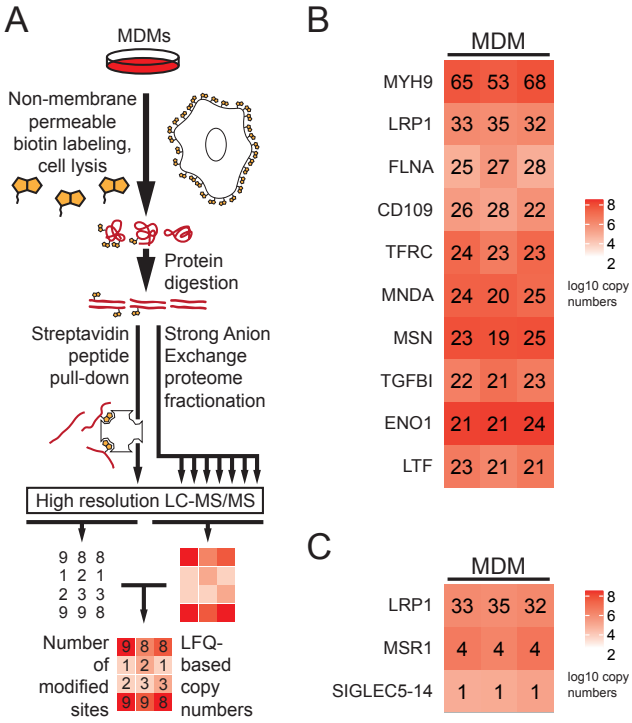

Supplemental Figure S1. Cell surface receptors of MDMs
Whole-cell proteome and cell surface proteome of MDMs were analyzed by mass spectrometry to map putative VWF clearance receptors (n=3). (A) Workflow of sample preparation and data processing. (B) The cell surface top 10 proteins. Numbers indicate the number of unique peptides identified per protein in each of the samples. The color coding represents log10 values of the estimated copy numbers per cell. (C) Identified VWF clearance receptors that were previously described, represented as in panel B.

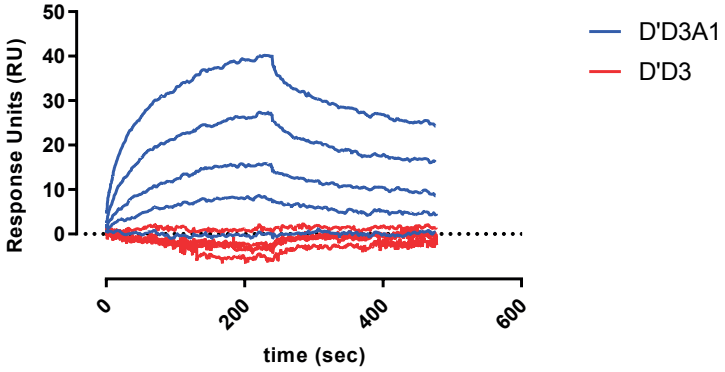

Supplemental Figure S2. Association of D'D3A1 to LRP-1 is dependent on the A1 domain
SPR analysis of D'D3A1 and D'D3 binding to immobilized LRP-1 (2 fmol/mm ^{2}). For each fragment a concentration series of 0, 31.25, 62.5, 125 and 250 nM was passed over the chip.

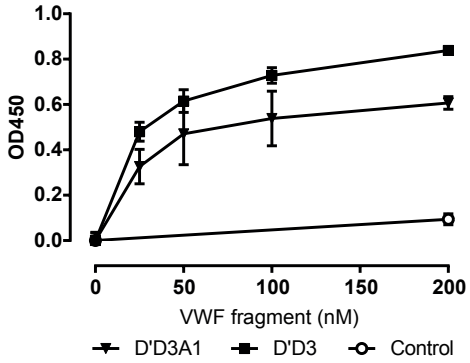

Supplemental Figure S3. The ability of VWF to bind sMSR-1 resides in the D'D3 region
Immunosorbent assay on D'D3A1 and D'D3 binding (0-200 nM) to wells coated with sMSR-1 or bovine serum albumin (BSA, control). Bound fragments were detected via TMB-hydrolysis following labeling with an anti-HPC4 antibody and polyclonal peroxidase-labeled goat anti-mouse antibody. Control data points represents the binding of 0 and 200 nM D'D3A1 to BSA.

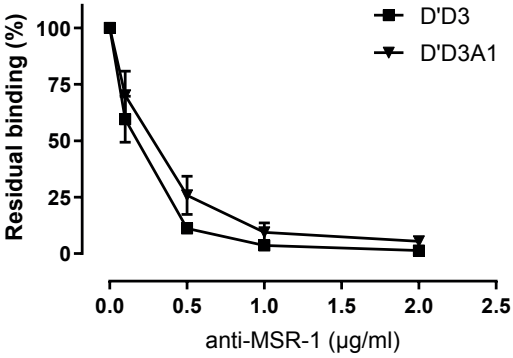

Supplemental Figure S4. Anti-MSR-1 competes with VWF-fragment binding to sMSR-1
Immunosorbent assay on D'D3A1 and D'D3 binding (40 nM) to wells coated with sMSR-1. Bound fragments were detected via TMB-hydrolysis following labeling with a polyclonal rabbit anti-HPC4 antibody and polyclonal peroxidase-labeled swine anti-rabbit antibody.

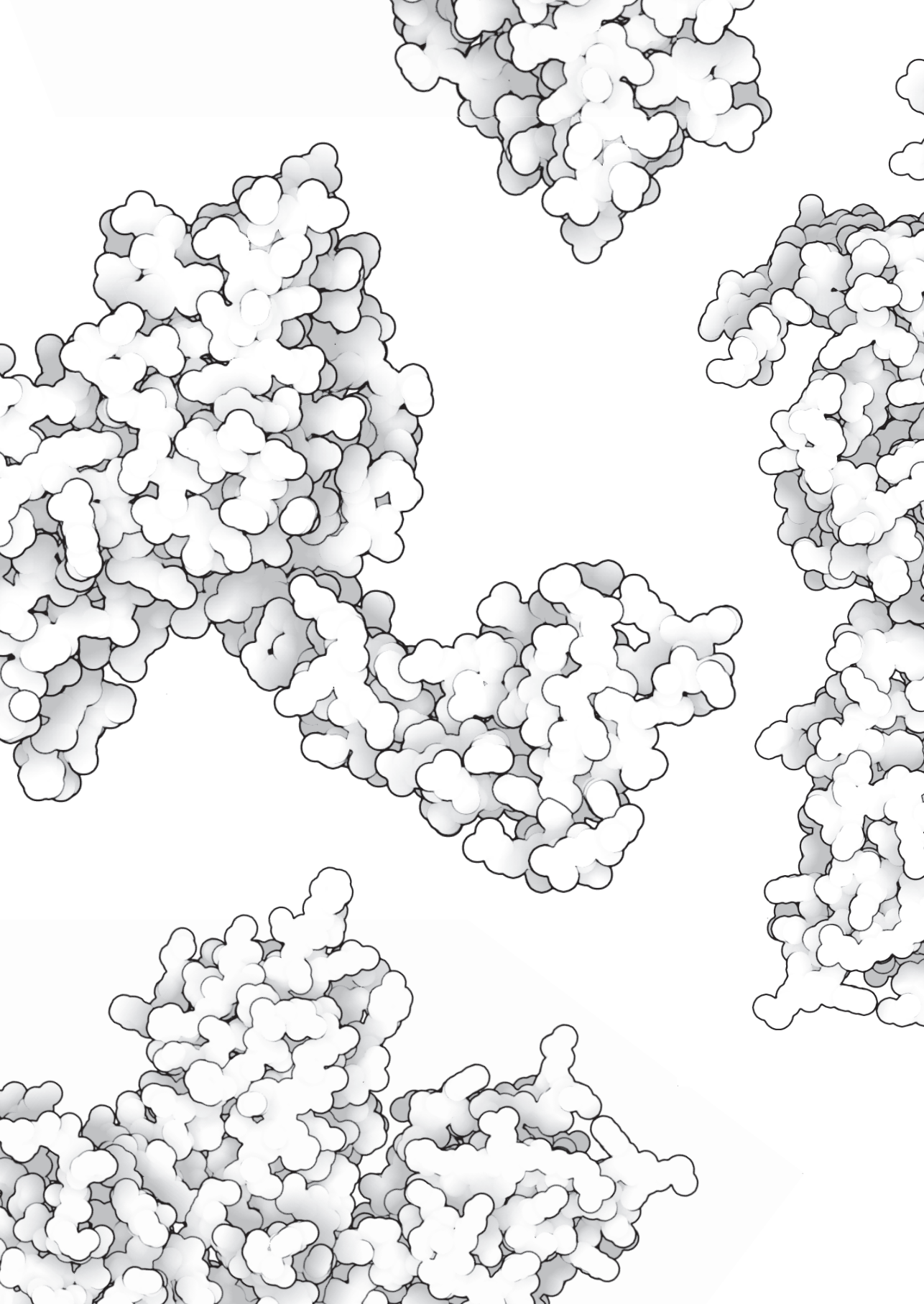

Chapter 5

Unique solvent-exposed hydrophobic residues in the C1 domain of factor VIII contribute to cofactor function and Von Willebrand Factor binding

Małgorzata A. Przeradzka*[1], Nadia Freato*[1], Mariette Boon-Spijker[1], Josse van Galen[1], Carmen van der Zwaan[1], Koen Mertens[1,2], Maartje van den Biggelaar[1], Alexander B. Meijer[1,3]

J Thromb Haemost. 2020;18(2):364-372

*authors contributed equally

[1]Molecular and Cellular Hemostasis, Sanquin Research, 1066 CX Amsterdam, The Netherlands,

[2]Department of Biomolecular Mass Spectrometry and Proteomics, Utrecht Institute for Pharmaceutical Sciences, Utrecht University, Utrecht, The Netherlands

ABSTRACT

Background

The identity of the amino acid regions of factor VIII (FVIII) that contribute to factor IXa (FIXa) and von Willebrand factor (VWF) binding has not been fully resolved. Previously, we observed that replacing the FVIII C1 domain for the one of factor V (FV) markedly reduces VWF binding and cofactor function. Compared to the FV C1 domain, this implies that the FVIII C1 domain comprises unique surface-exposed elements involved in VWF and FIXa interaction.

Objective

The aim of this study is to identify residues in the FVIII C1 domain that contribute to VWF and FIXa binding.

Methods

Structures and primary sequences of FVIII and FV were compared to identify surface-exposed residues unique to the FVIII C1 domain. The identified residues were replaced with alanine residues to identify their role in FIXa and VWF interaction. This role was assessed employing surface plasmon resonance analysis studies and enzyme kinetic assays.

Results

Five surface-exposed hydrophobic residues unique to the FVIII C1 domain, ie, F2035, F2068, F2127, V2130, I2139 were identified. Functional analysis indicated that residues F2068, V2130, and especially F2127 contribute to VWF and/or FIXa interaction. Substitution into alanine of the also surface-exposed V2125, which is spatially next to F2127, affected only VWF binding.

Conclusion

The surface-exposed hydrophobic residues in C1 domain contribute to cofactor function and VWF binding. These findings provide novel information on the fundamental role of the C1 domain in FVIII life cycle.

INTRODUCTION

Coagulation factor VIII (FVIII) is a large heterodimeric protein that serves its role in the coagulation cascade as a cofactor for activated factor IX (FIXa) during the proteolytic conversion of factor X (FX) into activated FX (FXa). FVIII is essential for proper functioning of the coagulation cascade as its functional absence has been associated with the X-linked bleeding disorder hemophilia A. [1]

FVIII is synthesized as a single chain protein of 2332 amino acids, which are organized into three homologous A domains, a B domain, and two homologous C domains. Short acidic amino acid regions comprising sulphated tyrosine amino acid residues are at the C-terminal side of A1 and A2 domains and at the N-terminal side of the A3 domain. [2, 3] Prior to secretion, FVIII is processed into a heavy chain (domains: A1-A2-B) and a light chain (domains: A3-C1-C2), which remain associated via electrostatic and metal ion-dependent interactions. [3] Because of limited proteolysis of the B domain, the molecular weight of FVIII in plasma ranges between 170 and 300 kDa. [2, 4-7] The crystal structures of FVIII show that the A domains are ordered in a triangular shape stacked on top of two C domains aligned in parallel. [8-10]

FVIII circulates in plasma in a tight complex with von Willebrand factor (VWF). In this complex, FVIII is protected from premature ligand binding, proteolytic degradation, and rapid plasma clearance. [11, 12] Upon initiation of the coagulation cascade, FVIII is activated by thrombin, which cleaves specific sites next to the acidic regions of FVIII. [3] This leads to the release of the B domain, disconnection of the A1 and A2 domains, and dissociation of the FVIII:VWF complex. After activation, FVIII can bind with high affinity to procoagulant phospholipid membranes that expose phosphatidylserine (PS) in the outer leaflet. Activated FVIII (FVIIIa) that is bound to the phospholipid surface provides a platform for effective interaction with FIXa resulting in the activated FX-generating complex.

Because of the high structural similarity between FVIII and factor V (FV), chimeric variants of FVIII and FV have been utilized in a number of studies to gain insight into the structure and function of FVIII and FV. [13-16] Factor V (FV) is the cofactor for FXa in the coagulation cascade and can form together with FXa and procoagulant phospholipid membranes the prothrombinase complex that efficiently converts prothrombin into thrombin. [8, 17] Using FVIII/FV chimeric proteins, the phospholipid binding role of the hydrophobic surface loops at the bottom of the C domains has, for instance, been addressed. [8, 13, 18-21] Another example is that contribution of the C domains to the intracellular trafficking of FVIII to the Weibel-Palade bodies has been studied in endothelial cells using chimeric FVIII/FV variants. [15]

Several FIXa and VWF interaction sites have been identified in FVIII. Competition studies with FVIII-derived peptides or isolated subunits indicated that the C2 domain may comprise a binding site for FIXa. [22] Using site-directed mutagenesis studies, inter-

action sites for FIXa have further been identified in the A2 and A3 domain. [23, 24] For the interaction with VWF, convincing evidence has been provided that the acidic region at the N-terminal side of the A3 domain is critical. [25-27] It has also been proposed that the C1 and C2 domains contribute to VWF binding as well. [18, 28, 29] However, a FVIII variant in which the C2 domain was replaced by the C2 domain of FV ($FVIII_{C2FVC2}$) displayed only a small reduction in VWF binding and nearly normal cofactor function. [15] This shows that the main interaction sites for VWF and FIXa are, most likely, outside the C2 domain.

In a previous study, we established that replacing the C1 domain of FVIII with that of FV ($FVIII_{C1FVC1}$) has a major impact on VWF binding and FVIII cofactor function. [15] This suggests that the C1 domain of FV lacks surface-exposed structural elements that can support the interaction with FIXa and VWF. In the present study, we now compare the C1 domains of FVIII and FV to identify the unique surface-exposed elements on the FVIII C1 domain that contribute to cofactor function and VWF binding. Results revealed five surface-exposed hydrophobic residues that were either more polar or more buried in the C1 domain core of FV, ie, F2035, F2068, F2127, V2130, I2139. Site-directed mutagenesis of FVIII followed by functional studies showed that these residues differentially contribute to FIXa and/or VWF binding. In particular F2127 proved to be important for both the interaction with VWF and FIXa.

MATERIALS AND METHODS

Materials

Fine chemicals were from Merck, unless otherwise stated. DMEM-F12 medium was from Lonza, Foetal Calf Serum (FCS) was from Bodinco. DMRIE-C reagent and Opti-MEM medium were from Thermo Fisher Scientific. Chicken egg L-α-phosphatidylcholine (PC), L-α-phosphatidylethanolamine (PE), and porcine brain L-α-phosphatidylserine (PS) were from Avanti Polar Lipids Inc. Geneticin G-418 sulphate, precast SDS/PAGE gels, and Brilliant Blue Coomassie were from Invitrogen. Tris-HCl was from Invitrogen, NaCl was obtained from Fagron, and HEPES was from Serva. Human serum albumin (HSA) was from the Division of Products of Sanquin. The FXa substrate S-2765 with the thrombin inhibitor I-2581 was from Chiralix.

Alignment of the FVIII and FV models

The crystal structure of the human B-domain deleted FVIII was aligned with the one of the bovine inactivated FVa with Pymol (PyMOL, Molecular Graphics System, v1.3, Schrödinger, LLC). Values of the accessible surface areas (ASA, $Å^2$) were obtained from the "Protein Interfaces, Surfaces and Assemblies Service" (PISA) at the European Bioin-

formatics Institute (EBI, **http://www.ebi.ac.uk/pdbe/prot_int/pistart.html**) using the PDB codes 2r7e for the FVIII crystal structure and 1sdd for the FVai crystal structure and then compared with each other. Hydrophobicity of amino acid residues residing on the C1 domain was evaluated according to the hydrophobicity scale. [9, 30-32] Alignments of the human FVIII to the bovine and human FV were taken from Liu et al. [33]

Proteins

B-domain deleted FVIII (GenBank accession number ABV90867.1) was codon optimized and purchased from Thermo Fisher Scientific (USA) in a pcDNA3.1(+) expression vector using NheI and NotI restriction. FVIII B domain-deleted variants with single amino acid substitutions F2035A, F2068A, V2125A, F2127A, V2130A, and I2139A were obtained by site-directed mutagenesis. Site-directed mutagenesis was performed using the QuikChange kit (Agilent Technologies) using appropriate primers (Table 1). DNA sequences were verified by sequencing analysis of the FVIII encoding parts on the mutated plasmid using BigDye Terminator Sequencing kit (Applied Biosystems). Stable transfection of Human Embryonic Kidney 293 cells (HEK293) and protein production was performed as described. [34] Recombinant FVIII mutants and wild-type were purified using VK34 monoclonal antibody [35] as described by Meems et al. [36] SDS-PAGE of the purified FVIII variants is shown in Figure S1 in supporting information. Recombinant VWF was prepared as described previously. [37] Human plasma derived FIXa, FX, and α-thrombin were purified as indicated. [38-40]

Table 1. Primers used in this study to obtain single substitutions of the C1 domain

Variant		Primer sequence
F2035A	sense	5'-AGCGGCCACATCCGGGACGCCCAGATCACCGCCTCCGGC-3'
	anti-sense	5'-GCCGGAGGCGGTGATCTGGGCGTCCCGGATGTGGCCGCT-3'
F2068A	sense	5'-TGGTCCACCAAAGAGCCCGCCAGCTGGATCAAGGTGGAC-3'
	anti-sense	5'-GTCCACCTTGATCCAGCTGGCGGGCTCTTTGGTGGACCA-3'
V2125A	sense	5'-AGCACCGGCACCCTGATGGCCTTCTTCGGCAACGTGGAC-3'
	anti-sense	5'-GTCCACGTTGCCGAAGAAGGCCATCAGGGTGCCGGTGCT-3'
F2127A	sense	5'-GGCACCCTGATGGTGTTCGCCGGCAACGTGGACAGCAGC-3'
	anti-sense	5'-GCTGCTGTCCACGTTGCCGGCGAACACCATCAGGGTGCC-3'
V2130A	sense	5'-ATGGTGTTCTTCGGCAACGCCGACAGCAGCGGCATCAAG-3'
	anti-sense	5'-CTTGATGCCGCTGCTGTCGGCGTTGCCGAAGAACACCAT-3'
I2139A	sense	5'-AGCGGCATCAAGCACAACGCCTTCAACCCCCCCATCATT-3'
	anti-sense	5'-AATGATGGGGGGGTTGAAGGCGTTGTGCTTGATGCCGCT-3'

Surface plasmon resonance

Binding studies were performed by surface plasmon resonance analysis employing Biacore T-200 biosensor system (GE Healthcare) as described.[41] For assessment of the FVIII-VWF interaction, recombinant VWF was immobilized at the density of 900 response units (RU) onto a CM5 sensor chip using the amine coupling method according to the manufacturer's instructions. Varying concentrations of FVIII and mutations thereof were passed over immobilized VWF at a flow rate of 30 µL/min in a buffer containing 20 mmol/L HEPES (pH 7.4), 150 mmol/L NaCl, 5 mmol/L $CaCl_2$, and 0.05% Tween 20 at 25°C. The sensor chip was regenerated after each protein injection using a regeneration buffer containing 20 mmol/L HEPES (pH 7.4), 1 mol/L NaCl, 20 mmol/L EDTA. FVIII binding to VWF was corrected for binding to an empty channel. Responses at equilibrium were plotted as a function of the FVIII concentration to estimate the K_D values.

Factor X activation studies

FXa generation assays were performed in the presence of sonicated lipids as described.[21] Briefly, 25 µmol/L of 15% PS, 20% PE, and 65% PC phospholipid vesicles were added to a mix containing 0.3 nmol/L FVIII and 0.2 µmol/L FX. FIXa was mixed in a concentration range from 0 to 16 nmol/L in a buffer containing 50 mmol/L Tris-HCl, 150 mmol/L NaCl 0.2% (w/v) Bovine Serum Albumin (BSA), pH 7.8. Complex formation was allowed as the result of the addition of 1 nmol/L of thrombin and 1.5 mmol/L of $CaCl_2$ at 25°C. The reaction was terminated by addition of 8.8 mmol/L EDTA. Quantity of FXa generated was assessed as described.[21]

RESULTS

The FVIII C1 domain comprises unique hydrophobic residues that are exposed to the surface

To identify the surface-exposed structural elements on the C1 domain that are unique to FVIII relative to FV, we compared structures of the C1 domain of human FVIII and FV. Unfortunately, no structure of human FV is available that comprises the complete light chain of human FV. Consequently, detailed information about intra- and inter-domain contacts is lacking. However, there is a crystal structure of inactivated bovine FV (FVai) in which the C1 domain shares more than 80% primary sequence identity with the C1 domain of human FV. We therefore compared the surface exposure of the amino acid residues of the human and bovine C1 domain in the crystal structure of human FVIII and bovine FVai (Figure 1A,B). Results revealed a unique set of five surface-exposed hydrophobic residues, ie, F2035, F2068, F2127, V2130, I2139 that are either more buried or more polar in FVai than in FVIII (Figure 1C). Sequence alignment

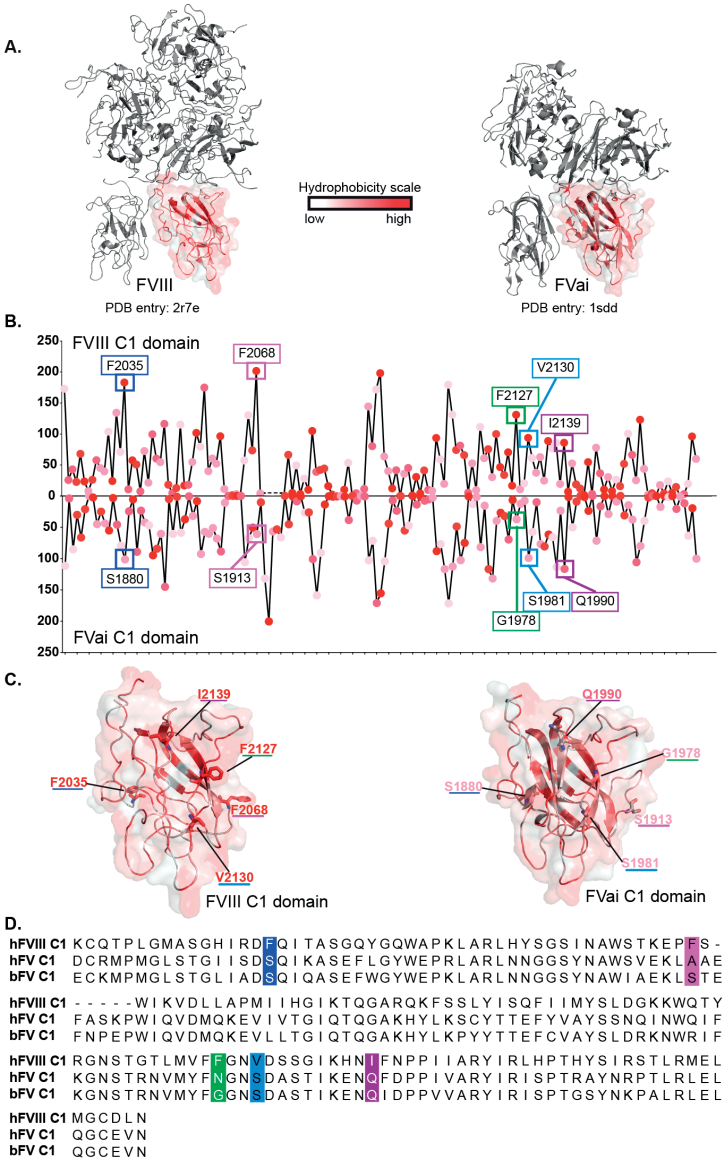

Figure 1. Comparison between C1 domains of FV and FVIII. A, On the left is displayed the crystal structure of FVIII [PDB entry: 2r7e] and on the right the structure of inactivated bovine FVa (FVai) [PDB entry: 1sdd].[9, 32] The transparent surfaces of the C1 domains are colored according to the local level of hydrophobicity.[31] B, The solvent accessible surface area is plotted as a function of the amino acid position in the C1 domain of FVIII (top) and FVai (bottom). The white to red color code represents the hydrophobicity of the amino acids.[31] C, Selected hydrophobic residues from panel B are indicated in the structures of the FVIII C1 domain and FVai C1 domain. D, Sequence alignment of human FVIII C1 domain (hFVIII C1), human FV C1 domain (hFV C1), and bovine FV C1 domain (bFV C1). Selected hydrophobic residues from panel B are indicated in the sequence

of the bovine FV C1 domain with human FV C1 domain showed that the polar nature of these residues is maintained in human FV C1 domain (Figure 1D). The findings together imply that the FVIII C1 domain comprises unique hydrophobic residues that are potentially in contact with the solvent rather than with the interior of the C1 domain core.

Amino acid residues V2125 and F2127 are crucial for high affinity binding to VWF

To assess the putative role of the surface-exposed hydrophobic residues for VWF binding, five new recombinant FVIII variants were constructed and purified. In these variants, each one of the identified hydrophobic residues was replaced by an alanine residue, ie, F2035A, F2068A, F2127A, V2130A, I2139A. Surface plasmon resonance (SPR) analysis was employed to evaluate the effect of the substitutions on VWF binding. To this end, increasing concentration of the FVIII variants were passed over VWF that was immobilized on a CM5 sensor chip (Figure 2). Results showed that the interaction between FVIII and VWF could not be accurately described by a single site binding model. This may be compatible with the observation that multiple contact sites have been identified between FVIII and VWF. [18, 25-29, 42] To still gain insight into the binding efficiency, we plotted the maximum binding response as a function of the employed FVIII concentration. The concentration at which half-maximum is reached is used as a measure for this binding efficiency. Results showed that replacement of F2035, V2130, and I2139 by an alanine residue had little, or no effect at all, on the interaction with VWF. In contrast, the substitution at position 2068 resulted in reduced VWF binding. A marked reduction in VWF binding was observed for the F2127A variant. This was reflected by a ~4-fold increase in FVIII concentration that was required to reach half-maximum binding (Figure 2H and Table 2). Notably, V2125 is in close proximity to F2127 (Cα-Cα distance = 6.9 Å according to the crystal structure by Shen et al[9]) and is also exposed to the solvent. We therefore decided to assess whether a FVIII V2125A variant exhibits reduced VWF binding as well. SPR analysis showed that replacement of V2125 to alanine indeed markedly reduces the binding to VWF. The FVIII concentration, at which half maximum binding is reached, was increased more than 6-fold compared to that required for FVIII-WT (Figure 2H and Table 2). These data suggest that F2068 and especially F2127 and V2125 contribute to the interaction with VWF.

Replacement of surface-exposed hydrophobic residues by alanine affects cofactor function

The FXa generation efficiency of the FVIII variants was assessed to verify the role of the exposed hydrophobic residues for cofactor function. FXa generation was evaluated at increasing concentrations of FIXa in presence of the thrombin-activated FVIII vari-

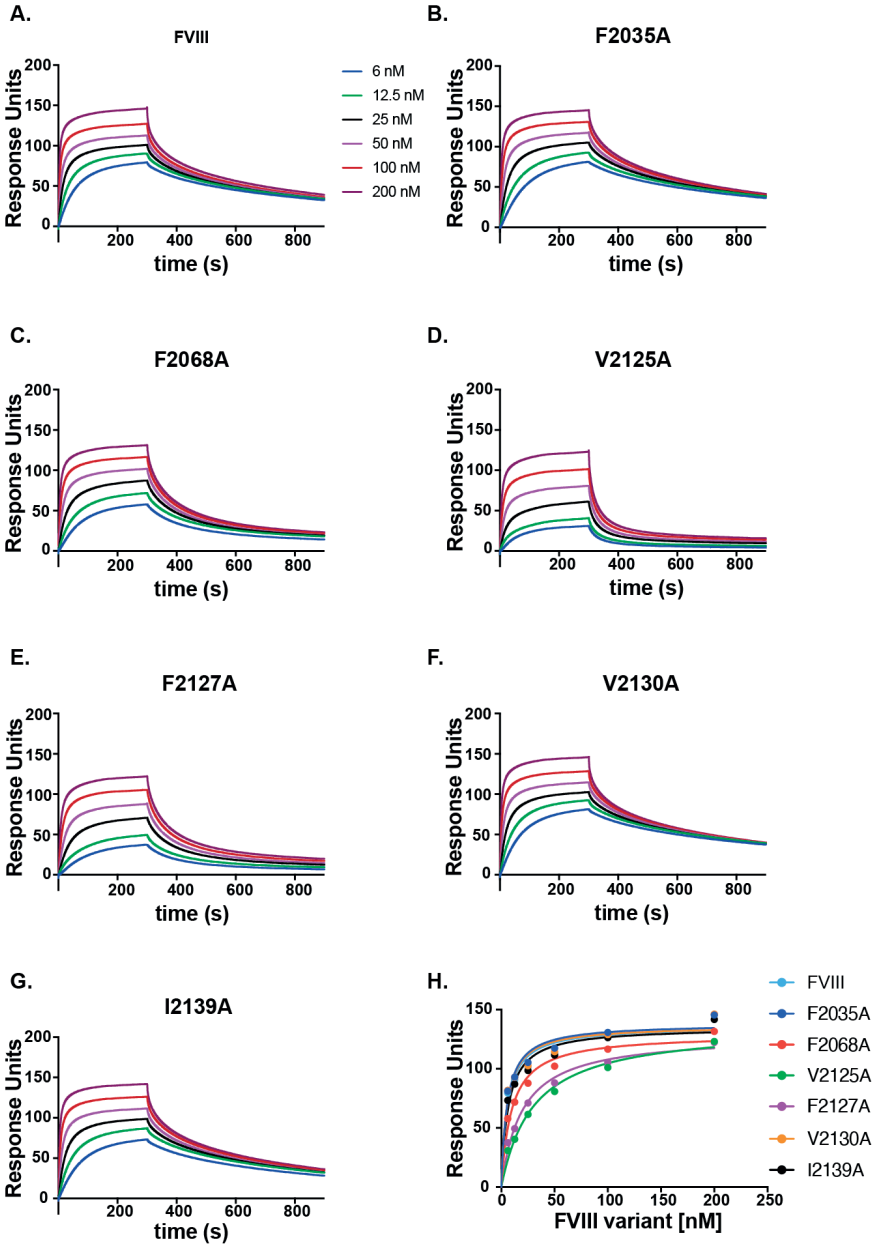

Figure 2. Binding of FVIII variants to VWF using SPR analysis. Panels A to G, Various concentrations (6-200 nmol/L) of the indicated FVIII variants were passed over VWF that was immobilized onto a CM5 sensor chip. The binding response is indicated as response units (RU) and was assessed in 20 mmol/L HEPES (pH 7.4), 150 mmol/L NaCl, 5 mmol/L $CaCl_2$ 0.05% (v/v) Tween 20 at a flow rate of 30 µL/min at 25°C. Binding to VWF was corrected for the binding to a channel without VWF. Panel H, the maximum RU plotted as a function of employed concentration of the FVIII variants.

ants, phospholipids, and calcium ions (Figure 3). The concentration of FIXa at which the half-maximum rate (half-Vmax) of FXa generation is reached can be used as an estimation of the apparent FIXa binding affinity of the FVIII variant (Table 2). The results show that V2125A and I2139A substitutions did not affect the efficiency of FX conversion in the presence of increasing concentrations of FIXa. F2035A presented only a minor reduction in its ability to stimulate FIXa compared to FVIII-WT, whereas for the F2068A and V2130A variant FXa generation was moderately impaired. The F2068A variant mainly displayed a reduced maximum rate of FXa generation. The variant F2127A showed the strongest defect in cofactor function. For this variant, the FIXa concentration to reach half-Vmax was more than 6-fold higher than required for FVIII-WT. These results suggest that the residues F2068 and V2130 and especially phenylalanine at position 2127 contribute to the interaction with FIXa.

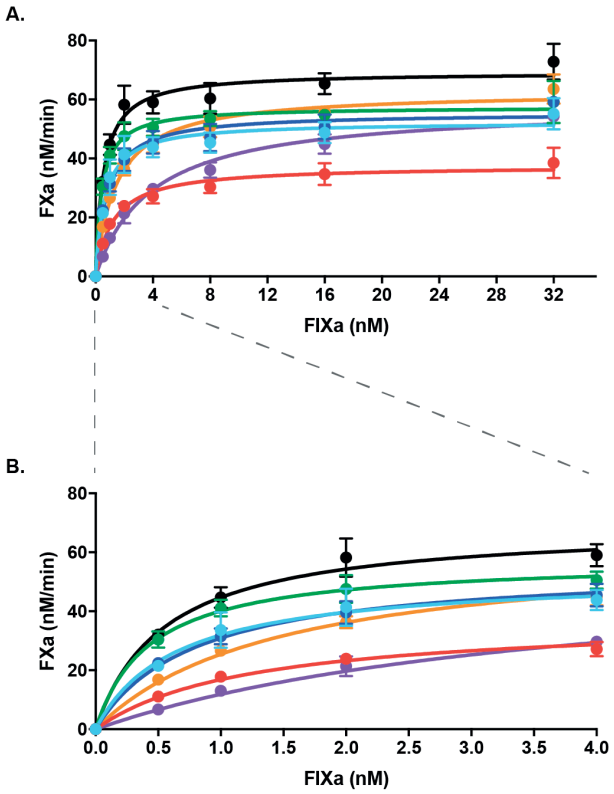

Figure 3. FXa generation by FIXa in presence of FVIII variants. A, B, FX was converted into FXa in presence of increasing concentrations of FIXa (0.5-16 nmol/L), phospholipids, Ca^{2+} ions, and 0.3 nmol/L of the FVIII variants as described in the Materials and Methods section. FVIII wild-type is represented in light blue, F2035A in blue, F2068A in red, V2125A in green, F2127A in purple, V2130A in orange, and I2139A in black. Data represent the mean value ± SD of three independent experiments.

Table 2. Apparent equilibrium dissociation constants (K_D) of FVIII variants in interaction with FIXa (Figure 3) and VWF (Figure 2)

	Apparent K_D (nM)	
FVIII Variant	**VWF binding**	**FIXa interaction**
FVIII	5.7 ± 1.8	0.6 ± 0.1
F2035A	5.5 ± 1.4	0.8 ± 0.1
F2068A	9.7 ± 1.9	1.2 ± 0.2
V2125A	29.9 ± 4.9	0.4 ± 0.1
F2127A	19.6 ± 2.9	3.9 ± 0.4
V2130A	5.4 ± 1.6	1.5 ± 0.1
I2139A	6.6 ± 1.7	0.6 ± 0.1

DISCUSSION

There is a strong structure and function relationship between FVIII and FV. This aspect has provided the unique opportunity in this and other studies to gain insight into the ligand-interactive regions of FVIII and FV.[13, 15-17] In the present study, we built upon the previous observation that replacement of the C1 domain of FVIII with that of FV ($FVIII_{C1FVC1}$) affects cofactor function.[15] These findings together suggest that the role of the C1 domain of FVIII is more important and complex than previously assumed. Wakabayashi et al[43] have come to a similar conclusion employing a FVIII variant comprising two FVIII C2 domains ($FVIII_{C2FVIIIC2}$). Intriguingly, the impaired cofactor function as a function of the FIXa concentration of the $FVIII_{C2FVIIIC2}$ variant was remarkably similar to that of the $FVIII_{C1FVC1}$ variant.[15, 43] The partial functional defect of both chimeras may be explained by a putative misalignment of the non-native FVIII A3 - FV C1 and FVIII A3 - FVIII C2 domain interface.[43] Although we do not exclude this possibility, we assessed in this study whether there may be unique structural elements in the FVIII C1 domain that mediate the interaction with FIXa and VWF.

The identification of the five surface-exposed hydrophobic amino acids in the FVIII C1 domain is remarkable in that hydrophobic residues are usually not interacting with the surrounding solvent (Figure 1).[44] Like in the FV C1 domain, structure and primary sequence comparison between the C1 and C2 domain of FVIII shows that the corresponding residues are also polar in the FVIII C2 domain (Figure 4). This further demonstrates the uniqueness of the surface-exposed hydrophobic residues in the FVIII C1 domain. Our study now reveals that the residues F2068, F2127, V2130 are of functional importance for FVIII biology as these residues contribute to VWF and/or FIXa interaction (Figures 2 and 3). No apparent role for FVIII cofactor function or VWF binding could be attributed to the other surface-exposed residues. Why the FVIII C1 domain comprises these hydrophobic residues remains therefore a topic for further investigation.

A previous Hydrogen Deuterium eXchange Mass Spectrometry (HDX-MS) study on FVIII in complex with the FVIII-binding D'-D3 fragment of VWF revealed altered hydrogen-deuterium exchange in three FVIII regions in presence of D'-D3, ie, W2062-S2069, T2086-S2095, and S2157-L2166.[28] Based on this observation, the authors concluded that these regions contribute to VWF binding. The VWF binding residue F2068 is indeed part of one of these regions, which is compatible with this conclusion (Table 2, Figure 2). Although the authors did find reduced deuterium incorporation in region M2124-Y2148, it was excluded from the analysis because of inconsistent results. Yet, residue F2127, which is part of this region, contributes the most to VWF binding among the identified residues in this study (Table 2, Figure 2). We propose that region M2124-Y2148 comprises a VWF binding region after all. It should be considered, however, that HDX-MS mainly records perturbations in deuterium uptake at the amide backbone level and does not provide any information on the side chains of amino acid residues. A direct interaction between the side chain of F2127 of FVIII and VWF without minimal alterations of the hydrogen bonding network of the protein backbone may, therefore, remain undetected by HDX-MS. This may provide an alternative explanation about why HDX-MS did not consistently identify M2124-Y2148 as a region that comprises VWF binding residues. Irrespective of these notions, our study and the HDX-MS study provide complementary information about the role of the C1 domain in VWF binding.

Multiple binding sites have been identified in FVIII for FIXa and VWF in this and other studies.[18, 25-29] The relative contribution of each of the identified residues for the overall interaction between FVIII and FIXa/VWF remains to be established. F2127, however, proves to be important for the interaction with both FIXa as well as for VWF binding. This observation is compatible with the protective role of VWF in preventing premature FIXa binding to FVIII. Most likely, VWF not only sterically hinders the interaction between FVIII and FIXa, it may partially share the binding regions on FVIII with FIXa. The proximity of F2127 to the hydrophobic V2125 suggests the involvement of the latter in VWF binding and cofactor function as well. Surprisingly, the variant V2125A displayed a marked reduction in VWF binding, but had no effect in FIXa interaction (Figures 2 and 3). As displayed in Figure 4, the counterpart of C1 V2125, in C2 is also a valine residue (V2282) suggesting that hydrophobicity at this level may be a conserved feature among the C domains. Therefore, while F2127 appears to be specific for VWF and FIXa interaction, V2125 could be rather of support in the interaction with VWF. The importance of F2127 for FVIII function is also demonstrated by the notion that substitution of this residue into a serine residue is associated with hemophilia A.[45-49] The results of our study now provide a possible mechanistic explanation for the cause of the bleeding observed in the patients with a F2127S variant of FVIII. VWF and/or FIXa binding to this FVIII variant may be affected in the patients.

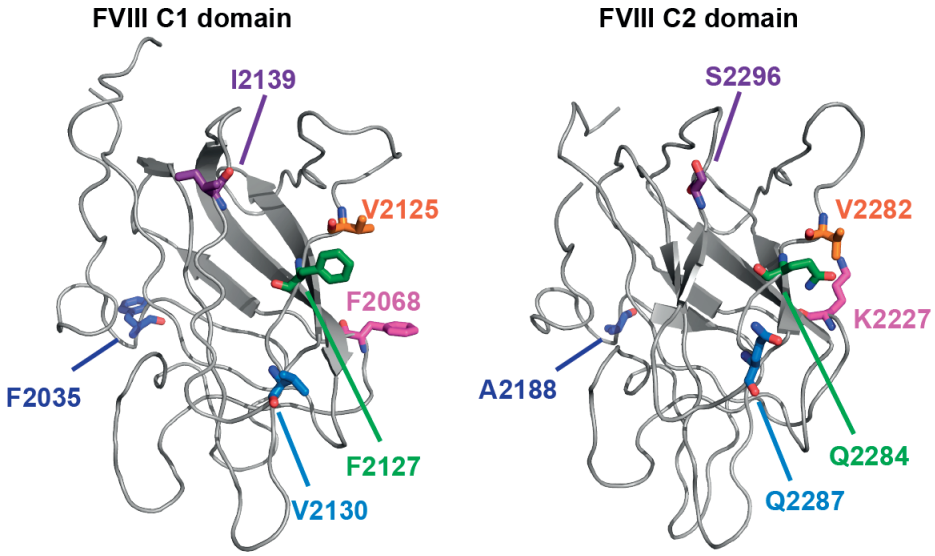

Figure 4. Comparison of the C1 and C2 domain of FVIII. On the left is displayed the crystal structure of the FVIII C1 domain [PDB entry: 2r7e9] and on the right the FVIII C2 domain. The analyzed surface exposed hydrophobic residues of the C1 residues and the corresponding residues in the C2 domain are indicated in the figure

Taken together, our findings provide novel information about the role of the C1 domain in supporting both VWF and FIXa binding. In this view, these findings also stress the importance of the FVIII C1 domain for enhancing the enzymatic activity of FIXa. We propose that activation of FVIII, followed by FVIII-VWF complex dissociation, liberates the now surface-exposed hydrophobic residues for optimal interaction with FIXa.

AUTHOR CONTRIBUTIONS

M.A.P., M.B.S., N.F., C.v.d.Z., and J.v.G. performed experiments; M.A.P., N.F., M.v.d.B, K.M., and A.B.M designed the research; M.A.P., M.B.S, N.F., and A.B.M. analyzed results; M.A.P. and N.F. made the figures; M.A.P., N.F., and A.B.M. wrote the paper.

FUNDING

This study has been funded by Product and Process Development, Sanquin, the Netherlands (PPOP-13-002).

REFERENCES

1. Mannucci PM, Tuddenham EG. The hemophilias-from royal genes to gene therapy. N Engl J Med. 2001; 344: 1773- 1779.
2. Vehar GA, Keyt B, Eaton D, et al . Structure of human factor VIII. Nature. 1984; 312: 337- 342.
3. Fay PJ. Factor VIII structure and function. Int J Hematol. 2006; 83: 103- 108.
4. Lenting PJ, van Mourik JA, Mertens K. The life cycle of coagulation factor VIII in view of its structure and function. Blood. 1998; 92: 3983- 3996.
5. Andersson LO, Forsman N, Huang K, Larsen K, Lundin A, Pavlu B, Sandberg H, Sewerin K, and Smart J. Isolation and characterization of human factor VIII: molecular forms in commercial factor VIII concentrate, cryoprecipitate, and plasma. Proc Natl Acad Sci USA. 1986; 83: 2979- 2983.
6. Fass DN, Knutson GJ, Katzmann JA. Monoclonal antibodies to porcine factor VIII coagulant and their use in the isolation of active coagulant protein. Blood. 1982; 59: 594- 600.
7. Truett MA, Blacher R, Burke RL, et al . Characterization of the polypeptide composition of human factor VIII: C and the nucleotide sequence and expression of the human kidney cDNA. DNA Mary Ann Liebert Inc. 1985; 4: 333- 349.
8. Ngo JCK, Huang M, Roth DA, Furie BC, Furie B. Crystal structure of human factor VIII: implications for the formation of the factor IXa-factor VIIIa complex. Structure. 2008; 16: 597- 606.
9. Shen BW, Spiegel PC, Chang C, Huh JW, Lee JS, Jeanman Kim, Kim JH, Stoddard BL.. The tertiary structure and domain organization of coagulation factor VIII. Blood. 2008; 111: 1240- 1247.
10. Svensson LA, Thim L, Olsen OH, Nicolaisen EM. Evaluation of the metal binding sites in a recombinant coagulation factor VIII identifies two sites with unique metal binding properties. Biol. Chem. 2013; 394(6): 761- 765.
11. Pipe SW, Montgomery RR, Pratt KP, Lenting PJ, Lillicrap D. Life in the shadow of a dominant partner: the FVIII-VWF association and its clinical implications for hemophilia A. Blood. 2016; 128: 2007- 2016.
12. Takeyama M, Nogami K, Okuda M, Shima M. von Willebrand factor protects the Ca2+-dependent structure of the factor VIII light chain. Br J Haematol. 2009; 146: 531- 537.
13. Gilbert GE, Novakovic VA, Kaufman RJ, Miao H, Pipe SW. Conservative mutations in the C2 domains of factor VIII and factor V alter phospholipid binding and cofactor activity. Blood. 2012; 120: 1923- 1932.
14. Bloem E, Meems H, van den Biggelaar M, Mertens K, Meijer AB. A3 domain region 1803-1818 contributes to the stability of activated factor VIII and includes a binding site for activated factor IX. J Biol Chem. 2013; 288: 26105- 26111.
15. Ebberink EH, Bouwens EA, Bloem E, Boon-Spijker M, van den Biggelaar M, Voorberg J, Meijer AB, Mertens K. Factor VIII/V C-domain swaps reveal discrete C-domain roles in factor VIII function and intracellular trafficking. Haematologica. 2017; 102: 686- 694.
16. Bovenschen N, Boertjes RC, van Stempvoort G, Voorberg J, Lenting PJ, Meijer AB, Mertens K. Low density lipoprotein receptor-related protein and factor IXa share structural requirements for binding to the A3 domain of coagulation factor VIII. J Biol Chem. 2003; 278: 9370- 9377.

17. Bos MHA, Camire RM. Blood coagulation factors V and VIII: molecular mechanisms of procofactor activation. J Coagul Disord. 2010; 2: 19- 27.
18. Gilbert GE, Kaufman RJ, Arena AA, Miao H, Pipe SW. Four hydrophobic amino acids of the factor VIII C2 domain are constituents of both the membrane-binding and von Willebrand factor-binding motifs. J Biol Chem. 2002; 277: 6374- 6381.
19. Lu J, Pipe SW, Miao H, Jacquemin M, Gilbert GE. A membrane-interactive surface on the factor VIII C1 domain cooperates with the C2 domain for cofactor function. Blood. 2011; 117: 3181- 3189.
20. Novakovic VA, Cullinan DB, Wakabayashi H, Fay PJ, Baleja JD, Gilbert GE. Membrane-binding properties of the Factor VIII C2 domain. Biochem J. 2011; 435: 187- 196.
21. Meems H, Meijer AB, Cullinan DB, Mertens K, Gilbert GE. Factor VIII C1 domain residues Lys 2092 and Phe 2093 contribute to membrane binding and cofactor activity. Blood. 2009; 114: 3938- 3946.
22. Soeda T, Nogami K, Nishiya K, Takeyama M, Ogiwara K, Sakata Y, Yoshioka A, Shima M. The factor VIIIa C2 domain (residues 2228-2240) interacts with the factor IXa Gla domain in the factor Xase complex. J Biol Chem. 2009; 284: 3379- 3388.
23. Vincent Jenkins P, Freas J, Schmidt KM, Zhou Q, Fay PJ. Mutations associated with hemophilia A in the 558-565 loop of the factor VIIIa A2 subunit alter the catalytic activity of the factor Xase complex. Blood. 2002; 100: 501- 508.
24. Lenting PJ, Donath MJ, van Mourik JA, Mertens K. Identification of a binding site for blood coagulation factor IXa on the light chain of human factor VIII. J Biol Chem. 1994; 269: 7150- 7155.
25. Leyte A, van Schijndel HB, Niehrs C, Huttner WB, Verbeet MP, Mertens K, van Mourik JA. Sulfation of Tyr1680 of human blood coagulation factor VIII is essential for the interaction of factor VIII with von Willebrand factor. J Biol Chem. 1991; 266: 740- 746.
26. Saenko EL, Scandella D. The acidic region of the factor VIII light chain and the C2 domain together form the high affinity binding site for von Willebrand factor. J Biol Chem. 1997; 272: 18007- 18014.
27. Lollar P, Hill-Eubanks DC, Parker CG. Association of the factor VIII light chain with von Willebrand factor. J Biol Chem. 1988; 263: 10451- 10455.
28. Chiu PL, Bou-Assaf GM, Chhabra ES, Chambers MG, Peters RT , Kulman JD, Walz T. Mapping the interaction between factor VIII and von Willebrand factor by electron microscopy and mass spectrometry. Blood. 2015; 126: 935- 938.
29. Jacquemin M, Lavend'homme R, Benhida A, Vanzieleghem B, d'Oiron R, Lavergne JM, Brackmann HH, Schwaab R, van den Driessche T, Chuah MK, Hoylaerts M, Gilles JG, Peerlinck K, Vermylen J, Saint-Remyet JM. A novel cause of mild/moderate hemophilia A: mutations scattered in the factor VIII C1 domain reduce factor VIII binding to von Willebrand factor. Blood. 2000; 96: 958- 965.
30. Krissinel E, Henrick K. Inference of macromolecular assemblies from crystalline state. J Mol Biol. 2007; 372: 774- 797.
31. Eisenberg D, Schwarz E, Komaromy M, Wall R. Analysis of membrane and surface protein sequences with the hydrophobic moment plot. J Mol Biol. 1984; 179: 125- 142.
32. Adams TE, Hockin MF, Mann KG, Everse SJ. The crystal structure of activated protein C-inactivated bovine factor Va: Implications for cofactor function. Proc Natl Acad Sci USA. 2004; 101: 8918- 8923.

33. Liu ML, Shen BW, Nakaya S, Pratt KP, Fujikawa K, Davie EW, Stoddard BL, Thompson AR. Hemophilic factor VIII C1- and C2-domain missense mutations and their modeling to the 1.5-angstrom human C2-domain crystal structure. Blood. 2000; 96: 979- 987.
34. Fribourg C, Meijer AB, Mertens K. The interface between the EGF2 domain and the protease domain in blood coagulation factor IX contributes to factor VIII binding and factor X activation. Biochemistry. 2006; 45: 10777- 10785.
35. van den Brink EN, Turenhout EA, Bank CM, Fijnvandraat K, Peters M, Voorberg J. Molecular analysis of human anti-factor VIII antibodies by V gene phage display identifies a new epitope in the acidic region following the A2 domain. Blood. 2000; 96: 540- 545.
36. Meems H, Van Den Biggelaar M, Rondaij M, van der Zwaan C, Mertens K, Meijer AB. C1 domain residues Lys 2092 and Phe 2093 are of major importance for the endocytic uptake of coagulation factor VIII. Int J Biochem Cell Biol. 2011; 43: 1114- 1121.
37. Van Den Biggelaar M, Bierings R, Storm G, Voorberg J, Mertens K. Requirements for cellular co-trafficking of factor VIII and von Willebrand factor to Weibel-Palade bodies. J Thromb Haemost. 2007; 5: 2235- 2242.
38. Mertens K, Bertina RM. Activation of human coagulation factor VIII by activated factor X, the common product of the intrinsic and the extrinsic pathway of blood coagulation. Thromb Haemost. 1982; 47: 96- 100.
39. Mertens K, Bertina RM. Pathways in the activation of human coagulation factor X. Biochem J. 1980; 185: 647- 658.
40. Hendrix H, Lindhout T, Mertens K, Engels W, Hemker HC. Activation of human prothrombin by stoichiometric levels of staphylocoagulase. J Biol Chem. 1983; 258: 3637- 3644.
41. Bloem E, van den Biggelaar M, Wroblewska A, Voorberg J, Fabe JHr, Kjalke M, Henning H, Stennicke R, Mertens K, Meijer AB. Factor VIII C1 domain spikes 2092-2093 and 2158-2159 comprise regions that modulate cofactor function and cellular uptake. J Biol Chem. 2013; 288: 29670- 29679.
42. van den Biggelaar M, Meijer AB, Voorberg J, Mertens K. Intracellular cotrafficking of factor VIII and von Willebrand factor type 2N variants to storage organelles. Blood. 2009; 113: 3102- 3109.
43. Wakabayashi H, Fay PJ. Replacing the factor VIII C1 domain with a second C2 domain reduces factor VIII stability and affinity for factor IXa. J Biol Chem. 2013; 288: 31289- 31297.
44. Dyson HJ, Wright PE, Scheraga HA. The role of hydrophobic interactions in initiation and propagation of protein folding. Proc Natl Acad Sci USA. 2006; 103: 13057- 13061.
45. Trossaërt M, Regnault V, Sigaud M, Boisseau P, Fressinaud E, Lecompte T. Mild hemophilia A with factor VIII assay discrepancy: using thrombin generation assay to assess the bleeding phenotype. J Thromb Haemost. 2008; 6: 486- 493.
46. Castaman G, Mancuso ME, Giacomelli SH, Tosetto A, Santagostino E, Mannucci PM, Rodeghiero F. Molecular and phenotypic determinants of the response to desmopressin in adult patients with mild hemophilia A. J Thromb Haemost. 2009; 7: 1824- 1831.
47. Green PM, Bagnall RD, Waseem NH, Giannelli F. Haemophilia A mutations in the UK: results of screening one-third of the population. Br J Haematol. 2008; 143: 115- 128.
48. Martín-Salces M, Venceslá A, Alvárez-Román MT, Rivas I, Fernandez I, Butta N, Baena M, Fuentes-Prior P, Tizzano, EF Jiménez-Yuste V. Clinical and genetic findings in five female patients with haemophilia A: Identification of a novel missense mutation, p.Phe2127Ser. Thromb Haemost. 2010; 104: 718- 723.

49. Johnsen JM, Fletcher SN, Huston H, Roberge S, Martin BK, Kircher M, Josephson NC, Shendure J, Ruuska S,Koerper MA, Morales J, Pierce GF, Aschman DJ, Konkle BA. Novel approach to genetic analysis and results in 3000 hemophilia patients enrolled in my life. Our future initiative. Blood Adv. 2017; 1: 824- 834.

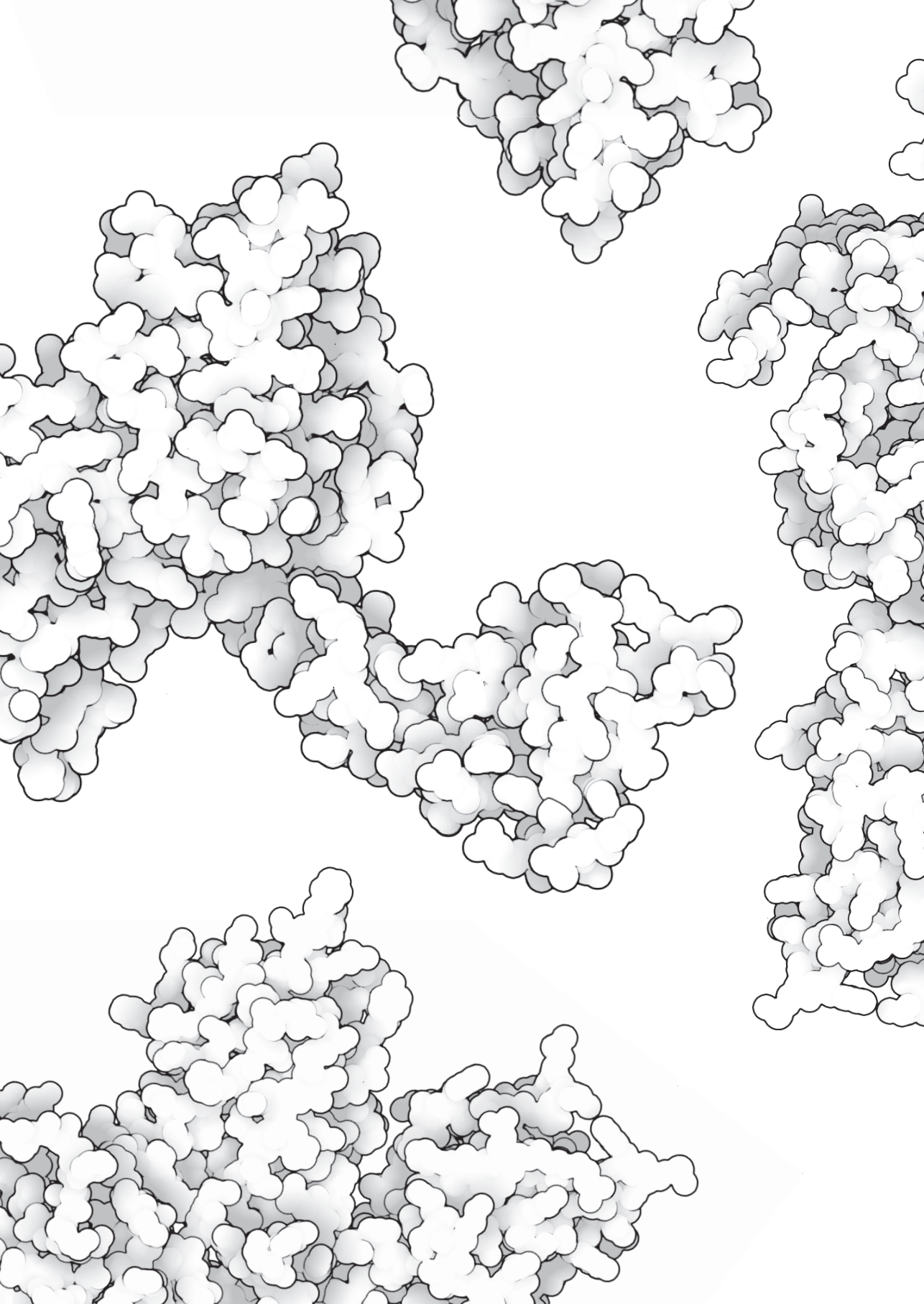

Chapter 6

General discussion

The mechanism of interaction between the multimeric VWF and FVIII has been extensively studied over the last decades[1-55]. Although much progress has been made, the amino acid residues that constitute the FVIII - VWF binding interface are still largely unknown. Another challenge that remains to be resolved involves the cellular mechanisms via which VWF is removed from the circulation[6,7]. The relative contribution to the cellular uptake of VWF of the growing list of putative VWF receptors remains to be clarified. Both these topics are important to gain insight into bleeding disorders associated with defects in FVIII binding or accelerated clearance of VWF. Interestingly, sites important for binding to FVIII, dimerization and clearance are all located in the N-terminal D'-D3 domains of VWF. In this chapter, the main conclusions of this thesis and possible implications thereof are discussed with reference to the key role of the D'-D3 domains in these processes.

MAPPING THE DIRECT FVIII BINDING SITE ON VWF D' REGION

It has been proposed that D'-D3 domains can be further subdivided into TIL'-E'-VWD3-C8_3-TIL3-E3[8]. In a recent study, Shiltaj et al. have proposed that the major FVIII binding site resides is in the TIL' subdomain of VWF[4]. In chapter 2, we have used Hydrogen/Deuterium eXchange Mass Spectrometry (HDX-MS) to identify sites involved in binding to FVIII. We found that the residues that contribute directly to FVIII binding are included in region Arg782-Cys799 of the TIL' subdomain. Based on the view that electrostatic interactions mediate FVIII binding, we replaced the charged residues, i.e. Arg782, Glu784, Glu787, Lys790, Asp796 and Glu798 in this region by alanine residues to assess the role thereof for FVIII binding[9,10]. We observed that variants Lys790Ala and Asp796Ala have a decreased affinity for FVIII. The Glu787Ala variant did not bind FVIII at all confirming the critical role for FVIII binding of the charged residues (Chapter 2, Figure 3).

Analysis of the Arg782-Cys799 architecture in the recently released crystal structure of D'-D3 revealed that Glu787 is a part of a short α-helix together with Leu786 and Cys788[11]. The latter forms a cysteine bridge with Cys799 which is most likely critical for stabilizing the helix[11]. We hypothesised that Leu786 may perform a similar role. To assess the role of Leu786 on the stability of the helix, we introduced variant Leu786Ala to probe its ability to bind FVIII. Our results showed a substantially decreased affinity to FVIII, which supports our hypothesis that the structural integrity of this helix is important for interaction with FVIII (Chapter 2, Figure 5).

The VWF variants were also evaluated for their efficiency to compete with immobilized VWF for binding FVIII. The Glu787Ala variant showed no competition with immobilized VWF. The Lys790Ala variant, however, revealed a biphasic competition behaviour (Chapter 2, Figure 4). This suggests that this variant may exist in two or

more conformations that bind with a distinct affinity to FVIII. The NMR-based 3D model of TIL' shows that side chains of Glu787 and Lys790 are in close proximity[4]. In the crystal structure of D'-D3, however, Glu787 is exposed to the solvent and Lys790 points in the opposite direction into the protein core[11]. The NMR model suggests that Glu787 and Lys790 may be connected via a salt bridge. If true, disturbance of this interaction may lead to conformational changes thereby affecting FVIII binding. To test the hypothesis of the existence of a salt bridge, we expressed a double mutant of D'-D3 with lysine and glutamic acid residues swapped. If present, we expect normal FVIII binding of the Glu787Lys/Lys790Glu variant. However, this mutant showed no binding to FVIII at all, implying that the conformational instability may not be caused by disruption of a salt bridge (data not shown). Therefore, the reason of the biphasic competition of the Lys790Ala remains as a topic for further investigation. In the crystal structure of D'-D3, Lys790 interacts with Tyr795 and Glu787 is exposed to the solved. An alternative model may be that Glu787 interacts directly with FVIII and Lys790 contributes to the local stability of D'-D3 by interacting with Tyr795.

THE D3 DOMAIN SUPPORTS THE INTERACTION BETWEEN THE TIL' DOMAIN AND FVIII

Our findings from chapter 2 fully support the previous view that the D' domain harbours a critical binding site for FVIII[4]. However, it has remained poorly understood why von Willebrand disease type 2N (VWD) variants, which lead to a reduced FVIII binding affinity, contain mutations of residues that are located outside the D' domain[12-16]. In chapter 3, we have therefore investigated the role of the subdomains of the D3 domain for FVIII binding. To challenge the role of these subdomains, we assessed the FVIII binding efficiency of D'-D3 fragments with subsequent C-terminal subdomain truncations. We found that the E3 subdomain can be removed without affecting FVIII binding. Removal of TIL3 and C8_3 subdomains results in a gradual decrease in FVIII binding affinity. The removal the VWD3 assembly completely abolishes VWF-FVIII interaction (Chapter 3, Figure 2). This could suggest that the VWD3 subdomain contains a binding site for FVIII, which was not identified in the HDX-MS study of chapter 2. The other domains may stabilize the conformation of the VWD3 domain via intermolecular interactions. Alternatively, the VWD3 domain does not comprise a FVIII binding site and may be only critical to stabilise the interaction between TIL' and FVIII.

To further address the above-mentioned issue, we also investigated putative structural changes in D'-D3 upon consecutive removal of C-terminal domains. To this end, we employed lysine-directed chemical footprinting with tandem mass tags (TMT) combined with mass spectrometry to assess the reactivity of the lysine residues in

the domain truncation variants. If the conformation is not altered as a consequence of a truncation, we do not expect a change in reactivity. The results did show changes in lysine reactivity in the truncation variants and mainly within the VWD3 module (Chapter 3, Figure 4). This implies that the conformation of VWD3 may be altered upon subdomain deletions. The crystal structure of D'-D3 revealed a tight hydrogen network connecting the VWD3, C8_3 and TIL3 modules[11]. This is compatible with the hypothesis that the C8_3 and TIL3 subdomains are required to stabilize the conformation of VWD3.

The findings together suggest that not only the binding site in the TIL' domain is required for high affinity FVIII binding, but also a proper conformation of the D3 domain. It has been suggested that dimerization of D'-D3 increases the affinity for FVIIII[17]. Notably, the two cysteine residues that mediate the dimerization are located within the D3 domain[18]. Dimerization may therefore further stabilise the hydrogen bonding network between the subdomains resulting in the most stable FVIII-binding conformation of VWF[17]. More studies are required to assess whether the D3 domain contains an additional binding sites for FVIII, or whether it solely plays a stabilizing role in the interaction between TIL' and FVIII.

THE ROLE OF D'-D3-A1 FOR THE CELLULAR UPTAKE OF VWF

Several receptors have been identified that may mediate the cellular uptake of VWF by macrophages including LDL receptor-related protein-1 (LRP-1), Macrophage scavenger receptor-1 (MSR-1, SR-AI or CD204), Macrophage Galactose-type lectin (MGL) Siglec-5 and the Asialoglycoprotein receptor (ASGPR[19-26]. The relative importance for VWF uptake by these receptors remained to be clarified. In chapter 4, we used cell surface proteomics to gain insight into the receptors that are expressed on monocyte-derived macrophages. We have previously found that these cells internalize VWF in a shear-dependent manner[23]. Our proteomics approach suggests abundant expression of mainly LRP-1 and MSR-1 on the macrophages implying that these receptors may be involved in the uptake of VWF (Chapter 4, Online Supplementary Figure S1).

It has been proposed that the D'-D3-A1 fragment of VWF comprises a binding site for LRP-1 in the A1 domain and for MSR-1 in the D'-D3 domains[21,24]. We therefore evaluated whether or not the isolated D'-D3 and D'-D3-A1 fragment can be internalized in a shear-independent manner by the macrophages. Our cellular uptake studies revealed that both fragments are indeed internalized.

Protein-binding studies and cellular uptake studies of D'-D3 and D'-D3-A1 by U87MG cells, which abundantly express LRP-1, confirmed previous findings that the A1 domain harbours an LRP-1 binding site. Yet, in presence of an LRP-1 antagonist, the cellular uptake by macrophages of not only D'-D3-A1 was blocked but also that of the

D'-D3 fragment (Chapter 4, Figure 1). Additional protein binding and cellular uptake studies revealed that the extracellular part of MSR-1 may interact directly with LRP-1 (Chapter 4, Online Supplementary Figure S3). This provided an explanation why D'-D3 is internalized by macrophages via LRP-1 although this VWF fragment lacks the LRP-1 binding site. MSR-1 may simultaneously interact with D'-D3 and LRP-1. To this end, LRP-1 may contribute to the uptake of D'-D3 as well. Additional studies are required to resolve the role of the other identified receptors in the endocytosis of VWF.

THE FVIII C1 DOMAIN COMPRISES A BINDING SITE FOR VWF

It has been well established that the acidic a3 region of FVIII is critical for VWF binding[27-30]. A recent cryo-EM study showed that the D' domain of D'-D3 may also interact with the C1 domain of FVIII[31]. This agrees with the observation that replacement of the C1 domain with homologous C1 domain of factor V (FV) completely impairs VWF binding[32]. FVIII cofactor function was also impaired suggesting that FIXa binding sites may be in the C1 domain as well[33]. In chapter 5 we therefore focused on sites in the C1 domain that may contribute to VWF and FIXa binding. We compared the crystal structures and primary sequences of the C1 domain of FV and FVIII to identify sites that are unique to FVIII. This comparison led to the identification of five hydrophobic residues that surprisingly are in contact with the solvent rather than the protein interior. To assess the role of each of these residues for FVIII functioning, five FVIII variants were constructed in which one of these residues was replaced by an alanine. Among the tested mutants, the Phe2068Ala variant showed a moderately affected ability to bind VWF. The variants Val2125A and Phe2127Ala revealed the strongest impact on VWF binding (Chapter 5, Figure 2). The crystal structure of FVIII shows that Val2125 and Phe2127 are in close proximity to each other on the same site of a surface loop[34]. Therefore, we argue that these residues may contribute to the binding to D'-D3. Interestingly, Phe2068Ala and Phe2127Ala also showed a reduced cofactor function compared to WT-FVIII suggesting a partial overlap between VWF and FIXa binding sites (Chapter 5, Figure 3). This may not be a surprise as FVIII does not interact with FIXa when it is in complex with VWF[35].

We also employed chemical footprinting mass spectrometry of FVIII in absence and presence of VWF to identify lysine residues that may contribute to the interaction with VWF as well. Lys1693/Lys1694 of the A3 domain and Lys2136 of the C1 domain showed a decreased reactivity in presence of VWF (data not shown). To assess their role in VWF binding, we substituted these residues for alanine residues. The Lys1693Als/Lys1694Ala variant of FVIII did not show any difference in binding to VWF. However, the Lys2136A variant did show a marked decrease in affinity for VWF (Figure 1). Interestingly, substitution of Lys2136 into glutamic acid has been associated

with haemophilia[36]. This suggests that a VWF binding defect may be the underlying cause of the disease. Coincidentally, Lys2136 is located in close proximity to Val2125 and Phe2127 at the same side of the C1 domain. We therefore propose that residues Lys2136, Val2125 and Phe2127 are part of the VWF binding interface.

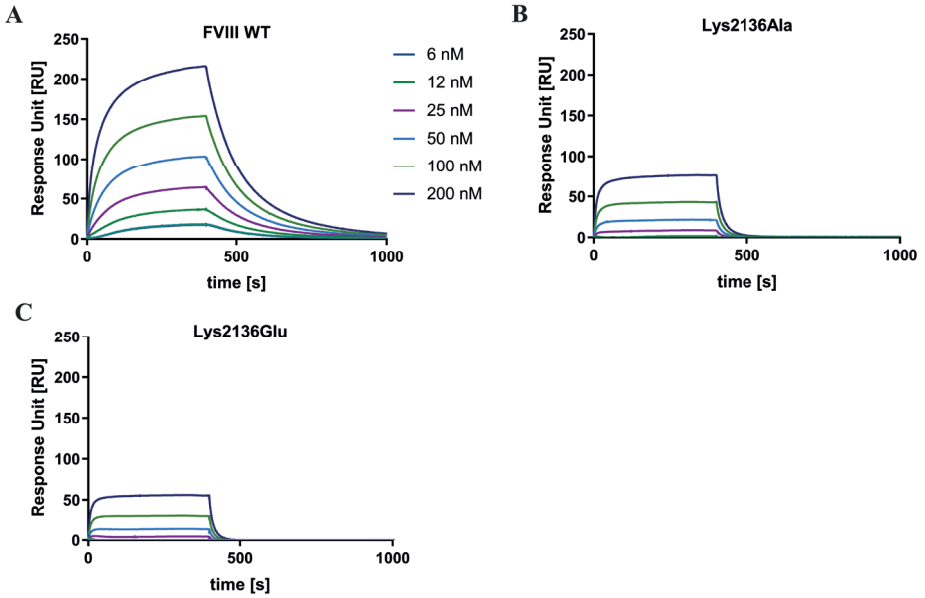

Figure 1. Binding of D'-D3 to FVIII, FVIII-Lys2136Ala and FVIII-Lys2136Glu variants. Various concentrations (0-200 nM) of D'-D3 were passed over FVIII, FVII-Lys2136Ala and FVIII-Lys2136Glu that were immobilized to the same density on CM5 sensor chip via C2 domain-directed antibody CLB-EL14. The binding response are indicated as Response Unit. Binding was assessed in 20 mM HEPES (pH 7.4), 150 mM NaCl, 5 mM $CaCl_2$, 0.05% (v/v) Tween 20 at a flow rate of 30 ml/min at 25°C. To correct for background binding we used a CM5 channel coated with CLB-EL14 lacking FVIII.

A MODEL OF THE FVIII - D'-D3 COMPLEX

We employed the Haddock protein-protein docking tool (https://haddock.science.uu.nl/) to predict the three-dimensional structure of the complex between D'-D3 and FVIII[37]. Our experimental data were used to set distance restraints between amino acids and amino acid regions to assist the docking process. To this end, we speculated that Lys2136 of FVIII interacts with Glu787 of VWF. In addition, we imposed that hydrophobic residues Val2125 and Phe2127 of FVIII interact with region Arg786-Cys799 of the TIL' subdomain. Molecular dynamics simulations and binding free energy calculations were employed on the docked solutions of the two interacting molecules. Two candidate models were selected as a putative complex (Figure 2). Model A supports the possibility that Glu1078 of C8_3 assembly might be located on the region taking

part in direct interaction with FVIII. Model B depicts the VWD3 subdomain as the main region of D3 domain in close proximity to FVIII C1 domain. Both models fit the EM data presenting close proximity between D3 domain and the C domains of FVIII[31].

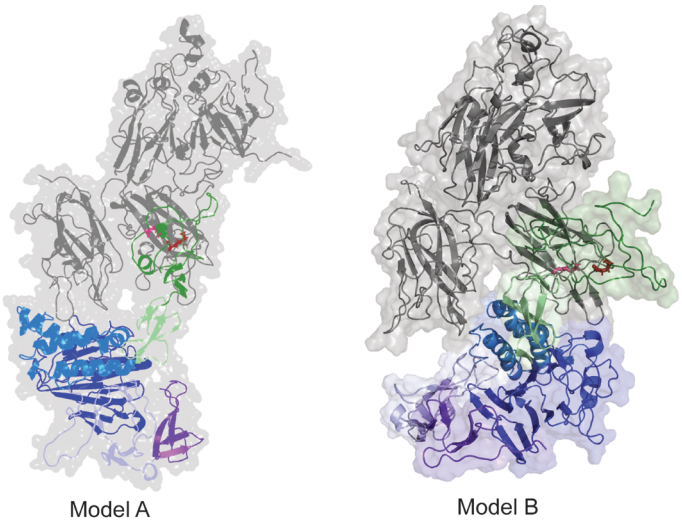

Figure 2. Haddock models of D'-D3 in complex with FVIII. Model (A) and (B) are the most favourable models obtained with data-driven docking using Haddock web server. The models were optimized using molecular dynamics simulations Amber16. Crystal structures of FVIII [PDB entry: 3cdz] and D'-D3 [PDB entry: 6n29] were used for the modelling[11,38]. FVIII is shown in grey with Lys2136 in a ball-and-stick representation in red. The TIL' of D'-D3 is shown in dark green, the E' domain in light green, the VWD3 domain in dark blue, the C8_3 domain in light blue and the E2 domain in purple. Glu787 of the TIL' domain is shown in a ball-and-stick representation in pink.

FURTHER DIRECTIONS AND CONCLUDING REMARKS

The last years have brought various strategies and improvements in treatment of haemophilia A patients. Besides replacement therapies with FVIII concentrates, gene therapy showed the promise of achieving long-term corrective plasma levels[39]. Recently, a bispecific antibody has reached the marked that binds both FIXa and FX thereby bypassing the need for FVIII as a therapeutic agent[40]. However, FVIII is still the most effective in enhancing the activity of FIXa. FVIII based "biobetters" may still present the treatment option of choice.

FVIII variants have been designed with the aim to improve the half-life of FVIII *in vivo*. These include PEGylated and Fc fusion FVIII variants[41-43]. There is, however, only a limited improvement of FVIII half-life as these FVIII variants are still effectively removed from the circulation via VWF. A FVIII variant that circulates independently of VWF may provide a solution for this phenomenon. Yet, tight complex formation with VWF has undeniable benefits such as protection of FVIII from proteolytic degradation,

stabilisation of the heterodimeric structure of FVIII, modulation of its immunogenicity, and prevention from premature clearance[5]. The optimal use of the advantages of VWF in a new therapeutic variant of FVIII may provide a promising alternative for future treatment strategies. To achieve this goal, one study focused on the improvement of the FVIII-VWF complex stability by employing FVIII fused to VWF-directed nanobodies[44]. In this manner, the complex is further stabilized. Results showed reduced anti-FVIII antibody formation and prolonged FVIII survival *in vivo*. This approach could be further explored to evaluate its feasibility as a new therapeutic option for the treatment of haemophilia A[44].

Cross-linking mass spectrometry combined with molecular modelling is one of the techniques that could help to further improve our understanding of the VWF-FVIII complex. Using cross linkers of different lengths, information can be obtained about the spatial positioning and proximity of amino acid regions of the two proteins[45]. Molecular modelling techniques may be employed to predict which residues should be replaced to improve the affinity of the complex[46].

Another topic that should be addressed is that the FVIII binding affinity of the D'-D3 dimer is similar to that of full length VWF, but drops about 20-fold in case of monomeric D'-D3[17]. This suggests that dimerization may affect protein structure, probably also changing the regions in close proximity to or in the FVIII binding site. Consequently, it would be important to study the properties of D'-D3 dimer and structural differences upon dimerization of D'-D3 in comparison to the monomer. The high-resolution crystal structure of the dimer in complex with FVIII would especially provide full understanding of the interaction between VWF and FVIII. This would facilitate the design of novel D'-D3-FVIII variants for therapeutic purposes resulting in FVIII with an improved *in vivo* half-life.

REFERENCES

1 Vlot, A. J., Koppelman, S. J., Meijers, J. C., Dama, C., van den Berg, H. M., Bouma, B. N., Sixma, J. J. and Willems, G. M. (1996) Kinetics of factor VIII-von Willebrand factor association. *Blood* **87**, 1809-1816.

2 Vlot, A. J., Koppelman, S. J., Bouma, B. N. and Sixma, J. J. (1998) Factor VIII and von Willebrand factor. *Thromb. Haemost.* **79**, 456-465.

3 Gensana, M., Altisent, C., Aznar, J. A., Casaña, P., Hernández, F., Jorquera, J. I., Magallón, M., Massot, M. and Puig, L. (2001) Influence of von Willebrand factor on the reactivity of human factor VIII inhibitors with factor VIII. *Haemophilia* **7**, 369-374.

4 Shiltagh, N., Kirkpatrick, J., Cabrita, L. D., Mckinnon, T. a J., Thalassinos, K., Tuddenham, E. G. D., Hansen, D. F., Tuddenham, Edward GD, Hansen, D. F., Tuddenham, E. G. D., et al. (2014) Solution structure of the major factor VIII binding region on von Willebrand factor. *Blood* **123**, 4143-4152.

5 Pipe, S. W., Montgomery, R. R., Pratt, K. P., Lenting, P. J. and Lillicrap, D. (2016) Life in the shadow of a dominant partner: the FVIII-VWF association and its clinical implications for hemophilia A. *Blood* **128**, 2007-2016.

6 Casari, C., Lenting, P. J., Wohner, N., Christophe, O. D. and Denis, C. V. (2013) Clearance of von Willebrand factor. *J. Thromb. Haemost.* **11**, 202-211.

7 O'Sullivan, J. M., Ward, S., Lavin, M. and O'Donnell, J. S. (2018) von Willebrand factor clearance - biological mechanisms and clinical significance. *Br. J. Haematol.* **183**, 185-195.

8 Zhou, Y. F., Eng, E. T., Zhu, J., Lu, C., Walz, T. and Springer, T. A. (2012) Sequence and structure relationships within von Willebrand factor. *Blood* **120**, 449-458.

9 Dimitrov, J. D., Christophe, O. D., Kang, J., Repesse, Y., Delignat, S., Kaveri, S. V and Lacroix-Desmazes, S. (2012) Thermodynamic analysis of the interaction of factor VIII with von Willebrand factor. *Biochemistry* **51**, 4108-4116.

10 Owen, W. G. and Wagner, R. H. (1972) Antihemophilic factor: separation of an active fragment following dissociation by salts or detergents. *Thromb. Diath. Haemorrh., Germany* **27**, 502-515.

11 Dong, X., Leksa, N. C., Chhabra, E. S., Arndt, J. W., Lu, Q., Knockenhauer, K. E., Peters, R. T. and Springer, T. A. (2019) The von Willebrand factor D'D3 assembly and structural principles for factor VIII binding and concatemer biogenesis. *Blood* **133**, 1523-1533.

12 Sadler, J. E., Mannucci, P. M., Mazurier, C., Meyer, D., Nichols, W. L., Nishino, M., Peake, I. R., Rodeghiero, F., Schneppenheim, R., Ruggeri, Z. M., et al. (2006) Update on the pathophysiology and classification of von Willebrand disease: a report of the Subcommittee on von Willebrand Factor. *J. Thromb. Haemost.* **4**, 2103-2114.

13 de Jong, A. and Eikenboom, J. (2017) Von Willebrand disease mutation spectrum and associated mutation mechanisms. *Thromb. Res.* **159**, 65-75.

14 Jorieux, S., Gaucher, C., Goudemand, J. and Mazurier, C. (1998) A Novel Mutation in the D3 Domain of von Willebrand Factor Markedly Decreases Its Ability to Bind Factor VIII and Affects Its Multimerization. *Blood* **92**, 4663-4670.

15 Allen, S., Abuzenadah, A. M., Blagg, J. L., Hinks, J., Nesbitt, I. M., Goodeve, A. C., Gursel, T., Ingerslev, J., Peake, I. R. and Daly, M. E. (2000) Two novel type 2N von Willebrand disease-causing mutations that result in defective factor VIII binding, multimerization, and secretion of von Willebrand factor. *Blood* **95**, 2000-2007.

16 Hilbert, L., D'Oiron, R., Fressinaud, E., Meyer, D. and Mazurier, C. (2004) First identification and expression of a type 2N von Willebrand disease mutation (E1078K) located in exon 25 of von Willebrand factor gene. *J. Thromb. Haemost.* **2**, 2271-2273.

17 Yee, A., Gildersleeve, R. D., Gu, S., Kretz, C. a., McGee, B. M., Carr, K. M., Pipe, S. W. and Ginsburg, D. (2014) A von Willebrand factor fragment containing the D'-D3 domains is sufficient to stabilize coagulation factor VIII in mice. *Blood* **124**, 445-52.

18 Purvis, A. R., Gross, J., Dang, L. T., Huang, R.-H., Kapadia, M., Townsend, R. R. and Sadler, J. E. (2007) Two Cys residues essential for von Willebrand factor multimer assembly in the Golgi. *Proc. Natl. Acad. Sci. U. S. A.* **104**, 15647-15652.

19 Grewal, P. K., Uchiyama, S., Ditto, D., Varki, N., Le, D. T., Nizet, V. and Marth, J. D. (2008) The Ashwell receptor mitigates the lethal coagulopathy of sepsis. *Nat. Med.* **14**, 648-655.

20 O'Sullivan, J. M., Aguila, S., McRae, E., Ward, S. E., Rawley, O., Fallon, P. G., Brophy, T. M., Preston, R. J. S. S., Brady, L., Sheils, O., et al. (2016) N-linked glycan truncation causes enhanced clearance of plasma-derived von Willebrand factor. *J. Thromb. Haemost.* **14**, 2446-2457.

21 Rastegarlari, G., Pegon, J. N., Casari, C., Odouard, S., Navarrete, A. M., Saint-Lu, N., Van Vlijmen, B. J., Legendre, P., Christophe, O. D., Denis, C. V., et al. (2012) Macrophage LRP1 contributes to the clearance of von Willebrand factor. *Blood* **119**, 2126-2134.

22 Wohner, N., Legendre, P., Casari, C., Christophe, O. D., Lenting, P. J. and Denis, C. V. (2015) Shear stress-independent binding of von Willebrand factor-type 2B mutants p.R1306Q & p.V1316M to LRP1 explains their increased clearance. *J. Thromb. Haemost.* **13**, 815-820.

23 Castro-Núñez, L., Dienava-Verdoold, I., Herczenik, E., Mertens, K. and Meijer, A. B. (2012) Shear stress is required for the endocytic uptake of the factor VIII-von Willebrand factor complex by macrophages. *J. Thromb. Haemost.* **10**, 1929-37.

24 Wohner, N., Muczynski, V., Mohamadi, A., Legendre, P., Proulle, V., Aymé, G., Christophe, O. D., Lenting, P. J., Denis, C. V. and Casari, C. (2018) Macrophage scavenger receptor sr-ai contributes to the clearance of von willebrand factor. *Haematologica* **103**, 728-737.

25 Ward, S. E., O'Sullivan, J. M., Drakeford, C., Aguila, S., Jondle, C. N., Sharma, J., Fallon, P. G., Brophy, T. M., Preston, R. J. S., Smyth, P., et al. (2018) A novel role for the macrophage galactose-type lectin receptor in mediating von Willebrand factor clearance. *Blood* **131**, 911-916.

26 Pegon, J. N., Kurdi, M., Casari, C., Odouard, S., Denis, C. V., Christophe, O. D. and Lenting, P. J. (2012) Factor VIII and von Willebrand factor are ligands for the carbohydrate-receptor Siglec-5. *Haematologica* **97**, 1855-1863.

27 Leyte, A., Verbeet, M. P., Brodniewicz-Proba, T., Van Mourik, J. A. and Mertens, K. (1989) The interaction between human blood-coagulation factor VIII and von Willebrand factor. Characterization of a high-affinity binding site on factor VIII. *Biochem. J.* **257**, 679-83.

28 Leyte, A., van Schijndel, H. B., Niehrs, C., Huttner, W. B., Verbeet, M. P., Mertens, K. and van Mourik, J. A. (1991) Sulfation of Tyr 1680 of human blood coagulation factor VIII is essential for the interaction of factor VIII with von Willebrand factor. *J. Biol. Chem.* **266**, 740-746.

29 Jacquemin, M., Lavend, R., Benhida, A., Vanzieleghem, B., Oiron, R., Lavergne, J., Brackmann, H. H., Schwaab, R., Vandendriessche, T., Chuah, M. K. L., et al. (2000) A novel cause of mild / moderate hemophilia A : mutations scattered in the factor VIII C1 domain reduce factor VIII binding to von Willebrand factor. *Blood* **96**, 958-965.

30 Saenko, E. L. and Scandella, D. (1997) The Acidic Region of the Factor VIII Light Chain and the C2 Domain Together Form the High Affinity Binding Site for von Willebrand Factor. *J. Biol. Chem.* **272**, 18007-14.

31 Yee, A., Oleskie, A. N., Dosey, A. M., Kretz, C. a., Gildersleeve, R. D., Dutta, S., Su, M., Ginsburg, D. and Skiniotis, G. (2015) Visualization of an N-terminal fragment of von Willebrand factor in complex with factor VIII. *Blood* **126**, 939-943.

32 Ebberink, E. H. T. M., Bouwens, E. A. M., Bloem, E., Boon-Spijker, M., van den Biggelaar, M., Voorberg, J., Meijer, A. B. and Mertens, K. (2017) Factor VIII/V C-domain swaps reveal discrete C-domain roles in factor VIII function and intracellular trafficking. *Haematologica* **102**, 686-694.

33 Wakabayashi, H. and Fay, P. J. (2013) Replacing thefactor VIII C1 domain with a second C2 domain reduces factor VIII stability and affinity for factor IXa. *J. Biol. Chem.* **288**, 31289-31297.

34 Shen, B. W., Spiegel, P. C., Chang, C., Huh, J., Lee, J., Kim, J., Kim, Y. and Stoddard, B. L. (2008) The tertiary structure and domain organization of coagulation factor VIII. *Blood* **111**, 1240-1247.

35 Lenting, P. J., van Mourik, J. A. and Mertens, K. (1997) The life cycle of coagulation factor VIII in view of its structure and function. *Blood* **92**, 3983-3996.

36 Kemball-Cook, G., Tuddenham, E. G. and Wacey, A. I. (1998) The factor VIII Structure and Mutation Resource Site: HAMSTeRS version 4. *Nucleic Acids Res.* **26**, 216-9.

37 Dominguez, C., Boelens, R. and Bonvin, A. M. J. J. (2003) HADDOCK: a protein-protein docking approach based on biochemical or biophysical information. *J. Am. Chem. Soc.* **125**, 1731-7.

38 Ngo, J. C. K., Huang, M., Roth, D. A., Furie, B. C. and Furie, B. (2008) Crystal Structure of Human Factor VIII: Implications for the Formation of the Factor IXa-Factor VIIIa Complex. *Structure* **16**, 597-606.

39 Kohn, D. B. (2019) Gene therapy for blood diseases. *Curr. Opin. Biotechnol.* **60**, 39-45.

40 Kitazawa, T., Igawa, T., Sampei, Z., Muto, A., Kojima, T., Soeda, T., Yoshihashi, K., Okuyama-nishida, Y., Saito, H., Tsunoda, H., et al. (2012) A bispecific antibody to factors IXa and X restores factor VIII hemostatic activity in a hemophilia A model. *Nat. Med.* **18**, 1570-1577.

41 Mei, B., Pan, C., Jiang, H., Tjandra, H., Strauss, J., Chen, Y., Liu, T., Zhang, X., Severs, J., Newgren, J., et al. (2010) Rational design of a fully active, long-acting PEGylated factor VIII for hemophilia A treatment. *Blood* **116**, 270-279.

42 Bloem, E., Karpf, D. M., Nørby, P. L., Johansen, P. B., Loftager, M., Rahbek-Nielsen, H., Petersen, H. H., Blouse, G. E., Thim, L., Kjalke, M., et al. (2019) Factor VIII with a 237 amino acid B-domain has an extended half-life in F8 -knockout mice. *J. Thromb. Haemost.* **17**, 350-360.

43 Pipe, S. W. (2012) The hope and reality of long-acting hemophilia products. *Am. J. Hematol.* **87**, S33-S39.

44 Muczynski, V., Casari, C., Moreau, F., Aymé, G., Kawecki, C., Legendre, P., Proulle, V., Christophe, O. D., Denis, C. V. and Lenting, P. J. (2018) A factor VIII-nanobody fusion protein forming an ultrastable complex with VWF: effect on clearance and antibody formation. *Blood* **132**, 1193-1197.

45 Sinz, A. (2018) Cross-Linking/Mass Spectrometry for Studying Protein Structures and Protein-Protein Interactions: Where Are We Now and Where Should We Go from Here? *Angew. Chemie - Int. Ed.* **57**, 6390-6396.

46 Kastritis, P. L. and Bonvin, A. M. J. J. (2012) On the binding affinity of macromolecular interactions: daring to ask why proteins interact. *J. R. Soc. Interface* **10**, 20120835-20120835.

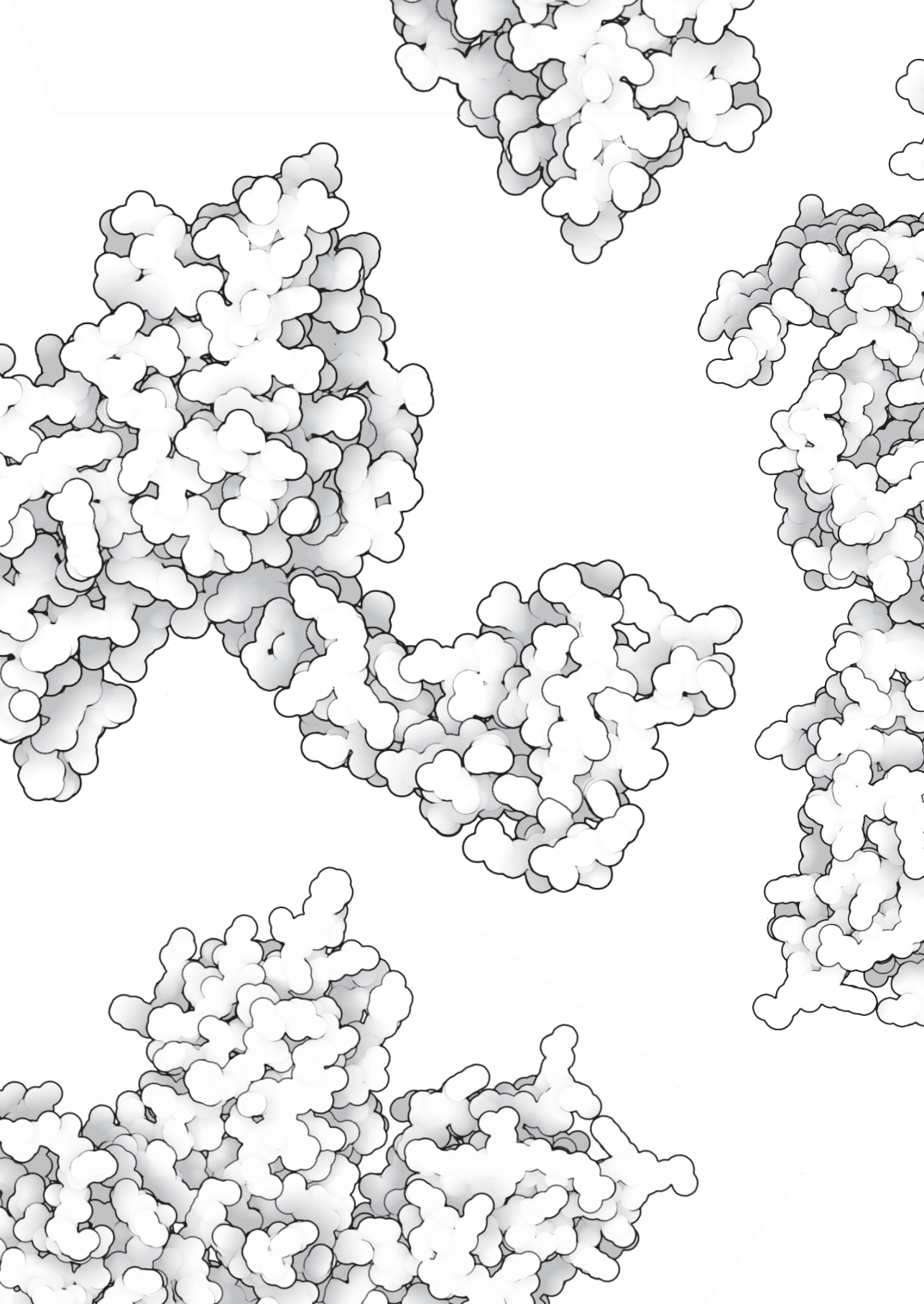

Appendix

Samenvatting

Curriculum vitae

Publication list

Acknowledgments

SAMENVATTING

Factor VIII (FVIII) circuleert in het bloed als een macromoleculair eiwitcomplex met Von Willebrand Factor (VWF). Hoewel FVIII door deze complexvorming wordt beschermd tegen snelle eliminatie uit de bloedsomloop, verloopt de klaring van FVIII paradoxaal via cellulaire receptoren die VWF uit het bloedplasma verwijderen. Inzicht in de duale rol die VWF speelt in de biologische processen die de levenscyclus van FVIII bepalen is van belang voor het begrijpen en behandelen van bloedingsstoornissen die worden veroorzaakt door lage plasma waarden van FVIII (Hemofilie A) en VWF (de ziekte van von Willebrand). Deze kennis is essentieel voor de ontwikkeling van verbeterde FVIII- en/of VWF-afgeleide therapieën. In dit proefschrift worden zowel het mechanisme van de complexvorming tussen VWF en FVIII, als de cellulaire opname van VWF, bestudeerd.

Hoofdstuk 1 beschrijft de algemene achtergrond met betrekking tot de biologie van FVIII en VWF. Er wordt een overzicht gegeven van de functie van FVIII en VWF in de primaire en secundaire hemostase en van de bloedingsstoornissen die verband houden met de functionele afwezigheid van deze eiwitten. Daarnaast wordt de huidige kennis over de complexe interactie tussen FVIII en VWF besproken, evenals de klaringsmechanismen voor beide eiwitten uit de circulatie. Ten slotte wordt massaspectrometrie besproken als technologie om eiwit-eiwit interacties op moleculair niveau verder te ontrafelen.

In hoofdstuk 2 wordt Hydrogen / Deuterium eXchange Mass Spectrometry (HDX-MS) gebruikt om regionen op VWF te identificeren die betrokken zijn bij de interactie met FVIII. Met behulp van een VWF fragment dat het FVIII interactieve gebied omvat, de zogenaamde N-terminale D'-D3 domeinen, ontdekten we dat een belangrijke bindingsplaats voor FVIII is gelegen tussen aminozuur residuen Arg782-Cys799 in het D' domein. Aminozuur specifieke mutagenese in het D'-D3 fragment gevolgd door eiwit-eiwit interactie studies met behulp van Surface Plasmon Resonance (SPR) analyse toonde aan dat met name de geladen residuen in deze regio, en in het bijzonder Glu787, belangrijk zijn voor de interactie met FVIII.

Het is niet goed begrepen waarom aminozuursubstituties in het D3-domein, dat ruim buiten het belangrijkste FVIII-bindingsgebied Arg782-Cys799 in het D' domain valt, leiden tot een Von Willebrand Disease type 2 Normandy ziektebeeld, dat gekarakteriseerd wordt door een verminderde affiniteit voor FVIII. In hoofdstuk 3 hebben we daarom de rol onderzocht van de VWD3-C8_3-TIL3-E3-subdomeinen in het D3-domein met betrekking tot de interactie met FVIII. Met behulp van Surface Plasmon Rsonance (SPR) analyse ontdekten we dat het E3-subdomein kan worden verwijderd uit het D'-D3 fragment zonder de binding aan FVIII te beïnvloeden. Het verwijderen van de TIL3- en C8_3-subdomeinen resulteerde in een geleidelijke afname van de affiniteit voor FVIII, terwijl het verwijderen van het VWD3 subdomein de interactie tussen VWF en

FVIII vrijwel volledig teniet deed. Chemische modificatie van specifieke aminozuren gecombineerd met massaspectrometrie analyse (zogenaamde *footprinting*) impliceerde dat het verwijderen van C-terminale subdomeinen resulteert in een verhoogde instabiliteit van het D3-domein. De gecombineerde bevindingen suggereerden dat een stabiele conformatie van het D3-domein vereist is om de interactie tussen D 'en FVIII te ondersteunen.

In hoofdstuk 4 hebben we massaspectrometrie technologie gebruikt om receptoren te identificeren die tot expressie komen op van monocyten afgeleide macrofagen die VWF internaliseren onder hemodynamische condities. De bevindingen suggereerden een hoge expressie van de vermeende VWF klaringsreceptoren Low-density lipoprotein receptor-Related Protein (LRP)-1 en Macrophage Scavenger Receptor (MSR)-1. In overeenstemming met de waarneming dat de bindingsplaatsen voor deze receptoren zich in het D'-D3-A1-fragment van VWF bevinden, ontdekten we dat geïsoleerde D'-D3- en D'-D3-A1-fragmenten konden worden geïnternaliseerd, onafhankelijk van hemodynamische condities. Eiwit-eiwit interactie studies en cellulaire opnamestudies van D'-D3 en D'-D3-A1 door U87MG-cellen die een hoge expressie van LRP-1 vertonen, toonden aan dat LRP-1 direct kan bijdragen aan de opname van het D'-D3-A1-fragment. Echter, in aanwezigheid van een antagonist voor LRP-1 werd niet alleen de cellulaire opname van het D'-D3-A1 fragment door macrofagen geblokkeerd, maar ook de cellulaire opname van het D'-D3-fragment. Aanvullende studies met een oplosbaar fragment van MSR-1 suggereerden dat MSR-1 tegelijkertijd D'-D3 en LRP-1 kan binden. Vervolgens bleek dat MSR-1 samenwerkt met LRP-1 bij de opname van de D'-D3- en D'-D3-A1-fragmenten van VWF.

In hoofdstuk 5 hebben we de complementaire bindingsregio van VWF op FVIII onderzocht. Eerdere studies suggereerden dat het C1-domein van FVIII een bindingsplaats voor VWF zou kunnen omvatten. Dit is in overeenstemming met onze waarneming dat het vervangen van het C1-domein van FVIII door het homologe C1-domein van Factor (F)V de binding aan VWF vrijwel volledig teniet doet. Door het vergelijken van de kristalstructuren van de C1-domeinen van FV en FVIII konden we vijf unieke hydrofobe aminozuur residuen identificeren in FVIII die geëxposeerd zijn aan de buitenkant van het eiwit. Aminozuur-specifieke mutagenese gecombineerd met eiwit-eiwit interactie studies toonden aan dat Val2125 en Phe2127 deel uitmaken van het oppervlak dat aan VWF bindt, dat daarnaast gedeeltelijk overlapt met oppervlak dat aan geactiveerd Factor (F)IX bindt.

In hoofdstuk 6 worden de belangrijkste bevindingen van dit proefschrift samengevat en besproken. Daarnaast geven we richting aan toekomstig onderzoek om een op VWF-gebaseerd fragment te ontwikkelen dat toegepast zou kunnen worden als therapeutisch eiwit om de *in vivo* halfwaardetijd van intraveneus toegediend FVIII te verlengen voor de behandeling van hemofilie A.

PUBLICATION LIST

Przeradzka, M. A.*, Freato, N.*, Boon-Spijker, M., van Galen, J., van der Zwaan, C., Mertens, K., van den Biggelaar, M. and Meijer, A. B. (2019) **Unique surface-exposed hydrophobic residues in the C1 domain of factor VIII contribute to cofactor function and von Willebrand factor binding**. J. Thromb. Haemost. jth.14668.

Przeradzka, M. A., van Galen, J., Ebberink, E. H. T. M., Hoogendijk, A. J., van der Zwaan, C., Mertens, K., van den Biggelaar, M. and Meijer, A. B. (2019) **D'domain Region Arg782-Cys799 of Von Willebrand Factor contributes to Factor VIII binding**. Haematologica 475, 2819-2830.

Béguin, E. P., Przeradzka, M. A., Janssen, E. F. J., Meems, H., Sedek, M., van der Zwaan, C., Mertens, K., van den Biggelaar, M., Meijer, A. B. and Mourik, M. J. (2020) **Endocytosis by macrophages: Interplay of macrophage scavenger receptor-1 and LDL receptor-related protein-1**. Haematologica 105, E133-E137

Przeradzka, M. A., Meems, H., van der Zwaan, C., Ebberink, E. H. T. M., van den Biggelaar, M., Mertens, K. and Meijer, A. B. (2018) **The D' domain of von Willebrand factor requires the presence of the D3 domain for optimal factor VIII binding**. Biochem. J. 475, 2819-2830.

In revision

van Galen, J.*, Freato, N.*, Przeradzka, M. A., Ebberink, E. H. T. M., Boon-Spijker, M., van der Zwaan, C., van der Biggelaar, M. and Meijer, A. B. **Hydrogen-deuterium exchange mass spectrometry identifies activated factor IX-induced molecular changes in activated factor VIII.**

*authors contributed equally

CURRICULUM VITAE

Małgorzata Aniela Przeradzka was born on 17th March 1989 in Łódź, Poland. She grew up in Łódź where she also attended High School no 12 with scientific orientation on math and physics. In September 2009, she started the Interdisciplinary Natural Science Bachelor Programme with a specialization in Chemistry at the University of Łódź under the supervision of prof. Jarosław Lewkowski. To follow her interest in principles of drug design, in September 2011 she moved to Wrocław for her master studies in Medicinal Chemistry at the Wrocław University of Technology. During that time, she did an additional internship at Durham University in England in the lab of prof. Steven Cobb. She completed the final master internship at the Institute of Immunology and Experimental Therapy of the Polish Academy of Science in the group of prof. Andrzej Rapak. After finishing studies, in May 2014 she moved to Amsterdam to start her PhD project under the supervision of Sander Meijer, Koen Mertens, and Maartje van den Biggelaar. The results of her studies are described in this thesis. Currently, she works as a scientist at Janssen Vaccines and Prevention in Leiden.

ACKNOWLEDGMENTS

I thought that the PhD project makes you an island, separated and individually focused on the work. That is totally not the case. There would be no thesis without the help and support of many different people. Now, "the mission is completed" and I would like to thank everyone without whom this thesis would not have been possible.

Sander, I would like to thank you for the supervision throughout my whole PhD path. I appreciate your passion for science and enthusiasm for this project. You always had thousands of ideas for new experiments and solutions to tackle any issue. These years were very challenging and I undoubtedly gained a lot.

Koen, thank you for your trust, without giving me a chance I wouldn't be where I am now. I still clearly remember my first trip to Amsterdam for the interview in early winter 2014. I value your input, down-to-earth judgment of the situation and support during this PhD project.

Maartje, I would like to thank you for teaching me the basis of molecular biology, helping me in the lab, for the critical and challenging comments and the inspiration for experiments.

Jan, I very much appropriate your interest in the project and all the asked questions. You have never missed any surprising band on my SDS-PAGE. Joost, I am grateful for all the discussion during our Tuesday morning seminars.

#The girls; I am really lucky to have my dear friends as my paranymphs. Ellie, you've never stopped teasing me, and please don't stop! I enjoyed hanging out, practicing presentations, having lunch and I enjoyed our time outside of Sanquin even more. I am very happy to see that you pursue your passion for science with your academic carrier adventure in Dubin. I wish you plenty of great successes and discoveries. Nadia, without you I wouldn't survive these last years of the PhD project, and even if I would, it will be not fun at all. Having you in the lab just opposite of me made long experiments joyful. You've been always there for me, I appreciate a lot your help, thoughtful words and sharp eye for details. Girls, I cherish this PhD time thanks to you!

#Y417: the memorable office allowed me to have a smooth landing at Sanquin. Our coffee breaks were so 'gezellig' that They even had to split us up :D Esther, you have pioneered TMT- labeling in our lab and we all benefit from it! Thank you for the intro to Biacore, despite very little time due to end of your contract, you always tried to help me out in the lab. Magda Sędek, dzięki za wszystkie pogaduchy o nauce i wszystkim

dookoła, nie zapomnę ze to właśnie Ty mnie odebrałaś z dworca, gdy przyjechałam pociągiem z dalekiej Polski z walizka i plecakiem. Annemarie, always ready for tea break and mental support. Eelke, that PhD time was definitely a fun time, starting together and ending together, it wouldn't be the same without you! Josse, I know I wasn't the easiest person to work with, but I have to admit that I have learned a lot from our collaboration on HDX project, the core of this thesis, and I am grateful for your input and help. Esmee, you were always very empathic thank you for the warmth you brought to our office.

#CoolKids; My secret nickname for people who were always willing to do fun things outside of Sanquin. There were lot of adventures, starting from bouldering, blow carting, climbing the trees, to dancing parties; Maaike, you are by far the bravest girl I know, and not only because you did mountain biking but also because you had more oral presentations than anybody, covering not only your projects, and you calmly faced them all in great style. Arjan, exceptional talent in dancing not only in the lab, thank you very much for all the advice on the statistical analysis of my HDX-MS experiments. Marjon, I love your sarcastic sense of humour, we had a lot of fun in the lab and outside of work. Eduard, thankfully we align in music taste otherwise you wouldn't have taught me all the little tips and tricks in the lab. You have dedicated lot of time to make the HDX experiments work, that later became the essential part of my thesis. Boğaç, it was great fun to hang out after work, thank you for all the effort with modelling the complex, the cherry of the general discussion, it was a totally awesome piece of work! Ivan, always challenging and demanding to reach higher level of quality, which almost broke our friendship :p thank you for never giving up on it.

#VintageSanquiners; The pioneers of the core projects held by the next generations, you have created this friendly supportive atmosphere at Plasma Proteins. Nicoletta, you have an unbelievable talent to make people feel special and welcomed, I remember how you took care of me when I just started at Sanquin and didn't know anybody, I am very grateful for all the advice through all these years; your passion for science is contagious! Some people show care in silence actions, that's for sure Robin. Not only did you bring me peanut butter 100% when I couldn't find one in the store, but also baby powder for when my shoes where too squeaky. And even closer to my heart, you brought me to your piano store where I could choose my instrument. Mar, we had lots of fun outside Sanquin, among others, the unforgettable night of dancing till the morning after the Spanish film festival, it was always great to hang out with you. Ruben, I am so happy that you didn't offer me the job, you have a good intuition, that project was not for me. Thank you for all the constructive comments during my

presentations. Henriët, I appreciate a lot your help with writing process, especially with my first paper; you have always made time to advise me.

#Technicians; let's face the truth: without you, none of us would have ever finished this mission, you kept the standards and the quality at a high level. Marleen, you have showed me how to culture the FreeStyle cells, which produced my whole PhD :D Paul, always ready to help with finding solutions. Floris, guard of the Mass Spec, thankfully my samples rarely caused any issues ;) Mariëtte, my lab-bench mate, you have been a great companion in the lab and taught me the most challenging assay: pipetting on the shaker! Carmen, you have been there in all the projects, taught me most of the lab work I needed and saved quite a few of the purifications, when my columns where getting dry in the morning. I admire your dedication and positive energy, thank you for the great help and support.

#HEP/IP our science fellows and party companions, dear Fiamma, Tati, Peter-Paul and Felix, it was always fun to hang out at Sanquin and after work.

#Rodzinka; Moja baza i oaza, zawsze odliczam dni do przyjazdu do domu. Mamo, Tato bez Waszego wsparcia i wiary we mnie nie ruszyłabym się z kraju. Od zawsze budziliście we mnie ciekawość do świata i nauki, wspieraliście i motywowaliście bym zawsze starała się dać z siebie co mogę. Dziękuje za wszystko, i jeszcze za to jakim jestem dzisiaj człowiekiem. Magdo, siostrzyczko i co wyszło? Przetarłaś mi szlaki i wygląda na to ze wylądowałam na dobre w Holandii. Dziękuję Ci za wszystkie słowa otuchy i wparcia, kiedy tego najbardziej potrzebowałam. Jesteś niesamowicie wnikliwa i spostrzegawcza, bardzo to cenię.

#Love&soulmate; Bart
Funny enough, I was sitting next you in the office since day one, you were a nice and friendly colleague, living outside of Amsterdam, so rarely joining for the spontaneous drinks after work. Quite some time has passed and here we are. There are no words that can express what I feel. Still, I want to thank you for the great support and understanding during the last and toughest parts of my PhD time. Going smoothly through all these moments makes it clear: we are a great team. Having you by my side makes me smile to the future.